Eur. Phys. J. C (2024) 84:1309
https://doi.org/10.1140/epjc/s10052-024-13190-x

THE EUROPEAN PHYSICAL JOURNAL C

Regular Article - Experimental Physics

Measurement of the W-boson mass and width with the ATLAS detector using proton–proton collisions at $\sqrt{s} = 7$ TeV

ATLAS Collaboration[⋆]

CERN, 1211 Geneva 23, Switzerland

Received: 22 March 2024 / Accepted: 2 August 2024

Abstract Proton–proton collision data recorded by the ATLAS detector in 2011, at a centre-of-mass energy of 7 TeV, have been used for an improved determination of the W-boson mass and a first measurement of the W-boson width at the LHC. Recent fits to the proton parton distribution functions are incorporated in the measurement procedure and an improved statistical method is used to increase the measurement precision. The measurement of the W-boson mass yields a value of $m_W = 80{,}366.5 \pm 9.8$ (stat.) $\pm$ 12.5 (syst.) MeV $= 80{,}366.5 \pm 15.9$ MeV, and the width is measured as $\Gamma_W = 2202 \pm 32$ (stat.) ± 34 (syst.) MeV $= 2202 \pm 47$ MeV. The first uncertainty components are statistical and the second correspond to the experimental and physics-modelling systematic uncertainties. Both results are consistent with the expectation from fits to electroweak precision data. The present measurement of m_W is compatible with and supersedes the previous measurement performed using the same data.

Contents

1 Introduction

At lowest order in the Standard Model (SM) electroweak theory [1–3] the W-boson mass, m_W, can be expressed solely as a function of the Z-boson mass, m_Z, the fine-structure constant, α, and the Fermi constant, G_F. Higher-order corrections introduce an additional dependence of the W-boson mass on the gauge couplings and the masses of the heavy particles of the SM, such as the top-quark mass, m_t, and the Higgs boson mass, m_H [4,5]. In extended theories, the loop corrections receive contributions from additional particles and interactions. The consistency of the SM and potential effects of new physics can therefore be probed by comparing the measured values of m_W with the results of global fits to the relevant physical parameters [6–8]. The SM fit yields $m_W^{\mathrm{SM}} = 80{,}355 \pm 6$ MeV [6,7]. The present experimental situation is characterised by a significant tension between the precise measurement from the CDF Collaboration, $m_W = 80{,}433.5 \pm 9.4$ MeV [9], and the average of the LEP [10], D0 [11], ATLAS [12] and LHCb [13] measurements, $m_W = 80{,}369.2 \pm 13.3$ MeV [14].

The electroweak theory also predicts the total decay width of the W boson, Γ_W. It is expected to be equal to the sum of the partial widths over three generations of lepton doublets

⋆ e-mail: atlas.publications@cern.ch

Published online: 21 December 2024

and two generations of quark doublets, yielding an expected value of $\Gamma_W^{\mathrm{SM}} = 2088 \pm 1$ MeV [6]. New particle candidates that couple to the W boson and are lighter than m_W would open a new decay channel and alter Γ_W [15]. Examples are supersymmetric models in which the W boson decays into the lightest super-partner of the charged gauge bosons and the lightest super-partner of the neutral gauge bosons [16]. The current world average of W-boson width determinations yields a value of $\Gamma_W = 2085 \pm 42$ MeV [17], and is based on measurements at LEP-2 [10] and the Tevatron [18,19]. No measurement of Γ_W has been previously performed at the Large Hadron Collider (LHC).

In this paper, an improved measurement of the W-boson mass as well as a first measurement of its width is presented, which is based on data from $\sqrt{s} = 7$ TeV recorded by the ATLAS detector in 2011, i.e., the same data as was used for the first measurement of m_W at the LHC [12]. This was based on a χ^2 considering statistical uncertainties only, where systematic uncertainties were included a posteriori through variations of the physics and calibration models within their uncertainties (the so-called 'offset' method).

The present analysis uses an improved statistic based on the profile likelihood (PLH) [20]. This technique performs a simultaneous determination of m_W together with a set of nuisance parameters describing the experimental and modelling uncertainties. The nuisance parameters are adjusted to optimally describe the data, yielding an overall improved model and some reduction in uncertainty compared with the fitting technique used previously. With few sub-dominant exceptions, the sources of uncertainty considered in this measurement are either of experimental nature, or phenomenological, with model parameters derived from the data. A nuisance parameter representation is therefore adequate and the PLH technique can be applied. The measurement of Γ_W relies on the same PLH statistic and on the same physics, detector and background model as those used for the determination of m_W.

Recent parton distribution functions (PDFs) are studied within this work, and the dependence of the measurement results on the assumed PDF set is presented and discussed. The present analysis also aims at consolidating the earlier result of ATLAS, in the perspective of the latest measurement by CDF.

2 ATLAS detector

The ATLAS experiment [21] is a multipurpose particle detector with a forward–backward symmetric cylindrical geometry. It consists of an inner tracking detector surrounded by a thin superconducting solenoid, electromagnetic and hadronic calorimeters, and a muon spectrometer incorporating three large superconducting toroid magnets[1].

The inner-detector system (ID) is immersed in a 2 T axial magnetic field and provides charged-particle tracking in the range of $|\eta| < 2.5$. At small radii, a high-granularity silicon pixel detector covers the vertex region and typically provides three measurements per track. It is followed by the silicon microstrip tracker, which usually provides eight measurement points per track. These silicon detectors are complemented by a gas-filled straw-tube transition radiation tracker, which enables radially extended track reconstruction within $|\eta| = 2.0$. The transition radiation tracker also provides electron identification information based on the fraction of hits (typically 35 in total) above a higher energy-deposit threshold corresponding to transition radiation.

The calorimeter system covers the pseudorapidity range $|\eta| < 4.9$. Within the region $|\eta| < 3.2$, electromagnetic (EM) calorimetry is provided by high-granularity lead/liquid-argon (LAr) calorimeters, with an additional thin LAr presampler covering $|\eta| < 1.8$ to correct for upstream energy-loss fluctuations. The EM calorimeter is divided into a barrel section covering $|\eta| < 1.475$ and two endcap sections covering $1.375 < |\eta| < 3.2$. For $|\eta| < 2.5$, it is divided into three layers in depth, which are finely segmented in η and ϕ. Hadronic calorimetry is provided by a steel/scintillator-tile calorimeter, segmented into three barrel structures within $|\eta| = 1.7$ and two copper/LAr hadronic endcap calorimeters covering $1.5 < |\eta| < 3.2$. The solid-angle coverage is completed with forward copper/LAr and tungsten/LAr calorimeter modules in $3.1 < |\eta| < 4.9$, optimised for electromagnetic and hadronic measurements, respectively.

The muon spectrometer (MS) comprises separate trigger and high-precision tracking chambers measuring the deflection of muons in a magnetic field generated by superconducting air-core toroids. The precision chamber system covers the region $|\eta| < 2.7$ with three layers of monitored drift tubes, complemented by cathode strip chambers in the forward region. The muon trigger system covers the range $|\eta| < 2.4$ with resistive plate chambers in the barrel, and thin gap chambers in the endcap regions.

A three-level trigger system is used to select events for offline analysis [22]. The level-1 trigger is implemented in hardware and uses a subset of detector information to reduce the event rate to a design value of at most 75 kHz. This is followed by two software-based trigger levels that together

[1] ATLAS uses a right-handed coordinate system with its origin at the nominal interaction point (IP) in the centre of the detector and the z-axis along the beam pipe. The x-axis points from the IP to the centre of the LHC ring, and the y-axis points upwards. Cylindrical coordinates (r, ϕ) are used in the transverse plane, ϕ being the azimuthal angle around the z-axis. The pseudorapidity is defined in terms of the polar angle θ as $\eta = -\ln\tan(\theta/2)$. Angular distance is measured in units of $\Delta R \equiv \sqrt{(\Delta\eta)^2 + (\Delta\phi)^2}$.

reduce the event rate to about 300 Hz. A software suite [23] is used in data simulation, in the reconstruction and analysis of real and simulated data, in detector operations, and in the trigger and data acquisition systems of the experiment.

3 Measurement overview and analysis strategy

3.1 Data samples and event simulation

The data sample consists of $W \to e\nu$ and $W \to \mu\nu$ candidate events, collected in 2011 with the ATLAS detector in proton–proton collisions at the LHC, at a centre-of-mass energy of $\sqrt{s} = 7$ TeV. The data collected with all relevant detector systems operational correspond to approximately 4.6 fb^{-1} and 4.1 fb^{-1} of integrated luminosity in the electron and muon channels, respectively.

The POWHEG Monte Carlo (MC) generator (v1/r1556) [24–26] is used for the simulation of W- and Z-boson production and decay in the electron, muon, and τ-lepton channels, and is interfaced to PYTHIA 8 (v8.170) for the modelling of the parton shower, hadronisation, and underlying event [27,28]. Parton shower and underlying event parameters are set according to the AZNLO tune [29]. The CT10 PDF set [30] is used for the hard process, and the CTEQ6L1 PDF set [31] is used in the parton shower. The Z-boson simulation includes the effect of virtual photon exchange. The W- and Z-boson rapidity and p_{T} distributions are reweighted to optimise the description of the data, as described in Sect. 5.2. The change in the final-state distributions from updating the distributions to more recent PDFs is evaluated using POWHEG.

QED final-state radiation (FSR) is simulated using PHOTOS (v2.154) [32]. Decays of τ-leptons are handled by PYTHIA 8, taking into account polarisation effects. The W- and Z-boson event yields are normalised according to their measured cross sections, and the experimental uncertainties of 1.8% and 2.3% are assigned to the W^+/Z and W^-/Z production cross-section ratios, respectively [33]. The W-boson production samples assume $m_W = 80{,}399$ MeV and $\Gamma_W = 2085$ MeV.

Background processes such as top-quark pair and single-top-quark production are modelled using the MC@NLO MC generator (v4.01) [34–36], interfaced to HERWIG and JIMMY for the parton shower. Gauge-boson pair production (WW, WZ, ZZ) is simulated with HERWIG (v6.520). The CT10 PDF set is used in all these samples.

The response of the ATLAS detector is simulated using a software suite [37] based on GEANT4 [38]. The hard-scattering process is overlaid with additional proton–proton interactions, simulated with PYTHIA 8 (v8.165) using the A2 tune [39]. The distribution of the average number of interactions per bunch crossing $\langle\mu\rangle$ spans the range 2.5–16.0, with a mean value of approximately 9.0.

3.2 Selection of electrons and muons and reconstruction of the recoil

Object definitions are unchanged compared to Ref. [12]. Electron candidates are reconstructed from clusters of energy deposited in the electromagnetic calorimeter and associated with at least one track in the ID [40,41]. Quality requirements are applied to the associated tracks in order to reject poorly reconstructed charged-particle trajectories. The energy of the electron is reconstructed from the energy collected in calorimeter cells within an area of size $\Delta\eta \times \Delta\phi = 0.075 \times 0.175$ in the barrel, and 0.125×0.125 in the endcaps. The energy measurement relies on a multivariate regression algorithm developed and optimised on simulated events. The kinematic properties of the reconstructed electron are inferred from the energy measured in the EM calorimeter and from the pseudorapidity and azimuth of the associated track. Electron candidates are required to fulfil tight identification requirements [40], and their transverse momentum, p_{T}^{ℓ}, and pseudorapidity should satisfy $p_{\mathrm{T}}^{\ell} > 15$ GeV and $|\eta| < 2.4$. As in the previous result, the pseudorapidity range $1.2 < |\eta| < 1.8$ is excluded from the measurement. Background from jets misidentified as electrons is reduced using additional isolation requirements using the activity in the ID and calorimeter nearby the electron candidates passing the kinematic and identification selections [12].

Muon candidates are reconstructed independently in the ID and in the MS, and a combined muon candidate is formed from the statistical combination of the ID and MS track parameters [42]. The kinematic properties of the reconstructed muon are defined using the ID track parameters alone, which allows a simpler calibration procedure. Muon candidates are required to have $p_{\mathrm{T}}^{\ell} > 20$ GeV and $|\eta| < 2.4$ [12]. Similarly to the electrons, the multijet background is reduced by applying an isolation requirement [12].

The recoil, $\vec{u}_{\mathrm{T}}$, is an estimator of the W- or Z-boson transverse momentum. It is reconstructed from the vector sum of the transverse energy of all clusters measured in the calorimeters, excluding clusters located at a distance $\Delta R < 0.2$ from electron or muon candidates. The definition of $\vec{u}_{\mathrm{T}}$ does not involve the explicit reconstruction of jets to avoid possible p_{T} threshold effects.

3.3 W-boson kinematics and event selection

The transverse momentum vector of charged leptons from the W-boson decay, $\vec{p}_{\mathrm{T}}^{\,\ell}$, is measured as summarised in the previous section. The transverse momentum of the decay neutrino is inferred from the missing transverse momentum vector, $\vec{p}_{\mathrm{T}}^{\,\mathrm{miss}}$, defined as $\vec{p}_{\mathrm{T}}^{\,\mathrm{miss}} = -\left(\vec{p}_{\mathrm{T}}^{\,\ell} + \vec{u}_{\mathrm{T}}\right)$. The W-boson transverse mass, m_{T}, is derived from $p_{\mathrm{T}}^{\mathrm{miss}}$ and from the transverse momentum of the charged lepton as

$m_{\mathrm{T}} = \sqrt{2p_{\mathrm{T}}^{\ell} p_{\mathrm{T}}^{\mathrm{miss}}(1-\cos\Delta\phi)}$, where $\Delta\phi$ is the azimuthal opening angle between the charged lepton and the missing transverse momentum.

The W-boson sample is collected using triggers requiring at least one muon candidate with transverse momentum larger than 18 GeV or at least one electron candidate with transverse momentum larger than 20 GeV. The transverse-momentum requirement for the electron candidate was raised to 22 GeV in later data-taking periods to cope with the increased instantaneous luminosity delivered by the LHC. Selected events are required to have a reconstructed primary vertex with at least three associated tracks.

The sample of W-boson candidate events is selected by requiring exactly one reconstructed electron or muon candidate with $p_{\mathrm{T}}^{\ell} > 30$ GeV. The leptons are required to match the corresponding trigger signal. The magnitude of the recoil is required to satisfy $u_{\mathrm{T}} < 30$ GeV, the missing transverse momentum $p_{\mathrm{T}}^{\mathrm{miss}} > 30$ GeV and the transverse mass $m_{\mathrm{T}} > 60$ GeV. Approximately 5.89×10^6 candidate events are selected in the $W \to e\nu$ channel and 7.84×10^6 events in the $W \to \mu\nu$ channel.

3.4 W-boson mass analysis updates

The selected W-boson event sample includes events from various background processes. Background contributions from Z-boson, $W \to \tau\nu$, boson pair, and top-quark production are estimated using simulation, and represent about 6.4% of the total sample in the muon channels, and about 3.1% in the electron channels. Contributions from multijet production are estimated with data-driven techniques, and are detailed in Ref. [12]. Compared with that reference, the multijet background yield was re-evaluated using the final luminosity calibration for Run 1 [43], resulting in a 1–2% decrease of the contamination of multijet background control regions by electroweak processes, and a corresponding 20% increase in the estimated multijet background yield in the electron channel. This background now represents 1.2% of the total sample, and agrees with the previous measurement within uncertainties. The multijet background in the muon channel is unaffected, due to the smaller contamination in this case. In addition, uncertainties in the multijet distributions were previously propagated to the m_W measurement through fluctuations of the extrapolation parameters; an eigenvector decomposition is used in the present analysis.

The results of Ref. [12] were obtained using the CT10nnlo PDF set and compared with results using the CT14 [44] and MMHT2014 PDF sets [45]. The present analysis extends the study of the PDF dependence of the fit results to the ATLASpdf21 [46], CT18, CT18A [47], MSHT20 [48], NNPDF3.1 [49] and NNPDF4.0 [50] sets.

In the previous measurement, m_W was determined with the W-boson width fixed to the SM prediction. In the present analysis, this assumption is relaxed by treating Γ_W as a source of systematic uncertainty, considering the SM value and uncertainty of $\Gamma_W^{\mathrm{SM}} = 2088 \pm 1$ MeV. The W-boson width is also extracted assuming the SM prediction and uncertainty of the W-boson mass, $m_W^{\mathrm{SM}} = 80{,}355 \pm 6$ MeV.

Finally, an improved statistic is used for the fit as described in the following section.

3.5 Statistical analysis

The previous measurement used separate template fits to the p_{T}^{ℓ} and m_{T} distributions observed in different event categories. The W-boson candidate events were classified according to the charge, flavour and pseudorapidity of the final state lepton, as summarised in Table 1. In the fit, the χ^2 of the comparison between data and simulation was minimised considering statistical uncertainties only; systematic uncertainties were included by varying the parameters determining the templates within their uncertainties, and repeating the fits.

The present analysis performs a simultaneous optimisation of m_W or Γ_W, and of nuisance parameters describing systematic uncertainties, through a global profile likelihood fit in all event categories for a given kinematic distribution. The likelihood function, which describes how compatible with each other the data and MC distributions are, is given by

$$\mathcal{L}(\vec{n}|\,\mu,\vec{\theta}) = \prod_j \prod_i \mathrm{Poisson}\left(n_{ji}|\nu_{ji}(\mu,\vec{\theta})\right) \cdot \mathrm{Gauss}\left(\vec{\theta}\right), \tag{1}$$

where $\vec{n}$ represents the observed distributions in data, and n_{ji} is the number of events observed in data in bin i of the distribution in a given category j. It is the input to the Poisson distribution with expectation $\nu_{ji}(\mu,\vec{\theta}) = S_{ji}(\mu,\vec{\theta}) + B_{ji}(\vec{\theta})$, of S_{ji} events from signal and B_{ji} events from background contributions. The parameter of interest, μ, represents variations in m_W or Γ_W with respect to a conventional reference, μ_{ref}. Uncertainties of the signal and background distributions are encapsulated as nuisance parameters (NPs), denoted by $\vec{\theta}$ in Eq. (1), for which a normal probability distribution is assumed. The expected number of events ν_{ji} is parameterised as

$$\begin{aligned}\nu_{ji}(\mu,\vec{\theta}) = \Phi \times &\left[S_{ji}^{\mathrm{nom}} + \mu \times \left(S_{ji}^{\mu} - S_{ji}^{\mathrm{nom}}\right)\right] \\ &+ \sum_s \theta_s \times \left(S_{ji}^{s} - S_{ji}^{\mathrm{nom}}\right) + B_{ji}^{\mathrm{nom}} \\ &+ \sum_b \theta_b \times \left(B_{ji}^{b} - B_{ji}^{\mathrm{nom}}\right),\end{aligned} \tag{2}$$

Table 1 Summary of the 28 categories and kinematic distributions used in the m_W measurement for the electron and muon decay channels

Decay channel	$W \to e\nu$	$W \to \mu\nu$
Kinematic distributions	p_{T}^{ℓ}, m_{T}	p_{T}^{ℓ}, m_{T}
Charge categories	W^+, W^-	W^+, W^-
$\lvert\eta_\ell\rvert$ categories	[0, 0.6], [0.6, 1.2], [1.8, 2.4]	[0, 0.8], [0.8, 1.4], [1.4, 2.0], [2.0, 2.4]

where Φ is an overall, unconstrained normalisation factor ensuring that the total $W^{\pm}$ signal rate always adjusts to the number of events in data, S_{ji}^{nom} and B_{ji}^{nom} are the nominal distributions of signal and background, respectively, while s and b represent nuisance parameters acting on signal and background contributions.

Changes in μ and $\vec{\theta}$ lead to changes in the expected signal and background distributions, which are interpolated using a polynomial morphing procedure. Signal templates for arbitrary values of m_W or Γ_W are obtained from the same simulation sample through a reweighting of the W-boson Breit–Wigner distribution. Templates representing systematic variations are determined from two-sided one- and two-sigma variations of the corresponding sources of uncertainty. The effect of varying m_W or Γ_W on the p_{T}^{ℓ} and m_{T} distributions is illustrated in Fig. 1. The procedure to interpolate between these points during the PLH fit was extensively tested, and excellent closure was observed.

As the new fitting method allows to better optimise the total uncertainty of the measurement due to the inclusion of NPs in the likelihood, the nominal fit ranges for the m_W measurement are re-evaluated. The updated optimal fit ranges are $30 < p_{\mathrm{T}}^{\ell} < 50$ GeV and $60 < m_{\mathrm{T}} < 100$ GeV, in contrast with $32 < p_{\mathrm{T}}^{\ell} < 45$ GeV and $66 < m_{\mathrm{T}} < 99$ GeV used in the previous measurement. For the determination of Γ_W, the same ranges are used as in the m_W measurement.

The baseline results rely on a numerical minimisation of the likelihood from Eq. (2). For ancillary studies, such as the decomposition of uncertainties, fit range variations, and to estimate the correlation between the m_{T} and p_{T}^{ℓ} fits, the following assumptions are made: in the limit where all uncertainties are Gaussian and the dependence of $\nu_{ji}(\mu, \vec{\theta})$ on μ and $\vec{\theta}$ is linear, the likelihood can be written as

$$
\begin{aligned}
&-2\ln\mathcal{L}\left(\vec{n}\,|\,\mu,\vec{\theta}\right) \\
&= \sum_j \sum_i \left(\frac{n_{ji} - \nu_{ji}(\mu_{\mathrm{ref}},\vec{0}) - \frac{\partial \nu_{ij}}{\partial \mu}(\mu - \mu_{\mathrm{ref}}) - \sum_t \frac{\partial \nu_{ij}}{\partial \theta_t}\theta_t}{\sigma_{ji}} \right)^2 \\
&\quad + \sum_t \theta_t^2,
\end{aligned}
\tag{3}
$$

and the minimisation and uncertainty estimation can be performed analytically [51]. This approach gives results within 2 MeV from the nominal fits and is much faster.

The decomposition of the post-fit uncertainties is performed according to the methods of Ref. [51]. The uncertainty components are defined to represent the contribution of the pre-fit uncertainty in the corresponding sources to the total uncertainty of the measurement, consistently with standard error propagation.

4 Experimental corrections and uncertainties

The p_{T}^{ℓ} and m_{T} distributions are affected by the lepton energy calibration and by the calibration of the recoil. Lepton momentum corrections are derived exploiting $Z \to \ell\ell$ event samples and the precisely measured value of m_Z [52], and the recoil response is calibrated using the expected momentum balance between u_{T} and $p_{\mathrm{T}}^{\ell\ell}$ [12]. Lepton identification and reconstruction efficiency corrections are determined from W- and Z-boson events using the tag-and-probe method [40,42].

A precision on the energy and momentum scale for electrons and muons of $O(10^{-4})$ is achieved, with somewhat larger uncertainty for the muons in the high-η region. The response and resolution of $u_{\mathrm{T}} = |\vec{u}_{\mathrm{T}}|$ is determined with a precision of a few percent. The experimental precision is limited by the finite size of the Z-boson sample, and by systematic uncertainties in the modelling of the distributions used in the calibration procedures.

4.1 Uncertainty propagation

Systematic uncertainties in the determination of m_W and Γ_W are evaluated by varying the calibration model parameters within their uncertainty. For two-sided systematic uncertainties, separate templates are produced for 68% confidence level (CL) upwards and downwards variations. Systematic uncertainties that are estimated independently in many kinematic bins are propagated through simultaneous random variations of the corresponding parameters within their uncertainty and generating templates for each variation. A principal component analysis (PCA) [53,54] is used to transform these variations into a set of uncorrelated two-sided uncertainties, preserving the total uncertainty. This approach is used for the statistical uncertainties of the electron and muon efficiencies, as well as for the recoil calibration, and allows a faithful representation of these uncertainties using a reduced set of nuisance parameters.

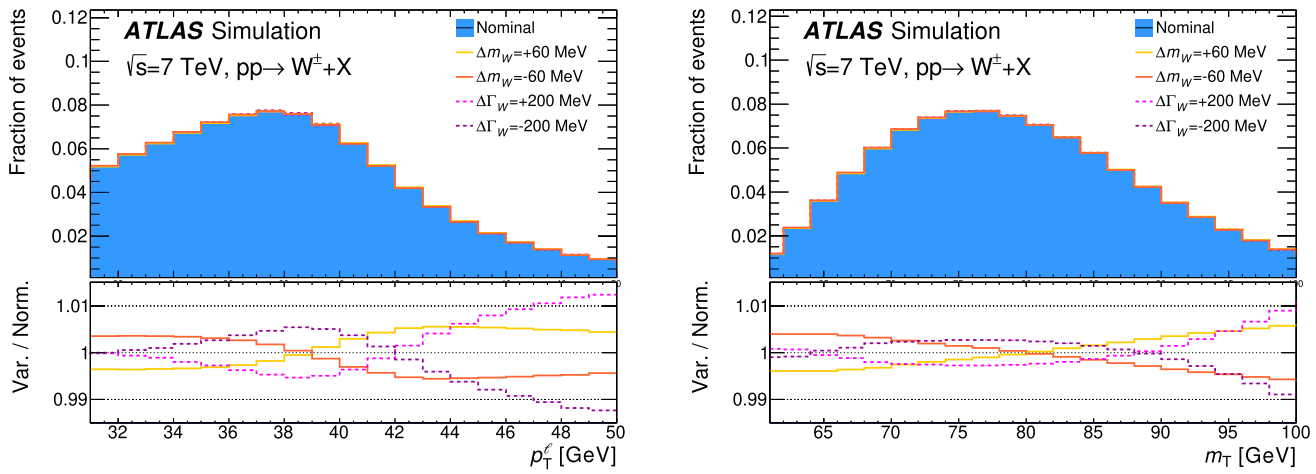

Fig. 1 Simulated kinematic distributions of **a** p_{T}^{ℓ} and **b** m_{T} in $W^{\pm} \to \mu^{\pm}\nu$ events, for W-boson mass and width values of $m_W = 80{,}399$ MeV and $\Gamma_W = 2085$ MeV. The ratio panels represent the relative effect of varying these parameters by ±60 MeV and ±200 MeV, respectively

Because of the finite size of the MC samples, some systematic variations contribute significant statistical fluctuations in the final-state distributions. A smoothing procedure is applied to remove such fluctuations, preserving the normalisation of each variation. For calibration systematic uncertainties, the effect of the upwards and downwards variations are symmetrised. The impact of the smoothing and symmetrisation procedures on the best-fit values and uncertainties are below 1 and 0.1 MeV, respectively.

The effect of each systematic variation is decomposed into corresponding uncertainties in the normalisation and in the shape of the final state distributions. Systematic uncertainties that yield differences smaller than 0.01% in the normalised p_{T}^{ℓ} distribution and smaller than 0.02% in the normalised m_{T} distribution are removed, reducing the number of shape systematic variations by a factor of two. The change in the total measurement uncertainty is less than 1% of itself, while central values change by less than 0.1 MeV. This pruning procedure simplifies the likelihood, stabilising and accelerating the fit procedure.

4.2 Sources of uncertainty

The electron calibration and selection efficiencies account for 75 sources of uncertainty in the p_{T}^{ℓ} distribution and 58 in the m_{T} distribution, including the energy scale and resolution as well as the electron identification, isolation, and trigger efficiencies. Of these uncertainties, 23 originate from the energy calibration and are treated as two-sided systematic uncertainties, while 52 (p_{T}^{ℓ}) and 35 (m_{T}) systematic variations come from the trigger, reconstruction, identification and isolation efficiencies. PCA is utilised to handle those systematic variations. Similarly, the muon response and efficiencies contribute 83 (p_{T}^{ℓ}) and 76 (m_{T}) sources of uncertainty, of which 6 are treated as two-sided uncertainties.

The calibration of the hadronic recoil yields 36 sources of systematic uncertainties for the m_{T} distributions, but only 7 sources for the p_{T}^{ℓ} distributions since the impact on the latter is only due to the hadronic recoil requirement in the signal selection. Of these uncertainties, 3 are two-sided uncertainties, while 4 (p_{T}^{ℓ}) and 33 (m_{T}) PCA variations are taken into account.

5 Physics corrections and uncertainties

5.1 Electroweak uncertainties

The dominant source of electroweak corrections to W-boson production originates from QED final-state radiation, and is simulated with PHOTOS. The effect of QED initial-state radiation (ISR) is also included through the PYTHIA 8 parton shower (PS). Other sources of electroweak corrections are not included in the simulated event samples, and their full effects are considered as systematic uncertainties. Systematic uncertainties from missing higher-order electroweak corrections are estimated considering the same sources of uncertainty as in Ref. [12]. An improvement of the present analysis is that the corresponding uncertainties are evaluated at detector level instead of generator level, which was a simplification used in the previous analysis as these are not leading uncertainties. The detector-level systematic variations are obtained by applying detector response and efficiency migration matrices derived from samples of simulated signal events described in Sect. 3.1. Their impact on m_W is larger than for generator-level variations by typically 20%.

5.2 QCD model and uncertainties

The rapidity, transverse momentum and decay distributions of the simulated W- and Z-boson samples are reweighted to include the effects of higher-order QCD corrections, which improves the agreement between the data and simulation. The differential cross section as a function of the boson rapidity, $\mathrm{d}\sigma(y)/\mathrm{d}y$, and the coefficients describing angular distributions of decay leptons, A_i [55], are calculated at $O(\alpha_s^2)$ in fixed-order QCD. The transverse-momentum spectrum at a given rapidity, $\mathrm{d}\sigma(p_\mathrm{T}, y)/(\mathrm{d}p_\mathrm{T}\,\mathrm{d}y) \cdot (\mathrm{d}\sigma(y)/\mathrm{d}y)^{-1}$, is modelled using the PYTHIA 8 MC generator, with parameters adjusted to reproduce the measured Z-boson p_T distribution at $\sqrt{s} = 7$ TeV [29]. The resulting tune, called AZ in the following, predicts W-boson p_T distributions that agree with measurements at $\sqrt{s} = 5.02$ and 13 TeV [56].

PDF uncertainties are calculated for the CT10, CT14, CT18, CT18A, MMHT2014, MSHT20, NNPDF3.1, NNPDF4.0 and ATLASpdf21 sets using the Hessian method [57], where each eigenvector of the PDF fit covariance matrix defines a pair of PDF uncertainty variations and a corresponding nuisance parameter in the PLH fit. The CT10, CT14, CT18 and CT18A variations correspond to 90% CL, and are rescaled to match the 68% CL. PDF uncertainty variations are constrained to leave the predicted p_T^Z distribution unchanged, propagating only the part of the PDF uncertainty in the p_T^W distribution that is uncorrelated to p_T^Z [12]. To achieve this, the impact of each PDF eigenvector on the p_T^W and p_T^Z distributions is calculated, and the corresponding uncertainty in the p_T^W distribution is defined from the ratio of the varied p_T^W and p_T^Z distributions. This procedure is equivalent to performing an explicit parton shower tune for each PDF variation but simpler in practice. The uncertainties in the AZ tune parameters are propagated separately as described below.

The PYTHIA 8 parton shower model contributes additional sources of uncertainty in the p_T^W distribution. The AZ tune parameters are assumed universal between Z- and W-boson production, and their uncertainties are propagated to the W-boson final-state distributions. The initial-state charm and bottom quark masses affect the p_T spectrum, and the corresponding uncertainties are estimated by varying their respective masses by ± 0.5 GeV and ± 0.8 GeV, respectively. Uncertainties in the shower evolution are parameterised through variations of the factorisation scale, μ_F, by factors of 0.5 and 2.0 with respect to the central choice $\mu_\mathrm{F}^2 = p_{\mathrm{T},0}^2 + p_\mathrm{T}^2$, where $p_{\mathrm{T},0}$ is an infrared cut-off, and p_T is the evolution variable of the parton shower [58]. The variations are applied independently to the light-quark, charm-quark and bottom-quark-induced processes, and are propagated considering only the relative impact on the p_T^W and p_T^Z distributions, as done for the PDF uncertainties. Differences between the PYTHIA 8 and HERWIG 7 predictions for this ratio were found to be negligible.

The accuracy of the next-to-next-to-leading-order (NNLO) predictions for the angular coefficients A_0–A_7 is validated by comparing to the corresponding measured values in Z-boson production [55]. The Z-boson data uncertainties are propagated to the W-boson predictions, which assumes that NNLO predictions have similar accuracy for the W- and Z-boson processes, and are validated within the experimental precision of the Z-boson data. The observed disagreement between data and prediction for the A_2 coefficient is taken as additional uncertainty. Similarly to some experimental uncertainties, random angular coefficient variations are treated with a PCA to produce uncorrelated two-sided uncertainties.

The effect of missing higher-order corrections on the NNLO predictions of the normalised rapidity distributions and the effect of the LHC beam-energy uncertainty of 0.65% were both found to be negligible.

6 Improved measurement of the W-boson mass

The improvements to the previous m_W measurement described in Sects. 3.4 and 3.5 are implemented in several steps. The impact of the analysis updates is evaluated using the same statistical method as in the previous measurement, and yields a change of the measured W-boson mass from $80{,}369.5 \pm 18.5$ MeV to $80{,}371.9 \pm 18.7$ MeV, corresponding to a shift of 2.4 MeV and a minimal increase of the total uncertainty. The analysis is then repeated using the CT10nnlo PDF set and unchanged systematic uncertainties but implementing the PLH approach. This provides a test of the stability of the measurement under the change of statistic used in the fit. The final step consists of updating the measurement to more recent PDF sets, one of which is used to define a new baseline.

6.1 Results with CT10nnlo and consistency tests

The PLH fits using the CT10nnlo PDF set are first performed with statistical uncertainties only. Excellent consistency with the previous results is obtained, which provides a basic validation for the technical aspects of the fit. The comparison is repeated for fits including all systematic uncertainties, with the results summarised in Fig. 2. The results of the PLH fits combining all categories yield $m_W = 80{,}357.0 \pm 15.8$ MeV and $m_W = 80{,}388.2 \pm 23.8$ MeV for the p_T^ℓ and m_T distributions, respectively. Compared to the original ATLAS measurement, this corresponds to shifts of m_W of -12.4 MeV and $+12.5$ MeV, respectively, while the total uncertainties are reduced by about 3 MeV due to the profiling of some sys-

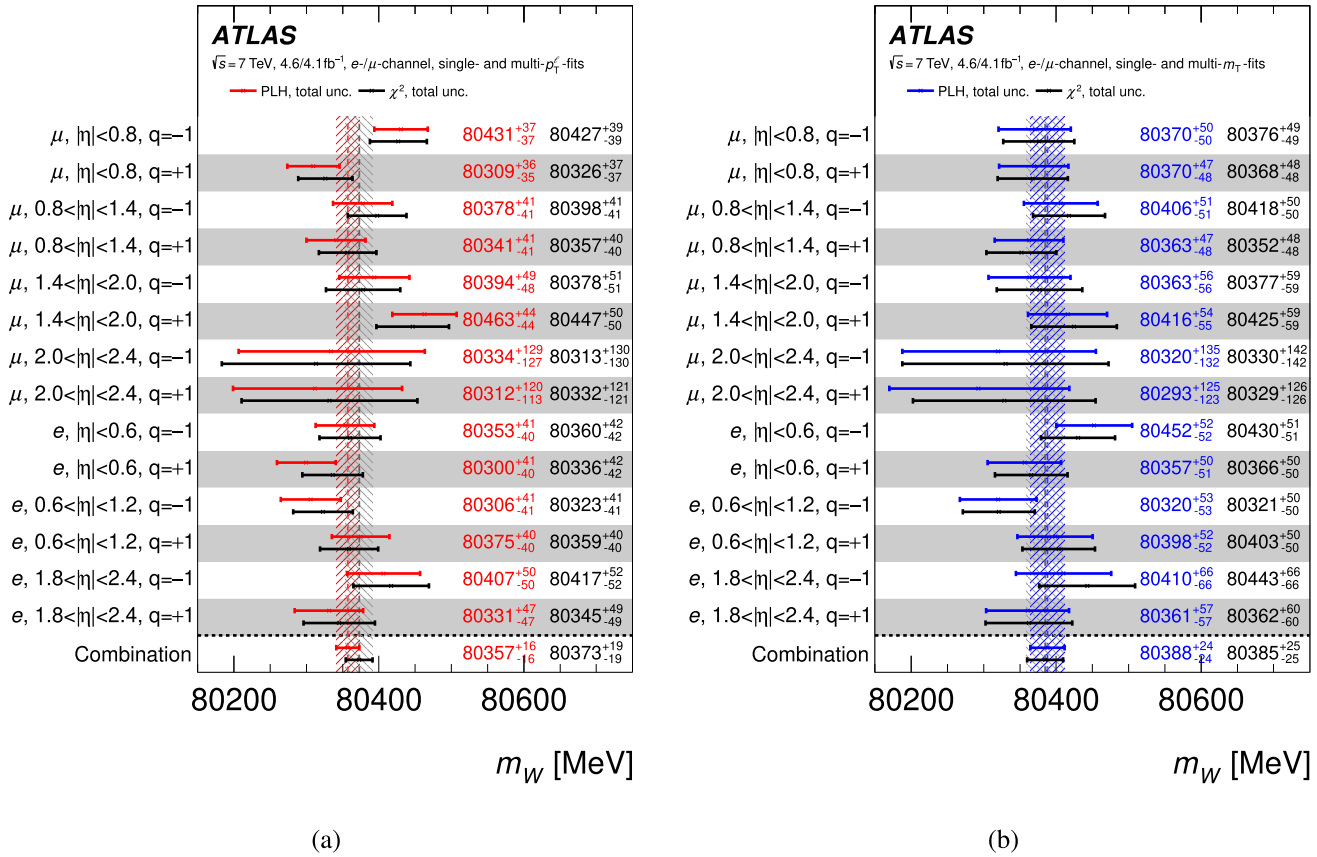

Fig. 2 Overview of the m_W fit results in all categories for the **a** p_{T}^{ℓ} and **b** m_{T} distributions, with the CT10nnlo PDF set, where q denotes the charge of the decay lepton. The results of the PLH fit are compared with the χ^2 fit, where systematic uncertainties are propagated using the offset method [12]. The points labelled as 'Combination' correspond to the result of a joint PLH fit to all categories and to a combination of individual χ^2 fits

tematic uncertainties. Repeating the present analysis with the fit range used in Ref. [12] increases the difference by 3 MeV.

The compatibility between the present and previous results is tested by repeating the PLH fits for an ensemble of models where the preferred values of the nuisance parameters are varied randomly within their pre-fit uncertainties. As shown in Fig. 3, the spread of fit results from pseudo-experiments with varied nuisance parameters is about 16 MeV, confirming that the change in central value introduced by the new statistical method corresponds to about one standard deviation. The distribution of the nuisance parameter pulls[2] is consistent with a normal distribution, indicating an overall correct estimate of the pre-fit uncertainties.

[2] For a given nuisance parameter θ, the pull is defined as $\hat{\theta}/\sqrt{1-\sigma_{\hat{\theta}}}$, where $\hat{\theta}$ and $\sigma_{\hat{\theta}}$ are the nuisance parameter post-fit value and uncertainty, respectively.

6.2 Impact of updated parton distribution functions

The impact of a change in the PDFs on the final state distributions is evaluated using POWHEG, both to calculate the extrapolation from the central CT10nnlo set to CT14, CT18, CT18A, MMHT2014, MSHT20, NNPDF3.1, NNPDF4.0 and ATLASpdf21, and to calculate the PDF uncertainty variations. All calculations are performed at generator level in full phase space, and the impact on the final-state distributions is evaluated using migration matrices as in Sect. 5.1. As in Sect. 5.2, the PDF extrapolations are constrained to leave p_{T}^{Z} unchanged. The impact of the extrapolations on the detector-level p_{T}^{ℓ} distributions is illustrated in Fig. 4.

6.3 Results and discussion

Fit results with updated PDF sets are listed in Table 2. A satisfactory fit quality is obtained for all PDF sets. Separate fits are performed to the p_{T}^{ℓ} and m_{T} distributions as they are projections of the same data, and the corresponding statistical correlations cannot be accounted for in the frame-

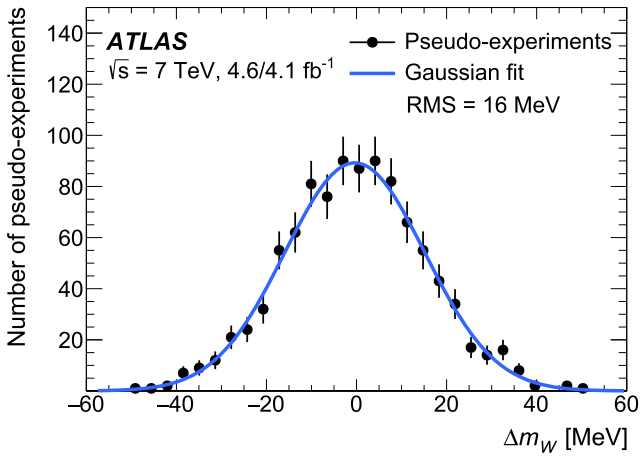

(a)

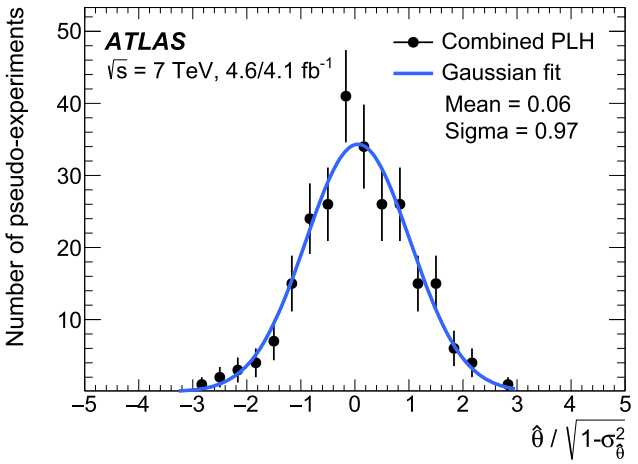

(b)

Fig. 3 **a** Distribution of the difference Δm_W between the nominal m_W PLH fit result and results obtained for pseudo-experiments using random variations of the sources of systematic uncertainty. The p_{T}^{ℓ} distribution is used. **b** Distribution of pull significances for the NPs in the combined PLH fit to the p_{T}^{ℓ} distribution

work of Eq. (1) in a straightforward way. Moreover, the PCA treatment applied for some classes of systematic uncertainties leads to different sets of nuisance parameters for the two distributions.

The best-fit values of m_W obtained with different PDF sets span a range of about 18 MeV for the p_{T}^{ℓ} fits, and about 42 MeV for the m_{T} fits. This envelope is dominated by the NNPDF3.1 and NNPDF4.0 fits, which yield the lowest fit values; the range spanned by the other sets is only 9 MeV for p_{T}^{ℓ} and 21 MeV for m_{T}.

As a cross-check, the influence of the size of the initial PDF uncertainties on the best-fit values is studied in Fig. 5, where the fits are repeated with pre-fit PDF uncertainties scaled by factors 1–3. Enlarged uncertainties allow the models to better adapt to the data, resulting in a reduced PDF model dependence. The differences between the central values found for five out of six PDF sets significantly decrease with larger PDF scaling factors. For factors of 2 and above, the residual model dependence is below 5 MeV for the p_{T}^{ℓ} fits, and 25 MeV for the m_{T} fits, with the total uncertainty increased by less than 1.5 MeV.

The baseline result is defined using CT18 with original uncertainties, which is compatible with the previous exercise and yields the most conservative uncertainty among the PDF sets considered except for ATLASpdf21. CT18 is also the only recent PDF set that does not include the W- and Z-boson cross sections measured by ATLAS at 7 TeV [33], which represent the same data as those used in the present analysis. The results for all measurement categories and for the CT18 PDF set are summarised in Fig. 6. The post-fit, $|\eta|$-inclusive p_{T}^{ℓ} distributions obtained with CT18 are shown in Fig. 7, and agree with the data within the uncertainties. Similarly to CT10nnlo, the distribution of the nuisance parameter pulls is consistent with a normal distribution.

The compatibility of the results for m_W in the different measurement categories is verified by repeating the fit assuming independent parameters of interest in each category. The differences to the baseline fit are small compared with the measurement uncertainties. As a further cross-check, partial fits are performed to the electron and muon channels separately. The electron and muon fit results are found to agree within one standard deviation. A similar exercise is performed for the W^+ and W^- channels, and the same conclusion is obtained. Finally, the dependence of the fit result on the p_{T}^{ℓ} and m_{T} ranges used for the fit is shown in Fig. 8, with good stability.

Figure 9 summarises the ten nuisance parameters that induce the largest shift of m_W in fits to the p_{T}^{ℓ} and m_{T} distributions. They are related to electron and muon calibration uncertainties, to the uncertainty in charm-induced production for the p_{T}^{W} description, to specific eigenvectors (EV) of the CT18 PDF set, and to missing higher-order electroweak corrections. The corresponding nuisance parameter pulls are also shown. By construction, the PLH fits induce shifts of the nuisance parameters from their nominal value and significant deviations would indicate an underestimation of systematic uncertainties. All observed pulls are within the expectation.

While uncertainties in the PDFs and in the AZ tune parameters have well defined confidence intervals and can be treated as nuisance parameters, this is more questionable for the other uncertainties in the W-boson p_{T} distribution, i.e., the factorisation scale and quark-mass variations. It was verified that the impact of the latter on the final-state distributions is very similar, in shape, to that of the AZ tune parameters,

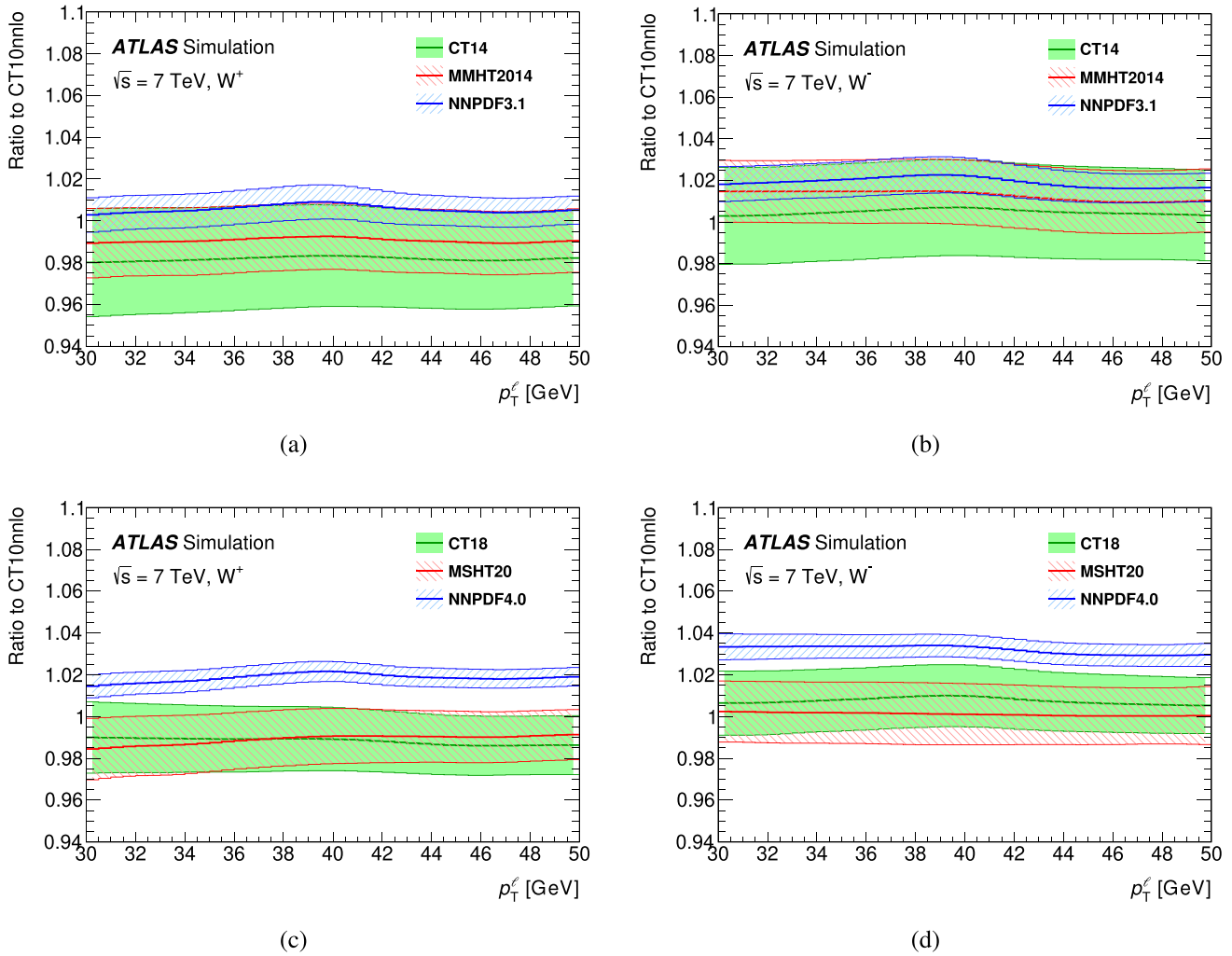

Fig. 4 Relative effect, with respect to CT10nnlo, of the indicated PDF extrapolations on the detector-level, η-inclusive p_{T}^{ℓ} distributions in **a**,**c** W^+ events and **b**,**d** W^- events. The thick lines show the central PDF set, and the envelopes show the associated 68% CL uncertainty

Table 2 Best-fit value of m_W, total and PDF uncertainties, in MeV, and goodness-of-fit for the p_{T}^{ℓ} and m_{T} distributions and the PDF sets described in the text. Each fit uses 14 event categories with 40 bins, for 558 degrees of freedom

PDF set	p_{T}^{ℓ} fit				m_{T} fit			
	m_W	σ_{tot}	σ_{PDF}	χ^2/n.d.f.	m_W	σ_{tot}	σ_{PDF}	χ^2/n.d.f.
CT14	80,358.3	$^{+16.1}_{-16.2}$	4.6	543.3/558	80,401.3	$^{+24.3}_{-24.5}$	11.6	557.4/558
CT18	80,362.0	$^{+16.2}_{-16.2}$	4.9	529.7/558	80,394.9	$^{+24.3}_{-24.5}$	11.7	549.2/558
CT18A	80,353.2	$^{+15.9}_{-15.8}$	4.8	525.3/558	80,384.8	$^{+23.5}_{-23.8}$	10.9	548.4/558
MMHT2014	80,361.6	$^{+16.0}_{-16.0}$	4.5	539.8/558	80,399.1	$^{+23.2}_{-23.5}$	10.0	561.5/558
MSHT20	80,359.0	$^{+13.8}_{-15.4}$	4.3	550.2/558	80,391.4	$^{+23.6}_{-24.1}$	10.0	557.3/558
ATLASpdf21	80,362.1	$^{+16.9}_{-16.9}$	4.2	526.9/558	80,405.5	$^{+28.2}_{-27.7}$	13.2	544.9/558
NNPDF3.1	80,347.5	$^{+15.2}_{-15.7}$	4.8	523.1/558	80,368.9	$^{+22.7}_{-22.9}$	9.7	556.6/558
NNPDF4.0	80,343.7	$^{+15.0}_{-15.0}$	4.2	539.2/558	80,363.1	$^{+21.4}_{-22.1}$	7.7	558.8/558

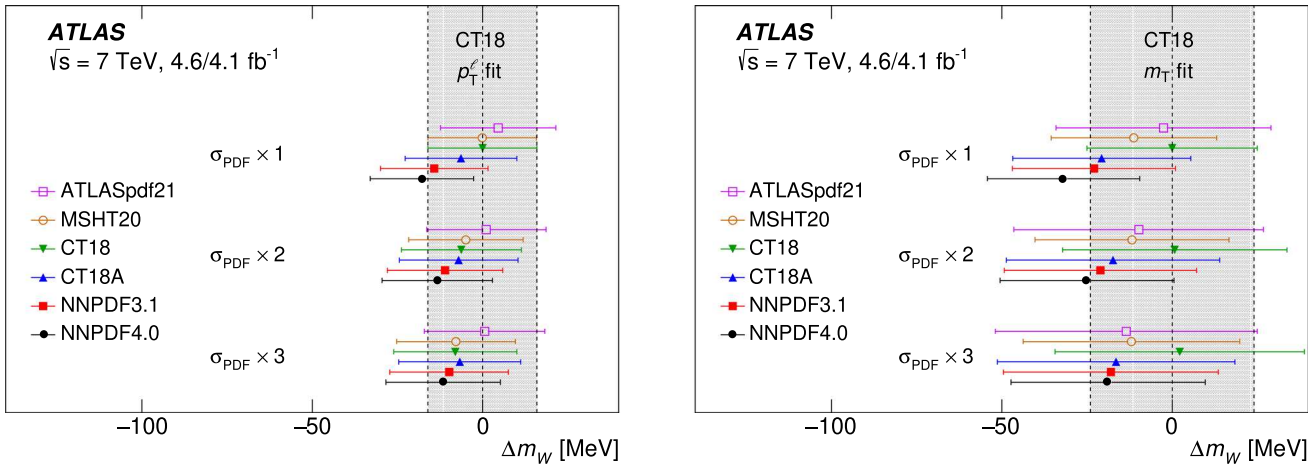

Fig. 5 Variation of the fitted value of m_W with the PDF set used in the fit, for the **a** p_{T}^{ℓ} and **b** m_{T} distributions and different scalings of the pre-fit PDF uncertainties. The reference value is defined by the CT18 PDF set

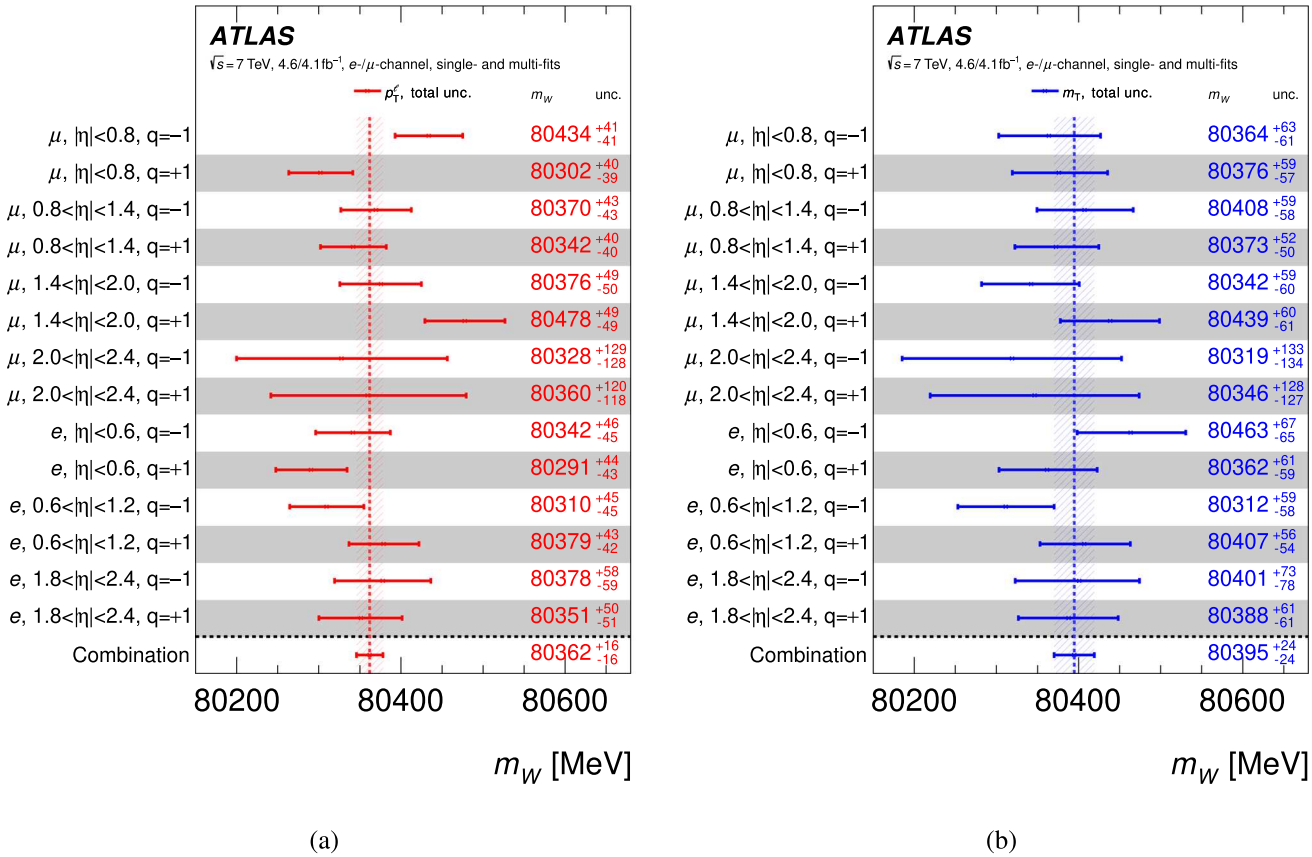

Fig. 6 Overview of the m_W PLH fit results in all categories for the **a** p_{T}^{ℓ} and **b** m_{T} distributions, with the CT18 PDF set. The points labelled as 'Combination' correspond to the result of a joint PLH fit to all categories

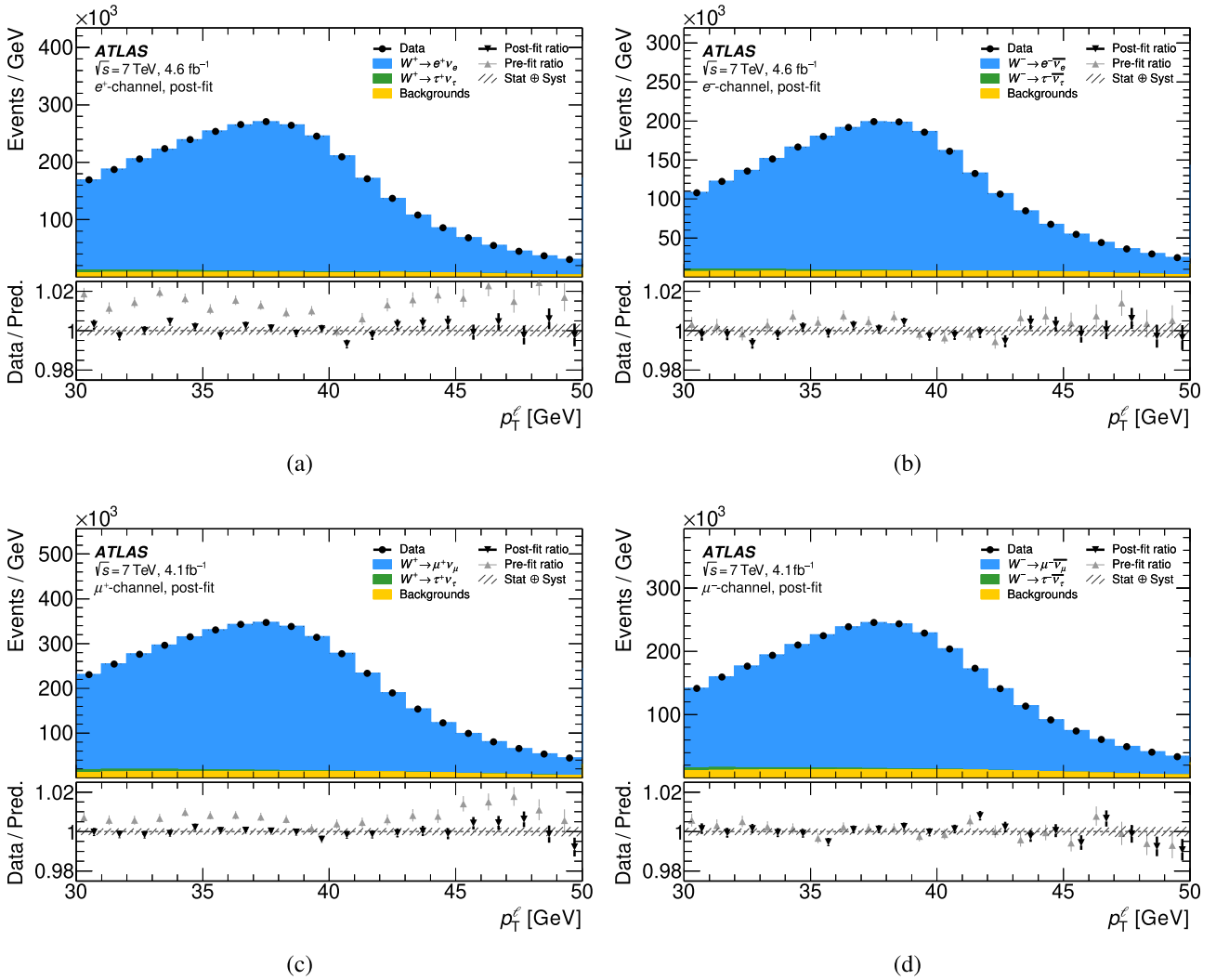

Fig. 7 Post-fit distributions of p_{T}^{ℓ} with data and MC for **a** $W^+ \to e^+\nu_e$, **b** $W^- \to e^-\overline{\nu}_e$, **c** $W^+ \to \mu^+\nu_\mu$ and **d** $W^- \to \mu^-\overline{\nu}_\mu$, inclusive over all η regions, and using the CT18 PDF set. In the bottom panels, the darker points represent the post-fit ratio of data to MC, while the lighter points indicate the ratio before the fit. The hatched band represents the total uncertainty of the data

and that these effects are thus not different from the other sources of uncertainty in this respect, and can be treated accordingly. The small post-fit value of the corresponding uncertainty is due to the strong discrimination between the effects of m_W and p_{T}^W variations on the p_{T}^{ℓ} distribution.

6.4 Combination

All event categories are statistically independent as long as only the p_{T}^{ℓ} or only the m_{T} distributions are considered. The correlation between the final p_{T}^{ℓ}- and m_{T}-based results for m_W is determined from an ensemble of fit results obtained by fluctuating the data and the most probable values of the nuisance parameters within their respective uncertainties. The p_{T}^{ℓ} and m_{T} results are then combined using the BLUE prescription [59]. The results of this procedure are given in Table 3. The weight of the p_{T}^{ℓ} fit ranges from 86% to 97%, depending on the PDF set, and dominates the final result. For the CT18 PDF set, the final result is:

$$\begin{aligned} m_W &= 80{,}366.5 \pm 9.8\ (\text{stat.}) \pm 12.5\ (\text{syst.})\ \text{MeV} \\ &= 80{,}366.5 \pm 15.9\ \text{MeV}, \end{aligned}$$

where the first uncertainty component is statistical and the second corresponds to the total systematic uncertainties.

The decomposition of the post-fit uncertainties is performed according to Ref. [51] and shown in Table 4. Statistical uncertainties contribute about 10 MeV in the present fit. This is in contrast with 6 MeV obtained from fits considering statistical uncertainties only, with all nuisance parameters fixed to their best-fit values. The increase reflects the

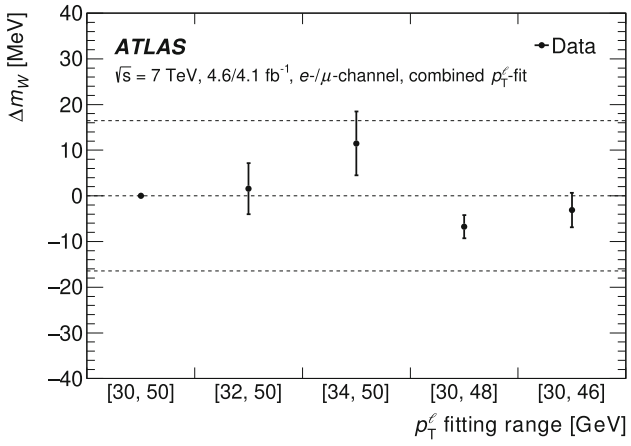

(a)

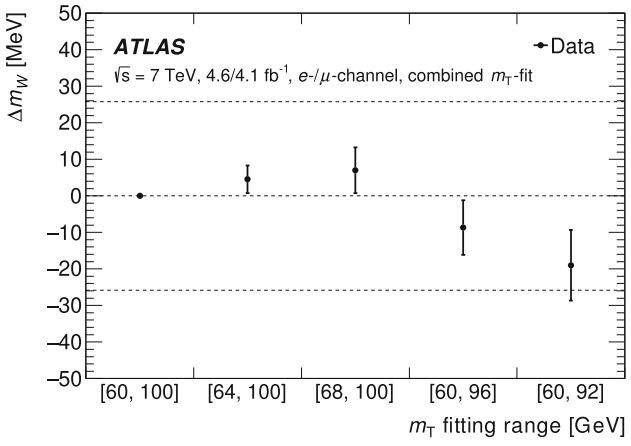

(b)

Fig. 8 Difference Δm_W between the W-boson mass measured using the **a** p_{T}^{ℓ} and **b** m_{T} distribution fit ranges indicated in the figure and the nominal fit range. The nominal ranges are $30 < p_{\mathrm{T}}^{\ell} < 50$ GeV and $60 < m_{\mathrm{T}} < 100$ GeV, respectively. The outer dashed lines indicate the total measurement uncertainty for the nominal range. Results are shown for the combined fit over all categories, and for the CT18 PDF set

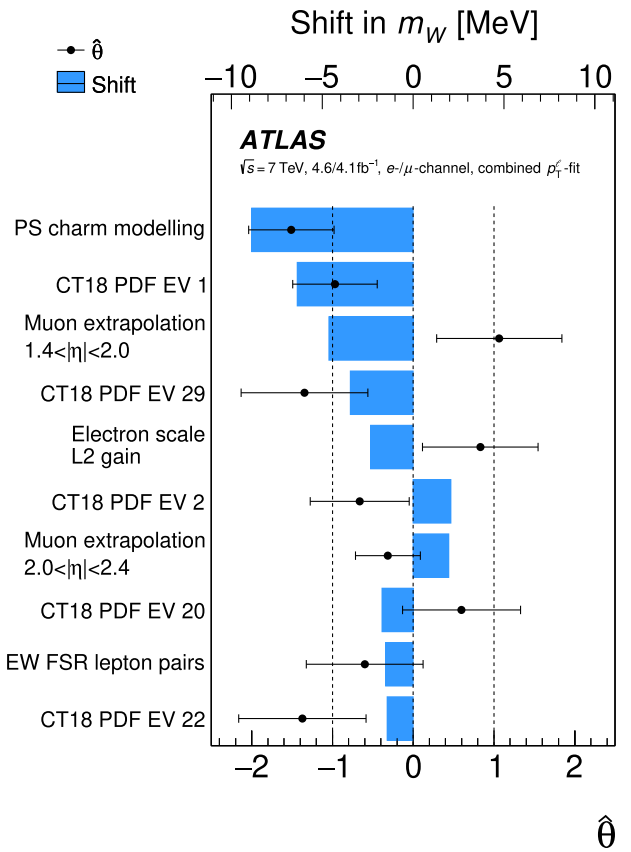

(a)

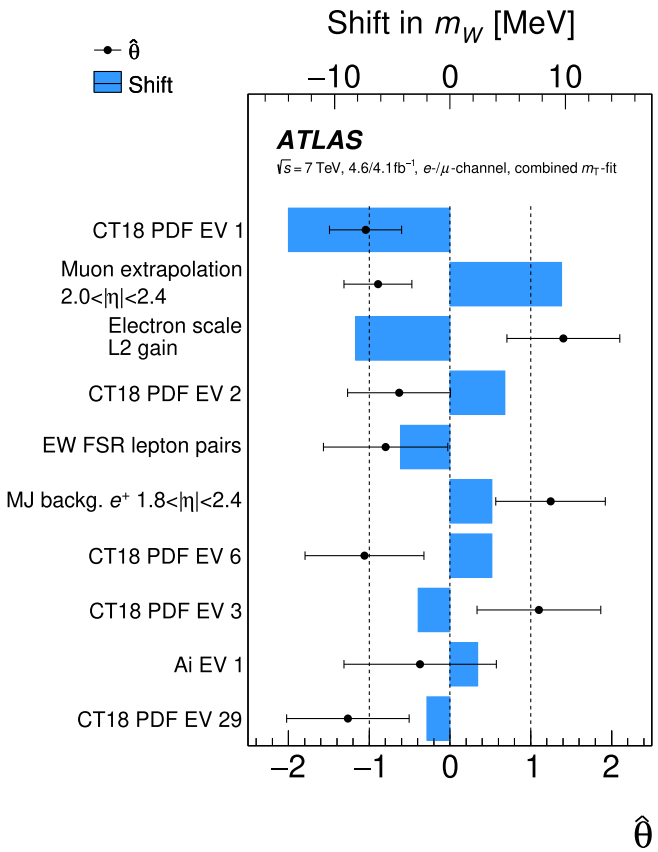

(b)

Fig. 9 The ten nuisance parameters inducing the largest shifts on the fitted value of m_W in the combined PLH fits, using the **a** p_{T}^{ℓ} and **b** m_{T} distributions and the CT18 PDF set. For a given NP θ, the shift is defined as the product of its post-fit value $\hat{\theta}$ and its pre-fit impact on m_W. The points, which are plotted according to the bottom horizontal scale, show $\hat{\theta}$ for each of the nuisance parameters. The error bars show the corresponding post-fit uncertainties, $\sigma_{\hat{\theta}}$. The nuisance parameters are ranked according to the shift induced on m_W, the NPs with the largest shifts at the top

Table 3 Uncertainty correlation between the p_{T}^{ℓ} and m_{T} fits, combination weights and combination results for m_W and the indicated PDF sets

PDF set	Correlation	Weight (p_{T}^{ℓ})	Weight (m_{T})	Combined m_W [MeV]
CT14	52.2%	88%	12%	80,363.6 ± 15.9
CT18	50.4%	86%	14%	80,366.5 ± 15.9
CT18A	53.4%	88%	12%	80,357.2 ± 15.6
MMHT2014	56.0%	88%	12%	80,366.2 ± 15.8
MSHT20	57.6%	97%	3%	80,359.3 ± 14.6
ATLASpdf21	42.8%	87%	13%	80,367.6 ± 16.6
NNPDF3.1	56.8%	89%	11%	80,349.6 ± 15.3
NNPDF4.0	59.5%	90%	10%	80,345.6 ± 14.9

larger number of parameters determined from the same data. Correspondingly, the systematic uncertainty components are smaller than systematic 'impacts' conventionally reported for PLH fits.[3] Systematic uncertainties contribute about 13 MeV, dominated by PDF uncertainties, missing higher-order electroweak corrections, and electron and muon calibration uncertainties.

The fits are performed assuming the SM value for the W-boson width, $\Gamma_W^{\mathrm{SM}} = 2088 \pm 1$ MeV [6]. The fitted value of m_W varies with the assumed value for Γ_W following $\Delta m_W = -0.06\,\Delta\Gamma_W$. Assuming an alternate SM prediction of $\Gamma_W^{\mathrm{SM}} = 2091 \pm 1$ MeV, as obtained in Ref. [7], does not change the measured value of the W-boson mass significantly.

The compatibility of the measured value of the W-boson mass using the CT18 PDF set with the Standard Model expectation is illustrated in Fig. 10a, together with selected previous measurements. The two-dimensional 68% and 95% confidence limits for the predictions of m_W and m_t in the context of the Standard Model electroweak fit are shown in Fig. 10b, and are compared to the present measurement of m_W and to the combined value of the LHC top-quark mass determinations at 7 and 8 TeV [60].

7 Measurement of the W-boson width

7.1 Overview

The p_{T}^{ℓ} and m_{T} distributions are not only sensitive to m_W but also to Γ_W, as shown in Fig. 1. In particular, the high tails of the p_{T}^{ℓ} and m_{T} distributions are sensitive to changes of Γ_W. The fit to the m_{T} distribution is expected to be more sensitive, because events with high m_{T} are more likely to come from the tail of the W-boson Breit–Wigner distribution than events with high p_{T}^{ℓ}. The measurement of Γ_W relies on the same statistical framework, the same calibration, and the same distributions as the previously presented measurement of m_W. However, Γ_W is left free in the fit, while the W-boson mass is treated as NP and set to its SM expectation within the global electroweak fit, $m_W^{\mathrm{SM}} = 80{,}355 \pm 6$ MeV [6]. The templates are generated with different values of Γ_W, centred around the reference value used in the Monte Carlo signal samples. All results are obtained using the same fit ranges as in the m_W measurement: $60 < m_{\mathrm{T}} < 100$ GeV and $30 < p_{\mathrm{T}}^{\ell} < 50$ GeV. The choice of fitting range is driven by the uncertainties in the lepton performance and the hadronic recoil.

7.2 Results and discussion

The results for each measurement category including all systematic uncertainties for the CT18 PDF set are summarised in Fig. 11 yielding the values of $\Gamma_W = 2221^{+68}_{-76}$ MeV and $\Gamma_W = 2200^{+47}_{-48}$ MeV for p_{T}^{ℓ} and m_{T} distributions respectively. Good agreement between the categories can be observed.

Contrary to m_W, the fitted value of Γ_W depends more strongly on the assumed value of the mass. The fitted value of Γ_W varies with the assumed value for m_W following $\Delta\Gamma_W = -1.25\,\Delta m_W$. In the Standard Model, the predicted value of m_W mainly depends on the assumed value of m_t. The present result is based on Ref. [6], which uses $m_t = 172.6$ GeV and is close to the LHC combined value used in Fig. 10b. Using $m_t = 171.8$ GeV [62] or $m_t = 173.1$ GeV [63] yields $m_W^{\mathrm{SM}} = 80{,}350$ MeV or 80,360 MeV, respectively, with corresponding variations of Γ_W by ±6 MeV.

The impact of different PDF sets (CT14, CT18, CT18A, MMHT2014, MSHT20, ATLASpdf21, NNPDF3.1, NNPDF4.0) on the Γ_W measurement is also studied. The results of full fits for all considered PDF sets are summarised in Table 5, with again a satisfactory fit quality for all PDF sets. The PDF dependence of the fit result is weaker than for m_W, and all central values are well within the uncertainties obtained with CT18. The CT18 PDF set is chosen for the baseline result, consistently with the m_W measurement.

[3] Impacts are obtained from the quadratic subtraction between the total fit uncertainty and the uncertainty of a fit with selected nuisance parameters removed and overestimate the genuine systematic uncertainty.

Table 4 Uncertainty components for the p_{T}^{ℓ}, m_{T} and combined m_W measurements using the CT18 PDF set. The first columns give the total, statistical and overall systematic uncertainty in the measurements. The following columns show the contributions of modelling and experimental systematic uncertainties, grouped into categories

Unc. [MeV]	Total	Stat.	Syst.	PDF	A_i	Backg.	EW	e	μ	u_{T}	Lumi	Γ_W	PS
p_{T}^{ℓ}	16.2	11.1	11.8	4.9	3.5	1.7	5.6	5.9	5.4	0.9	1.1	0.1	1.5
m_{T}	24.4	11.4	21.6	11.7	4.7	4.1	4.9	6.7	6.0	11.4	2.5	0.2	7.0
Combined	15.9	9.8	12.5	5.7	3.7	2.0	5.4	6.0	5.4	2.3	1.3	0.1	2.3

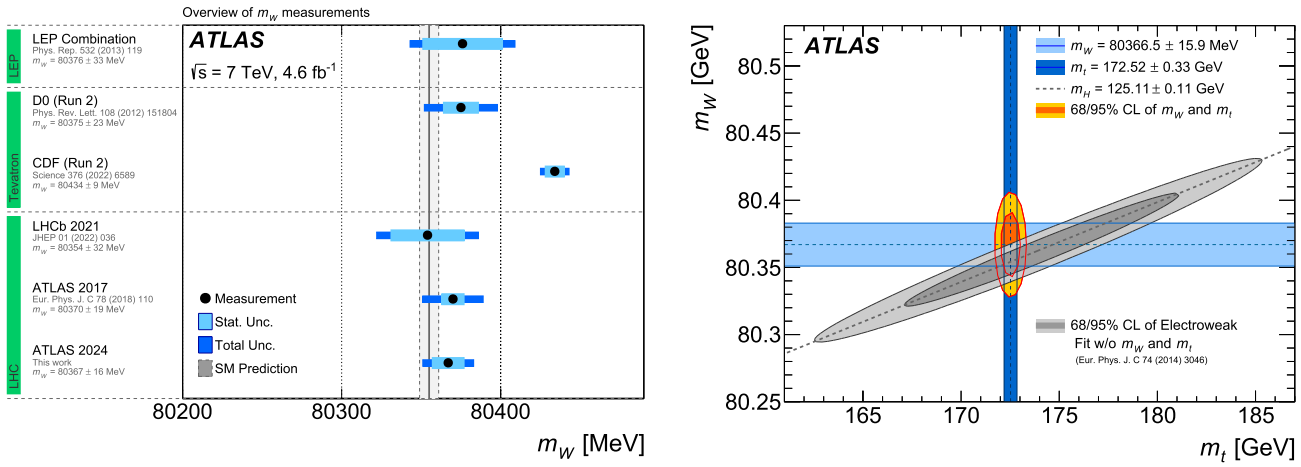

(a) (b)

Fig. 10 **a** Present measured value of m_W, compared to SM prediction from the global electroweak fit [6], and to the measurements of LEP [10], Tevatron [18,19] and the LHC [12,13]. **b** The 68% and 95% confidence level contours of the m_W and m_t indirect determinations from the global electroweak fit [7], compared to the 68% and 95% confidence-level contours of the present ATLAS measurement of m_W, the ATLAS measurement of m_H [61] and the LHC measurement of m_t [60]

Table 5 Best-fit value of Γ_W, total and PDF uncertainties, in MeV, and goodness-of-fit for the p_{T}^{ℓ} and m_{T} distributions and the PDF sets described in the text. Each fit uses 14 event categories with 40 bins, for 558 degrees of freedom

PDF set	p_{T}^{ℓ} fit				m_{T} fit			
	Γ_W	σ_{tot}	σ_{PDF}	χ^2/n.d.f.	Γ_W	σ_{tot}	σ_{PDF}	χ^2/n.d.f.
CT14	2228	$^{+67}_{-83}$	24	550.0/558	2202	$^{+48}_{-48}$	5	556.8/558
CT18	2221	$^{+68}_{-76}$	21	534.5/558	2200	$^{+47}_{-48}$	5	548.8/558
CT18A	2207	$^{+68}_{-75}$	18	533.0/558	2181	$^{+47}_{-48}$	5	550.6/558
MMHT2014	2155	$^{+71}_{-78}$	19	546.0/558	2186	$^{+48}_{-48}$	5	562.2/558
MSHT20	2206	$^{+66}_{-79}$	15	556.5/558	2179	$^{+47}_{-48}$	4	559.4/558
ATLASpdf21	2213	$^{+67}_{-73}$	18	531.3/558	2190	$^{+47}_{-48}$	6	545.6/558
NNPDF31	2203	$^{+65}_{-78}$	20	531.7/558	2180	$^{+47}_{-47}$	6	560.4/558
NNPDF40	2182	$^{+69}_{-68}$	12	550.5/558	2184	$^{+47}_{-47}$	4	564.0/558

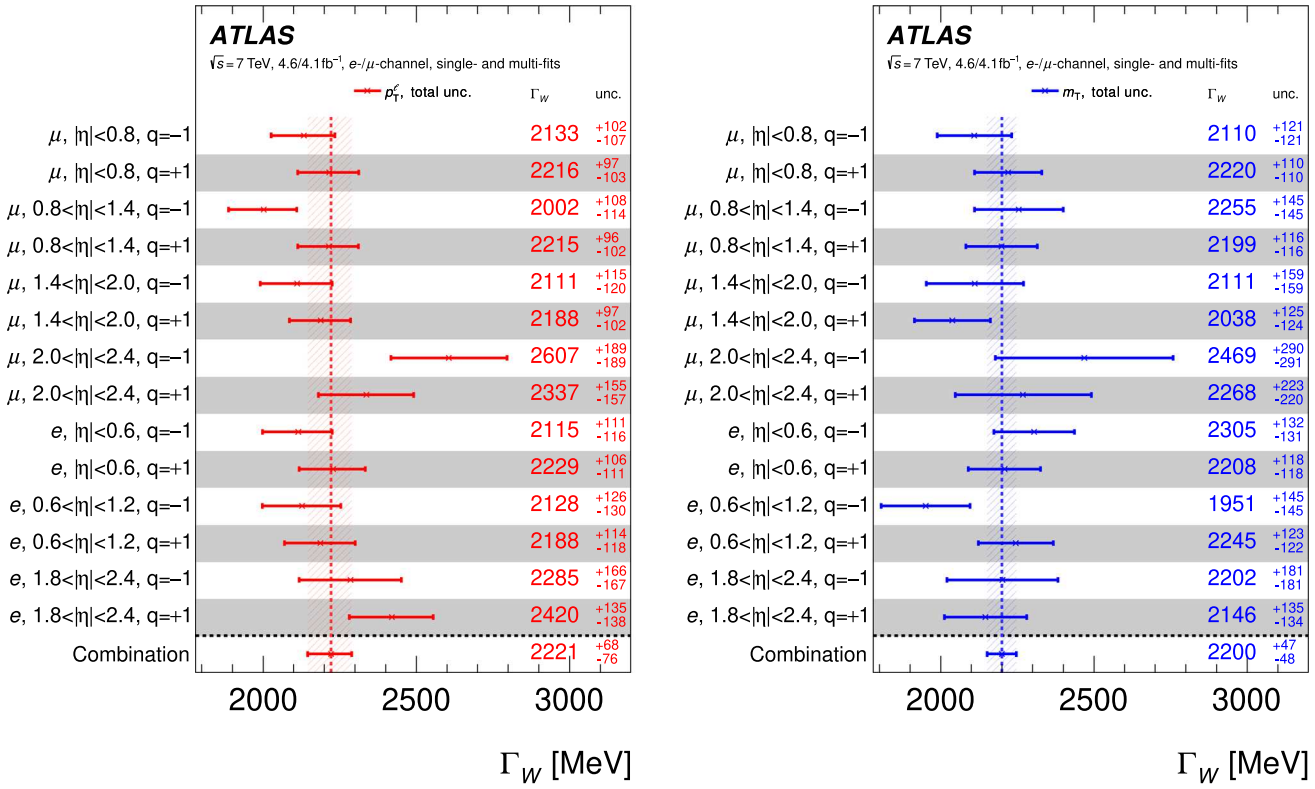

Fig. 11 Overview of the Γ_W PLH fit results in all categories for the **a** p_{T}^{ℓ} and **b** m_{T} distributions, with the CT18 PDF set. The points labelled as 'Combination' correspond to the result of a joint PLH fit to all categories

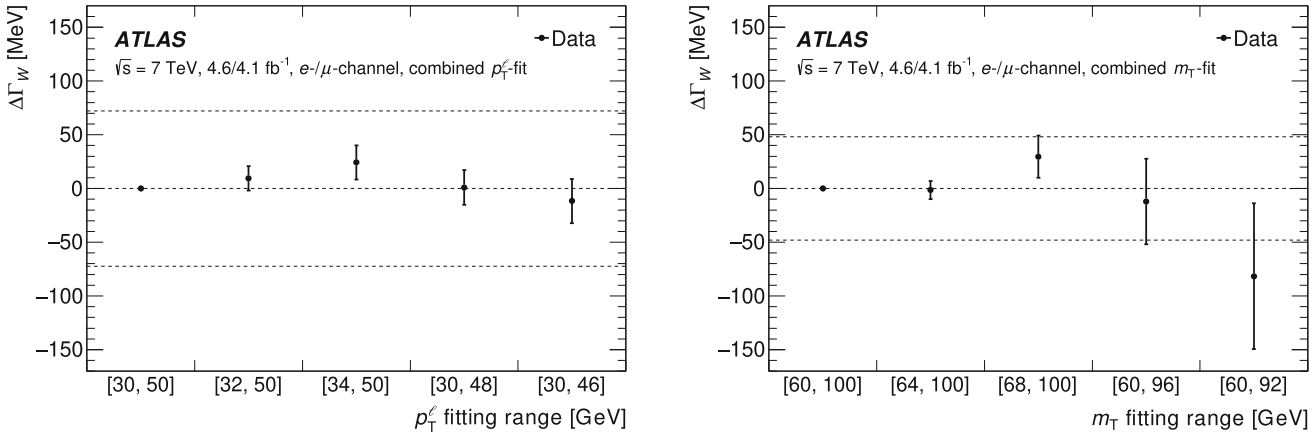

Fig. 12 Difference $\Delta\Gamma_W$ between the W-boson width measured using the **a** p_{T}^{ℓ} and **b** m_{T} distribution fit ranges indicated in the figure and the nominal fit range. The nominal ranges are $30 < p_{\mathrm{T}}^{\ell} < 50$ GeV and $60 < m_{\mathrm{T}} < 100$ GeV, respectively. The outer dashed lines indicate the total measurement uncertainty for the nominal range. Results are shown for the combined fit over all categories, and for the CT18 PDF set

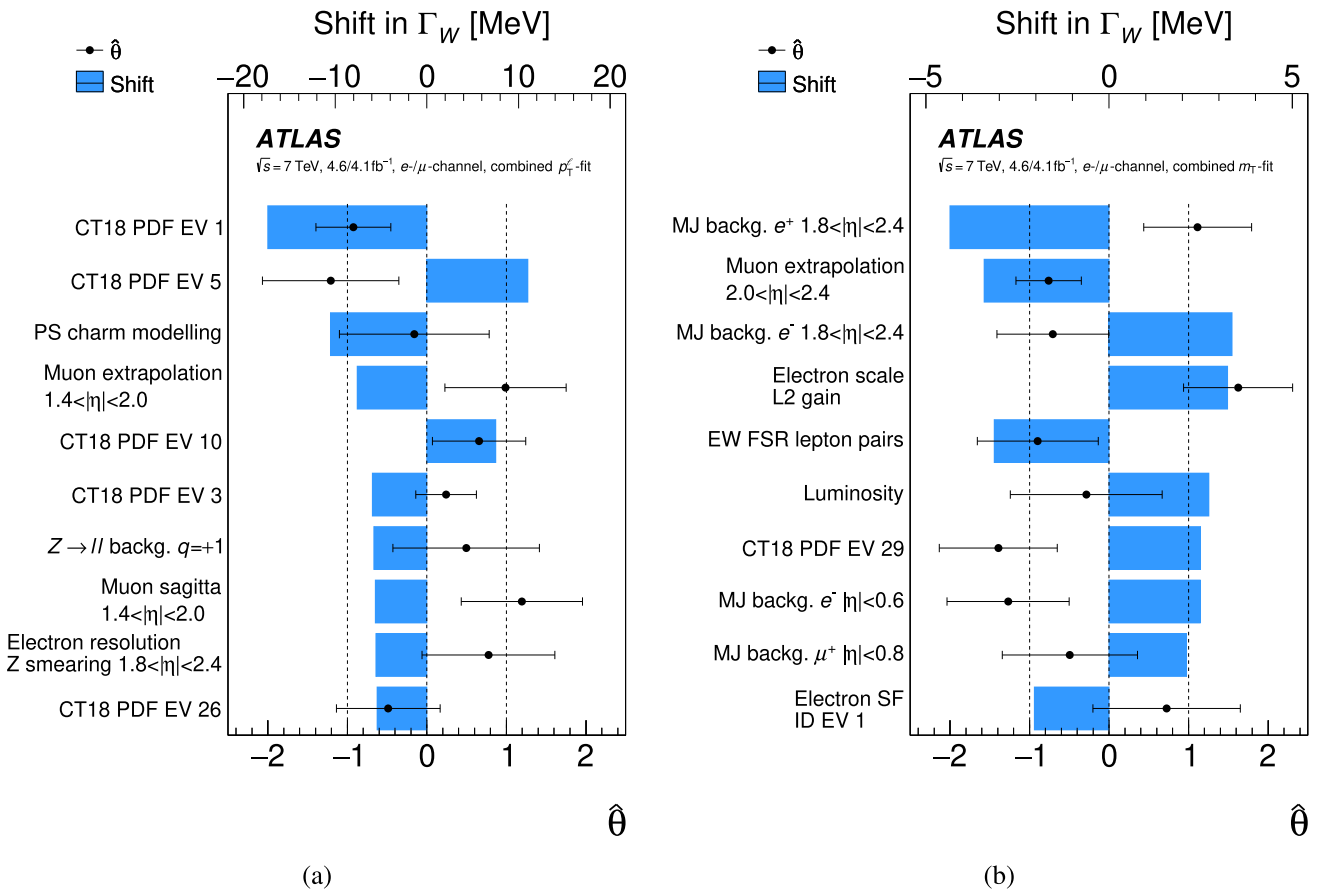

Fig. 13 The ten nuisance parameters inducing the largest shifts on the fitted value of Γ_W in the combined PLH fits, using the **a** p_T^ℓ and **b** m_T distributions and the CT18 PDF set. For a given NP θ, the shift is defined as the product of its post-fit value $\hat{\theta}$ and its pre-fit impact on Γ_W. The points, which are plotted according to the bottom horizontal scale, show $\hat{\theta}$ for each of the nuisance parameters. The error bars show the corresponding post-fit uncertainties, $\sigma_{\hat{\theta}}$. The nuisance parameters are ranked according to the shift induced on Γ_W, the NPs with the largest shifts at the top

Table 6 Uncertainty components for the p_T^ℓ, m_T and combined Γ_W measurements using the CT18 PDF set. The first columns give the total, statistical and overall systematic uncertainty in the measurements. The following columns show the contributions of modelling and experimental systematic uncertainties, grouped into categories

Unc. [MeV]	Total	Stat.	Syst.	PDF	A_i	Backg.	EW	e	μ	u_T	Lumi	m_W	PS
p_T^ℓ	72	27	66	21	14	10	5	13	12	12	10	6	55
m_T	48	36	32	5	7	10	3	13	9	18	9	6	12
Combined	47	32	34	7	8	9	3	13	9	17	9	6	18

As a check of compatibility, partial fits are performed to the electron and muon channels separately. These fit results are found to agree within one standard deviation. Similarly, separate fits are performed in the W^+ and W^- channels. The results for the two charges are consistent within the 68% CL contour of the two-dimensional likelihood function for the m_T fits, while for the p_T^ℓ fits the consistency between the two charges is within two standard deviations. Finally, the dependence of the measurement result on the m_T and p_T^ℓ ranges used for the fit is studied in Fig. 12, with stable results.

Figure 13 summarises the ten nuisance parameters that induce the largest shift of Γ_W in fits to the p_T^ℓ and m_T distributions. The largest shifts are related to the multijet (MJ) background, to the lepton calibration, to specific eigenvectors of the CT18 PDF set, to the luminosity, and to the uncertainty in charm-induced production for the p_T^W description.

The decomposition of post-fit uncertainties is done with the same method as in the m_W measurement, see Sect. 6.4. A summary of the uncertainties contributed by various sources is given in Table 6. The measurement is dominated by systematic uncertainties for the p_T^ℓ distribution, while for the

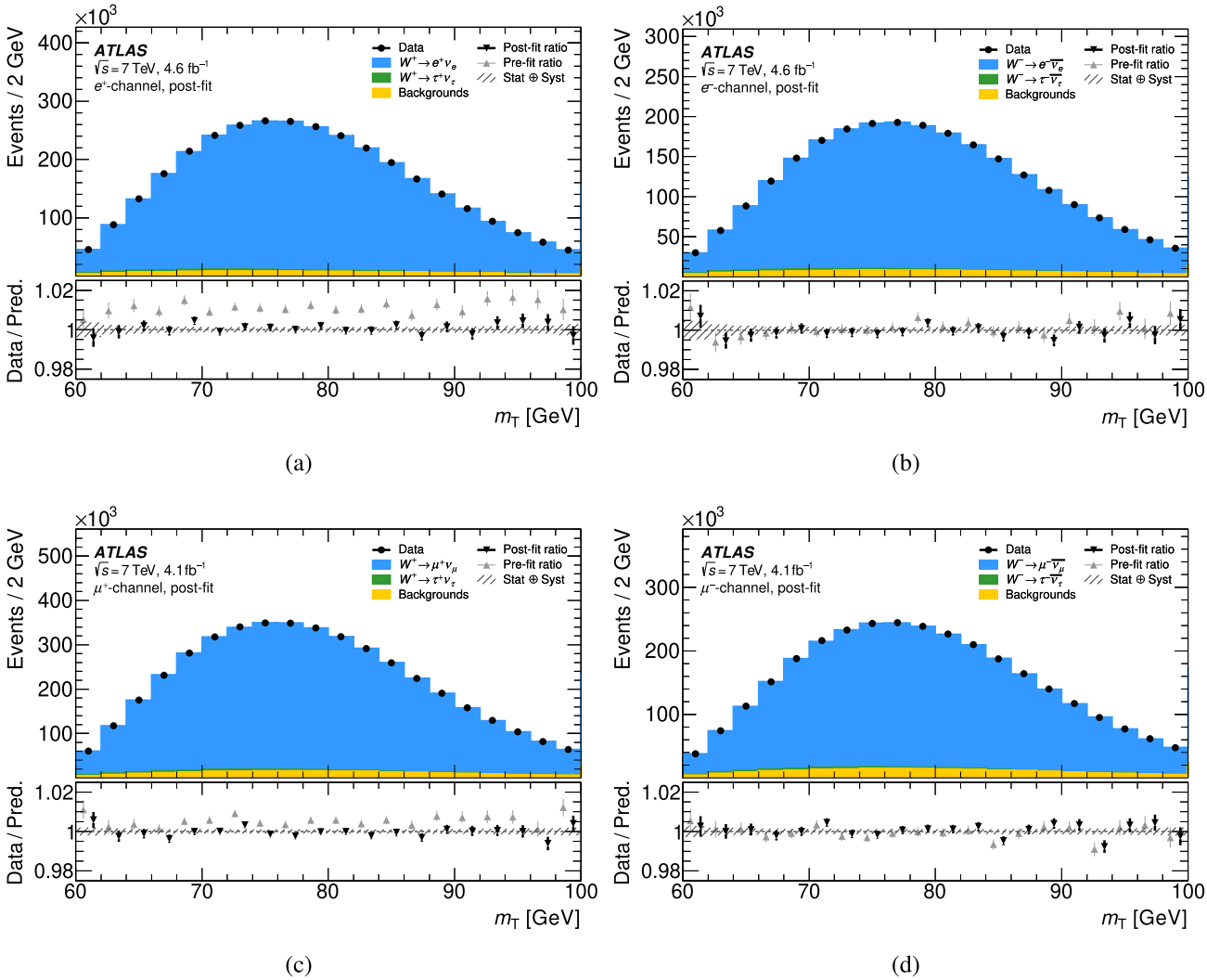

Fig. 14 Post-fit distributions of m_{T} with data and MC for **a** $W^+ \to e^+\nu_e$, **b** $W^- \to e^-\overline{\nu}_e$, **c** $W^+ \to \mu^+\nu_\mu$ and **d** $W^- \to \mu^-\overline{\nu}_\mu$, inclusive over all η regions, and using the CT18 PDF set. In the bottom panels, the darker points represent the post-fit ratio of data to MC, while the lighter points indicate the ratio before the fit. The hatched band represents the total uncertainty of the data

m_{T} distribution statistical and systematic uncertainties are of similar magnitude. The dominant systematic uncertainties are due to the parton shower modelling for p_{T}^{ℓ}, and lepton and recoil performance for m_{T}, respectively.

An overview of selected pre- and post-fit distributions of m_{T} is shown in Fig. 14, where a general better agreement can be observed for the post-fit case. The post-fit distributions use the final measured value of Γ_W.

7.3 Combination

The combination of results obtained from p_{T}^{ℓ} and m_{T} distributions follows the procedure described in Sect. 6.4. The p_{T}^{ℓ} and m_{T} results are fully compatible with each other in terms of central values and nuisance parameters. The results for all considered PDF sets are presented in Table 7. The weight of the m_{T} fit ranges from 84% to 89%, depending on the PDF set, and dominates the final result. For CT18, the final result yields:

$$\begin{aligned}\Gamma_W &= 2202 \pm 32\ (\text{stat.}) \pm 34\ (\text{syst.})\ \text{MeV} \\ &= 2202 \pm 47\ \text{MeV},\end{aligned}$$

where the first uncertainty component is statistical and the second corresponds to the total systematic uncertainties. The compatibility of the measured value with the SM expectation is illustrated in Fig. 15a, together with selected previous measurements.

Table 7 Uncertainty correlation between the p_{T}^{ℓ} and m_{T} fits, combination weights and combination results for Γ_W and the indicated PDF sets

PDF set	Correlation	Weight (m_{T})	Weight (p_{T}^{ℓ})	Combined Γ_W [MeV]
CT14	50.3%	88%	12%	2204 ± 47
CT18	51.5%	87%	13%	2202 ± 47
CT18A	50.0%	86%	14%	2184 ± 47
MMHT2014	50.8%	88%	13%	2182 ± 47
MSHT20	53.6%	89%	11%	2181 ± 47
ATLASpdf21	49.5%	84%	16%	2193 ± 46
NNPDF31	49.9%	86%	14%	2182 ± 46
NNPDF40	51.4%	85%	15%	2184 ± 46

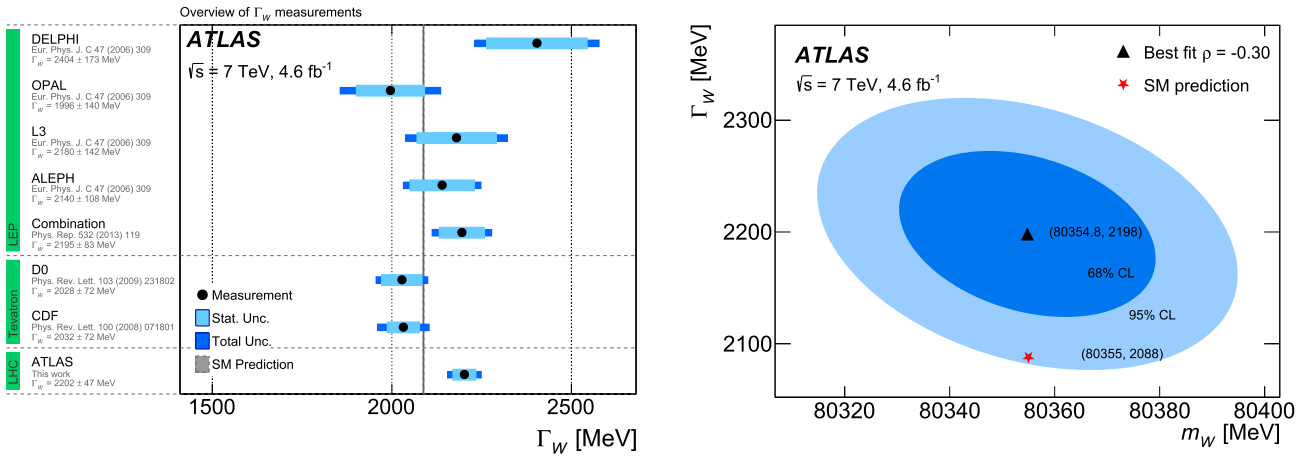

Fig. 15 **a** Present measurement of Γ_W, compared to the SM prediction from the global electroweak fit [6], and to the measurements of LEP [10] and Tevatron [64]. **b** 68% and 95% CL uncertainty contours for the simultaneous determination of m_W and Γ_W using the CT18 PDF set and combining results from the p_{T}^{ℓ} and m_{T} distributions. The triangular marker represents the best fit, while the star corresponds to the SM prediction of Ref. [6]

8 Simultaneous determination of the W-boson mass and width

The previously described determination of m_W assumes for the W-boson width its SM value and uncertainty, and similarly the Γ_W measurement uses the SM prediction for m_W. To further test the interplay between the two observables, the PLH fit is also performed with both m_W and Γ_W free in the fit. This fit with two parameters of interest relies on the same experimental calibrations and physics modelling. The fit yields values of $m_W = 80{,}351.8 \pm 16.7$ MeV and $\Gamma_W = 2216 \pm 73$ MeV for the p_{T}^{ℓ} distributions and $m_W = 80{,}369.4 \pm 26.8$ MeV and $\Gamma_W = 2186 \pm 53$ MeV for the m_{T} distributions using the CT18 PDF set. Compared with the separate m_W and Γ_W fits, the decrease of m_W by 10 MeV and 25 MeV for the p_{T}^{ℓ} and m_{T} distributions, respectively, is consistent with the larger measured value of Γ_W following the observed anti-correlation of m_W and Γ_W. The increase in total uncertainty is due to the removal of the constraints on Γ_W and m_W in the fit.

The combination of results obtained from p_{T}^{ℓ} and m_{T} distributions follows the procedure described in Sect. 6.4. The p_{T}^{ℓ} and m_{T} results are fully compatible with each other.

For the CT18 PDF set, the combination yields values of

$$m_W = 80{,}354.8 \pm 16.1 \text{ MeV}$$

and

$$\Gamma_W = 2198 \pm 49 \text{ MeV},$$

with a correlation of -30% that reflects the negative slope of the dependencies reported in Sects. 6.4 and 7.2. The 68% and 95% CL uncertainty contours are shown in Fig. 15b.

9 Conclusion

This paper reports on a first measurement of the W-boson width at the LHC as well as the reanalysis of the data

used in the published W-boson mass measurement, using an improved fitting technique and updated parton distribution functions. Both measurements are based on proton–proton collision data at a centre-of-mass energy of $\sqrt{s} = 7$ TeV recorded by the ATLAS detector at the LHC in 2011, and corresponding to an integrated luminosity of 4.6 fb^{-1} and 4.1 fb^{-1} in the electron and muon channels, respectively.

The measurements of m_W using the p_{T}^{ℓ} and m_{T} distributions are found to be consistent and their combination yields

$$m_W = 80{,}366.5 \pm 9.8\ (\text{stat.}) \pm 12.5\ (\text{syst.})\ \text{MeV} = 80{,}366.5 \pm 15.9\ \text{MeV}.$$

The present result is compatible with and supersedes the previous measurement of m_W at ATLAS using the same data. No significant deviation from the SM expectation is observed. The PDF dependence of the m_W result is driven by the prefit PDF uncertainties, and is strongly reduced when allowing for enlarged uncertainties. The final results are obtained using the CT18 PDF set, which is the most conservative PDF set for these measurements and compatible with the fits using enlarged PDF uncertainties of other sets.

The measurements of Γ_W using the p_{T}^{ℓ} and m_{T} distributions are also found to be consistent and their combination yields a value of

$$\Gamma_W = 2202 \pm 32\ (\text{stat.}) \pm 34\ (\text{syst.})\ \text{MeV} = 2202 \pm 47\ \text{MeV}.$$

It is the currently most precise single measurement of Γ_W and agrees with the SM expectation of $\Gamma_W^{\mathrm{SM}} = 2088 \pm 1$ MeV within 2.4 standard deviations. The dependence of Γ_W on the assumed PDF set is weak compared with the measurement uncertainties.

Acknowledgements We thank CERN for the very successful operation of the LHC and its injectors, as well as the support staff at CERN and at our institutions worldwide without whom ATLAS could not be operated efficiently. The crucial computing support from all WLCG partners is acknowledged gratefully, in particular from CERN, the ATLAS Tier-1 facilities at TRIUMF/SFU (Canada), NDGF (Denmark, Norway, Sweden), CC-IN2P3 (France), KIT/GridKA (Germany), INFN-CNAF (Italy), NL-T1 (Netherlands), PIC (Spain), RAL (UK) and BNL (USA), the Tier-2 facilities worldwide and large non-WLCG resource providers. Major contributors of computing resources are listed in Ref. [65]. We gratefully acknowledge the support of ANPCyT, Argentina; YerPhI, Armenia; ARC, Australia; BMWFW and FWF, Austria; ANAS, Azerbaijan; CNPq and FAPESP, Brazil; NSERC, NRC and CFI, Canada; CERN; ANID, Chile; CAS, MOST and NSFC, China; Minciencias, Colombia; MEYS CR, Czech Republic; DNRF and DNSRC, Denmark; IN2P3-CNRS and CEA-DRF/IRFU, France; SRNSFG, Georgia; BMBF, HGF and MPG, Germany; GSRI, Greece; RGC and Hong Kong SAR, China; ISF and Benoziyo Center, Israel; INFN, Italy; MEXT and JSPS, Japan; CNRST, Morocco; NWO, Netherlands; RCN, Norway; MNiSW, Poland; FCT, Portugal; MNE/IFA, Romania; MESTD, Serbia; MSSR, Slovakia; ARRS and MIZŠ, Slovenia; DSI/NRF, South Africa; MICINN, Spain; SRC and Wallenberg Foundation, Sweden; SERI, SNSF and Cantons of Bern and Geneva, Switzerland; MOST, Taipei; TENMAK, Turkey; STFC, UK; DOE and NSF, USA. Individual groups and members have received support from BCKDF, CANARIE, CRC and DRAC, Canada; PRIMUS 21/SCI/017, CERN-CZ and FORTE, Czech Republic; COST, ERC, ERDF, Horizon 2020, ICSC-NextGenerationEU and Marie Skłodowska-Curie Actions, European Union; Investissements d'Avenir Labex, Investissements d'Avenir Idex and ANR, France; DFG and AvH Foundation, Germany; Herakleitos, Thales and Aristeia programmes co-financed by EU-ESF and the Greek NSRF, Greece; BSF-NSF and MINERVA, Israel; Norwegian Financial Mechanism 2014-2021, Norway; NCN and NAWA, Poland; La Caixa Banking Foundation, CERCA Programme Generalitat de Catalunya and PROMETEO and GenT Programmes Generalitat Valenciana, Spain; Göran Gustafssons Stiftelse, Sweden; The Royal Society and Leverhulme Trust, UK. In addition, individual members wish to acknowledge support from CERN: European Organization for Nuclear Research (CERN PJAS); Chile: Agencia Nacional de Investigación y Desarrollo (FONDECYT 1190886, FONDECYT 1210400, FONDECYT 1230812, FONDECYT 1230987); China: Chinese Ministry of Science and Technology (MOST-2023YFA1605700), National Natural Science Foundation of China (NSFC - 12175119, NSFC 12275265, NSFC-12075060); Czech Republic: Czech Science Foundation (GACR - 24-11373 S), Ministry of Education Youth and Sports (FORTE CZ.02.01.01/00/22_008/0004632), PRIMUS Research Programme (PRIMUS/21/SCI/017); EU: H2020 European Research Council (ERC - 101002463); European Union: European Research Council (ERC - 948254, ERC 101089007), Horizon 2020 Framework Programme (MUCCA - CHIST-ERA-19-XAI-00), European Union, Future Artificial Intelligence Research (FAIR-NextGenerationEU PE00000013), Italian Center for High Performance Computing, Big Data and Quantum Computing (ICSC, NextGenerationEU); France: Agence Nationale de la Recherche (ANR-20-CE31-0013, ANR-21-CE31-0013, ANR-21-CE31-0022), Investissements d'Avenir Labex (ANR-11-LABX-0012); Germany: Baden-Württemberg Stiftung (BW Stiftung-Postdoc Eliteprogramme), Deutsche Forschungsgemeinschaft (DFG - 469666862, DFG - CR 312/5-2); Italy: Istituto Nazionale di Fisica Nucleare (ICSC, NextGenerationEU); Japan: Japan Society for the Promotion of Science (JSPS KAKENHI JP21H05085, JSPS KAKENHI JP22H01227, JSPS KAKENHI JP22H04944, JSPS KAKENHI JP22KK0227); Netherlands: Netherlands Organisation for Scientific Research (NWO Veni 2020 - VI.Veni.202.179); Norway: Research Council of Norway (RCN-314472); Poland: Polish National Agency for Academic Exchange (PPN/PPO/2020/1/00002/U/00001), Polish National Science Centre (NCN 2021/42/E/ST2/00350, NCN OPUS nr 2022/47/B/ST2/03059, NCN UMO-2019/34/E/ST2/00393, UMO-2020/37/B/ST2/01043, UMO-2021/40/C/ST2/00187, UMO-2022/47/O/ST2/00148, UMO-2023/49/B/ST2/04085); Slovenia: Slovenian Research Agency (ARIS grant J1-3010); Spain: Generalitat Valenciana (Artemisa, FEDER, IDIFEDER/2018/048), Ministry of Science and Innovation (MCIN & NextGenEU PCI2022-135018-2, MICIN & FEDER PID2021-125273NB, RYC2019-028510-I, RYC2020-030254-I, RYC2021-031273-I, RYC2022-038164-I), PROMETEO and GenT Programmes Generalitat Valenciana (CIDEGENT/2019/023, CIDEGENT/2019/027); Sweden: Swedish Research Council (Swedish Research Council 2023-04654, VR 2018-00482, VR 2022-03845, VR 2022-04683, VR 2023-03403, VR grant 2021-03651), Knut and Alice Wallenberg Foundation (KAW 2018.0157, KAW 2018.0458, KAW 2019.0447, KAW 2022.0358); Switzerland: Swiss National Science Foundation (SNSF - PCEFP2_194658); UK: Leverhulme Trust (Leverhulme Trust RPG-2020-004), Royal Society (NIF-R1-231091); USA: U.S. Department of Energy (ECA DE-AC02-76SF00515), Neubauer Family Foundation.

Data Availability Statement This manuscript has associated data in a data repository. [Authors' comment: All ATLAS scientific output is published in journals, and preliminary results are made available in Conference Notes. All are openly available, without restriction on use by external parties beyond copyright law and the standard conditions agreed by CERN. Data associated with journal publications are also made available: tables and data from plots (e.g. cross section values,

likelihood profiles, selection efficiencies, cross section limits, ...) are stored in appropriate repositories such as HEPDATA (http://hepdata.cedar.ac.uk/). ATLAS also strives to make additional material related to the paper available that allows a reinterpretation of the data in the context of new theoretical models. For example, an extended encapsulation of the analysis is often provided for measurements in the framework of RIVET (http://rivet.hepforge.org/). This information is taken from the ATLAS Data Access Policy, which is a public document that can be downloaded from http://opendata.cern.ch/record/413.]

Code Availability Statement My manuscript has no associated code/software.] [Authors' comment: Software sharing not applicable to this article.]

Funded by SCOAP[3].

References

1. S.L. Glashow, Partial-symmetries of weak interactions. Nucl. Phys. **22**, 579 (1961). https://doi.org/10.1016/0029-5582(61)90469-2
2. A. Salam, J.C. Ward, Electromagnetic and weak interactions. Phys. Lett. **13**, 168 (1964). https://doi.org/10.1016/0031-9163(64)90711-5
3. S. Weinberg, A Model of Leptons. Phys. Rev. Lett. **19**, 1264 (1967). https://doi.org/10.1103/PhysRevLett.19.1264
4. A. Sirlin, Radiative corrections in the $SU(2)_L \times U(1)$ theory: A simple renormalization framework. Phys. Rev. D **22**, 971 (1980). https://doi.org/10.1103/PhysRevD.22.971
5. M. Awramik et al., Precise prediction for the W-boson mass in the standard model. Phys. Rev. D **69**, 053006 (2004). https://doi.org/10.1103/PhysRevD.69.053006. arXiv:hep-ph/0311148
6. J. de Blas et al., Global analysis of electroweak data in the Standard Model. Phys. Rev. D **106**, 033003 (2022). https://doi.org/10.1103/PhysRevD.106.033003. arXiv:2112.07274 [hep-ph]
7. The GFitter Group, J. Haller et al. Update of the global electroweak fit and constraints on two-Higgsdoublet models. Eur. Phys. J. C **78**, 675 (2018). https://doi.org/10.1140/epjc/s10052-018-6131-3. arXiv:1803.01853 [hep-ph]
8. J. Erler. Global Fits to Electroweak Data Using GAPP. QCD and weak boson physics in Run II. Proceedings, Batavia, IL, March 4–6, June 3–4, November 4–6 (1999). arXiv: hep-ph/0005084
9. C.D.F. Collaboration, High-precision measurement of the W boson mass with the CDF II detector. Science **376**, 170 (2022). https://doi.org/10.1126/science.abk1781
10. The ALEPH Collaboration, The DELPHI Collaboration, The L3 Collaboration, The OPAL Collaboration, The LEP Electroweak Working Group. Electroweak measurements in electron-positron collisions at W-boson-pair energies at LEP. Phys. Rept. **532**, 119 (2013). https://doi.org/10.1016/j.physrep.2013.07.004. arXiv:1302.3415 [hep-ex]
11. D0 Collaboration, Measurement of the W Boson Mass with the D0 Detector. Phys. Rev. Lett. **108**, 151804 (2012). https://doi.org/10.1103/PhysRevLett.108.151804. arXiv:1203.0293 [hep-ex]
12. ATLAS Collaboration. Measurement of the W-boson mass in pp collisions at $\sqrt{s} = 7$ TeV with the ATLAS detector. Eur. Phys. J. C **78**, 110 (2018). https://doi.org/10.1140/epjc/s10052-017-5475-4. arXiv:1701.07240 [hep-ex]. Erratum: in: Eur. Phys. J. C 78 (2018), 898. https://doi.org/10.1140/epjc/s10052-018-6354-3
13. LHCb Collaboration. Measurement of the W boson mass. JHEP **01**, 036 (2022). https://doi.org/10.1007/JHEP01(2022)036. arXiv:2109.01113 [hep-ex]
14. S. Amoroso et al. Compatibility and combination of world W-boson mass measurements (2023). arXiv:2308.09417 [hep-ex]
15. M.E. Peskin, T. Takeuchi, Estimation of oblique electroweak corrections. Phys. Rev. D **46**, 381 (1992). https://doi.org/10.1103/PhysRevD.46.381
16. S. Heinemeyer et al., Implications of LHC search results on the W boson mass prediction in the MSSM. JHEP **12**, 084 (2013). https://doi.org/10.1007/JHEP12(2013)084. arXiv:1311.1663 [hep-ph]
17. Particle Data Group, R. L. Workman et al. Review of Particle Physics. PTEP 2022, 083C01 (2022). https://doi.org/10.1093/ptep/ptac097
18. C.D.F. Collaboration, Precise measurement of the W-boson mass with the CDF II detector. Phys. Rev. Lett. **108**, 151803 (2012). https://doi.org/10.1103/PhysRevLett.108.151803. arXiv:1203.0275 [hep-ex]
19. D0 Collaboration, Measurement of the W-boson mass with the D0 detector. Phys. Rev. D **89**, 012005 (2014). https://doi.org/10.1103/PhysRevD.89.012005. arXiv:1310.8628 [hep-ex]
20. W.A. Rólke, A.M. Lopez, J. Conrad, Limits and confidence intervals in the presence of nuisance parameters. Nucl. Instrum. Meth. A **551**, 493 (2005). https://doi.org/10.1016/j.nima.2005.05.068. arXiv:physics/0403059
21. ATLAS Collaboration. The ATLAS Experiment at the CERN Large Hadron Collider. JINST **3**, S08003 (2008). https://doi.org/10.1088/1748-0221/3/08/S08003
22. ATLAS Collaboration. Performance of the ATLAS Trigger System in 2010. Eur. Phys. J. C **72**, 1849 (2012). https://doi.org/10.1140/epjc/s10052-011-1849-1. arXiv:1110.1530 [hep-ex]
23. ATLAS Collaboration. The ATLAS Collaboration Software and Firmware. ATL-SOFT-PUB-2021-001 (2021). https://cds.cern.ch/record/2767187
24. P. Nason, A new method for combining NLO QCD with shower Monte Carlo algorithms. JHEP **11**, 040 (2004). https://doi.org/10.1088/1126-6708/2004/11/040. arXiv:hep-ph/0409146
25. S. Frixione, P. Nason, C. Oleari, Matching NLO QCD computations with parton shower simulations: the POWHEG method. JHEP **11**, 070 (2007). https://doi.org/10.1088/1126-6708/2007/11/070. arXiv:0709.2092 [hep-ph]
26. S. Alioli et al., A general framework for implementing NLO calculations in shower Monte Carlo programs: the POWHEG BOX. JHEP **06**, 043 (2010). https://doi.org/10.1007/JHEP06(2010)043. arXiv:1002.2581 [hep-ph]
27. T. Sjöstrand, S. Mrenna, P. Skands, PYTHIA 6.4 physics and manual. JHEP **05**, 026 (2006). https://doi.org/10.1088/1126-6708/2006/05/026. arXiv:hep-ph/0603175
28. T. Sjostrand, S. Mrenna, P. Skands. A brief introduction to PYTHIA 8.1. Comput. Phys. Commun. **178**, 852 (2008). https://doi.org/10.1016/j.cpc.2008.01.036. arXiv:0710.3820 [hep-ph]
29. ATLAS Collaboration. Measurement of the Z/γ^* boson transverse momentum distribution in pp collisions at $\sqrt{s} = 7$ TeV with the ATLAS detector. JHEP **09**, 145 (2014). https://doi.org/10.1007/JHEP09(2014)145. arXiv:1406.3660 [hep-ex]
30. H.-L. Lai et al., New parton distributions for collider physics. Phys. Rev. D **82**, 074024 (2010). https://doi.org/10.1103/PhysRevD.82.074024. arXiv:1007.2241 [hep-ph]

31. J. Pumplin et al., New Generation of Parton Distributions with Uncertainties from Global QCD Analysis. JHEP **07**, 012 (2002). https://doi.org/10.1088/1126-6708/2002/07/012. arXiv:hep-ph/0201195
32. P. Golonka, Z. Was, PHOTOS Monte Carlo: a precision tool for QED corrections in Z and W decays. Eur. Phys. J. C **45**, 97 (2006). https://doi.org/10.1140/epjc/s2005-02396-4. arXiv:hep-ph/0506026
33. ATLAS Collaboration. Precision measurement and interpretation of inclusive W^+, W^- and Z/γ^* production cross sections with the ATLAS detector. Eur. Phys. J. C **77**, 367. (2017). https://doi.org/10.1140/epjc/s10052-017-4911-9. arXiv:1612.03016 [hep-ex]
34. S. Frixione, B.R. Webber, Matching NLO QCD computations and parton shower simulations. JHEP **06**, 029 (2002). https://doi.org/10.1088/1126-6708/2002/06/029. arXiv:hep-ph/0204244
35. S. Frixione, P. Nason, B.R. Webber, Matching NLO QCD and parton showers in heavy flavour production. JHEP **08**, 007 (2003). https://doi.org/10.1088/1126-6708/2003/08/007. arXiv:hep-ph/0305252
36. S. Frixione et al., Single-top production in MC@NLO. JHEP **03**, 092 (2006). https://doi.org/10.1088/1126-6708/2006/03/092. arXiv:hep-ph/0512250
37. ATLAS Collaboration. The ATLAS Simulation Infrastructure. Eur. Phys. J. C **70**, 823 (2010). https://doi.org/10.1140/epjc/s10052-010-1429-9. arXiv:1005.4568 [physics.ins-det]
38. S. Agostinelli et al. GEANT4–*asimulationtoolkit*. Nucl. Instrum. Meth. A **506**, 250 (2003). https://doi.org/10.1016/S0168-9002(03)01368-8
39. ATLAS Collaboration. Summary of ATLAS Pythia 8 tunes. ATL-PHYS-PUB-2012-003 (2012). https://cds.cern.ch/record/1474107
40. ATLAS Collaboration. Electron reconstruction and identification efficiency measurements with the ATLAS detector using the 2011 LHC proton-proton collision data. Eur. Phys. J. C **74**, 2941 (2014). https://doi.org/10.1140/epjc/s10052-014-2941-0. arXiv:1404.2240 [hep-ex]
41. ATLAS Collaboration. Electron and photon energy calibration with the ATLAS detector using LHC Run 1 data. Eur. Phys. J. C **74**, 3071 (2014). https://doi.org/10.1140/epjc/s10052-014-3071-4. arXiv:1407.5063 [hep-ex]
42. ATLAS Collaboration. Measurement of the muon reconstruction performance of the ATLAS detector using 2011 and 2012 LHC proton–proton collision data. Eur. Phys. J. C **74**, 3130 (2014). https://doi.org/10.1140/epjc/s10052-014-3130-x. arXiv:1407.3935 [hep-ex]
43. ATLAS Collaboration. Improved luminosity determination in pp collisions at $\sqrt{s} = 7$ TeV using the ATLAS detector at the LHC. Eur. Phys. J. C **73**, 2518 (2013). https://doi.org/10.1140/epjc/s10052-013-2518-3. arXiv:1302.4393 [hep-ex]
44. S. Dulat et al., Newparton distribution functions from a global analysis of quantum chromodynamics. Phys. Rev. D **93**, 033006 (2016). https://doi.org/10.1103/PhysRevD.93.033006. arXiv:1506.07443 [hep-ph]
45. L.A. Harland-Lang et al., Parton distributions in the LHC era: MMHT 2014 PDFs. Eur. Phys. J. C **75**, 204 (2015). https://doi.org/10.1140/epjc/s10052-015-3397-6. arXiv:1412.3989 [hep-ph]
46. ATLAS Collaboration. Determination of the parton distribution functions of the proton using diverse ATLAS data from pp collisions at $\sqrt{s} = 7, 8$ and 13 TeV. Eur. Phys. J. C **82**, 438 (2022). https://doi.org/10.1140/epjc/s10052-022-10217-z. arXiv:2112.11266 [hep-ex]
47. T.-J. Hou et al., New CTEQ global analysis of quantum chromodynamics with high-precision data from the LHC. Phys. Rev. D **103**, 014013 (2021). https://doi.org/10.1103/PhysRevD.103.014013. arXiv:1912.10053 [hep-ph]
48. S. Bailey et al., Parton distributions from LHC, HERA, Tevatron and fixed target data: MSHT20 PDFs. Eur. Phys. J. C **81**, 341 (2021). https://doi.org/10.1140/epjc/s10052-021-09057-0. arXiv:2012.04684 [hep-ph]
49. NNPDF Collaboration. Parton distributions from high-precision collider data. Eur. Phys. J. C **77**, 663 (2017). https://doi.org/10.1140/epjc/s10052-017-5199-5. arXiv:1706.00428 [hep-ph]
50. NNPDF Collaboration, R. D. Ball et al. The path to proton structure at 1% accuracy. Eur. Phys. J. C **82**(5), 428 (2022). https://doi.org/10.1140/epjc/s10052-022-10328-7. arXiv:2109.02653 [hep-ph]
51. A. Pinto et al. Uncertainty components in profile likelihood fits (2023). arXiv:2307.04007 [physics.data-an]
52. The ALEPH Collaboration, The DELPHI Collaboration, The L3 Collaboration, The OPAL Collaboration, The SLD Collaboration, The LEP Electroweak Working Group, The SLD Electroweak and Heavy Flavour Groups. Precision electroweak measurements on the Z resonance. Phys. Rept. **427**, 257 (2006). https://doi.org/10.1016/j.physrep.2005.12.006. arXiv:hep-ex/0509008
53. K. Pearson. LIII. On lines and planes of closest fit to systems of points in space. Lond. Edinburgh Dublin Philos. Mag. J. Sci. **2**, 559 (1901). https://doi.org/10.1080/14786440109462720
54. H. Hotelling. Analysis of a complex of statistical variables into principal components. J. Educ. Psychol. 417 (1933). https://doi.org/10.1037/h0071325
55. ATLAS Collaboration. Measurement of the angular coefficients in Z-boson events using electron and muon pairs from data taken at $\sqrt{s} = 8$ TeV with the ATLAS detector. JHEP **08**, 159 (2016). https://doi.org/10.1007/JHEP08(2016)159. arXiv:1606.00689 [hep-ex]
56. ATLAS Collaboration. Precise measurements of W and Z transverse momentum spectra with the ATLAS detector at $\sqrt{s} = 5.02$ TeV and 13 TeV. CERN-EP-2024-080 (2024)
57. J. Pumplin et al. Uncertainties of predictions from parton distribution functions. II. The Hessian method. Phys. Rev. D **65**, 014013 (2001). https://doi.org/10.1103/PhysRevD.65.014013. arXiv:hep-ph/0101032
58. T. Sjöstrand, P.Z. Skands, Transverse-momentum-ordered showers and interleaved multiple interactions. Eur. Phys. J. C **39**, 129 (2005). https://doi.org/10.1140/epjc/s2004-02084-y. arXiv:hep-ph/0408302
59. L. Lyons, D. Gibaut, P. Clifford, How to combine correlated estimates of a single physical quantity. Nucl. Instrum. Meth. A **270**, 110 (1988). https://doi.org/10.1016/0168-9002(88)90018-6
60. ATLAS and CMS Collaborations. Combination of measurements of the top quark mass from data collected by the ATLAS and CMS experiments at $\sqrt{s}$=7 and 8 TeV. (2024). arXiv:2402.08713 [hep-ex]
61. ATLAS Collaboration. Combined Measurement of the Higgs Boson Mass from the $H\to\gamma\gamma$ and $H\to ZZ^*\to 4\ell$ Decay Channels with the ATLAS Detector Using $\sqrt{s}$=7, 8, and13 TeV pp Collision Data, Phys. Rev. Lett. **131**, 251802 (2023). https://doi.org/10.1103/PhysRevLett.131.251802. arXiv:2308.04775 [hep-ex]
62. J. de Blas et al., Impact of the Recent Measurements of the Top-Quark and W-Boson Masses on Electroweak Precision Fits. Phys. Rev. Lett. **129**, 271801 (2022). https://doi.org/10.1103/PhysRevLett.129.271801. arXiv:2204.04204 [hep-ph]
63. J. de Blas et al. The Global Electroweak and Higgs Fits in the LHC era. PoS EPS-HEP2017 (2017). Ed. by P. Checchia et al., 467. https://doi.org/10.22323/1.314.0467. arXiv:1710.05402 [hep-ph]
64. The Tevatron Electroweak Working Group. Combination of CDF and D0 Results on the Width of the W boson (2010). arXiv:1003.2826 [hep-ex]
65. ATLAS Collaboration. ATLAS Computing Acknowledgements. ATL-SOFT-PUB-2023-001 (2023). https://cds.cern.ch/record/2869272

ATLAS Collaboration*

G. Aad[103], E. Aakvaag[16], B. Abbott[121], S. Abdelhameed[117a], K. Abeling[55], N. J. Abicht[49], S. H. Abidi[29], M. Aboelela[44], A. Aboulhorma[35e], H. Abramowicz[152], H. Abreu[151], Y. Abulaiti[118], B. S. Acharya[69a,69b,k], A. Ackermann[63a], C. Adam Bourdarios[4], L. Adamczyk[86a], S. V. Addepalli[26], M. J. Addison[102], J. Adelman[116], A. Adiguzel[21c], T. Adye[135], A. A. Affolder[137], Y. Afik[39], M. N. Agaras[13], J. Agarwala[73a,73b], A. Aggarwal[101], C. Agheorghiesei[27c], A. Ahmad[36], F. Ahmadov[38,x], W. S. Ahmed[105], S. Ahuja[96], X. Ai[62e], G. Aielli[76a,76b], A. Aikot[164], M. Ait Tamlihat[35e], B. Aitbenchikh[35a], M. Akbiyik[101], T. P. A. Åkesson[99], A. V. Akimov[37], D. Akiyama[169], N. N. Akolkar[24], S. Aktas[21a], K. Al Khoury[41], G. L. Alberghi[23b], J. Albert[166], P. Albicocco[53], G. L. Albouy[60], S. Alderweireldt[52], Z. L. Alegria[122], M. Aleksa[36], I. N. Aleksandrov[38], C. Alexa[27b], T. Alexopoulos[10], F. Alfonsi[23b], M. Algren[56], M. Alhroob[168], B. Ali[133], H. M. J. Ali[92], S. Ali[31], S. W. Alibocus[93], M. Aliev[33c], G. Alimonti[71a], W. Alkakhi[55], C. Allaire[66], B. M. M. Allbrooke[147], J. F. Allen[52], C. A. Allendes Flores[138f], P. P. Allport[20], A. Aloisio[72a,72b], F. Alonso[91], C. Alpigiani[139], Z. M. K. Alsolami[92], M. Alvarez Estevez[100], A. Alvarez Fernandez[101], M. Alves Cardoso[56], M. G. Alviggi[72a,72b], M. Aly[102], Y. Amaral Coutinho[83b], A. Ambler[105], C. Amelung[36], M. Amerl[102], C. G. Ames[110], D. Amidei[107], K. J. Amirie[156], S. P. Amor Dos Santos[131a], K. R. Amos[164], S. An[84], V. Ananiev[126], C. Anastopoulos[140], T. Andeen[11], J. K. Anders[36], S. Y. Andrean[47a,47b], A. Andreazza[71a,71b], S. Angelidakis[9], A. Angerami[41,z], A. V. Anisenkov[37], A. Annovi[74a], C. Antel[56], E. Antipov[146], M. Antonelli[53], F. Anulli[75a], M. Aoki[84], T. Aoki[154], M. A. Aparo[147], L. Aperio Bella[48], C. Appelt[18], A. Apyan[26], S. J. Arbiol Val[87], C. Arcangeletti[53], A. T. H. Arce[51], E. Arena[93], J-F. Arguin[109], S. Argyropoulos[54], J.-H. Arling[48], O. Arnaez[4], H. Arnold[115], G. Artoni[75a,75b], H. Asada[112], K. Asai[119], S. Asai[154], N. A. Asbah[36], R. A. Ashby Pickering[168], K. Assamagan[29], R. Astalos[28a], K. S. V. Astrand[99], S. Atashi[160], R. J. Atkin[33a], M. Atkinson[163], H. Atmani[35f], P. A. Atmasiddha[129], K. Augsten[133], S. Auricchio[72a,72b], A. D. Auriol[20], V. A. Austrup[102], G. Avolio[36], K. Axiotis[56], G. Azuelos[109,ad], D. Babal[28b], H. Bachacou[136], K. Bachas[153,o], A. Bachiu[34], F. Backman[47a,47b], A. Badea[39], T. M. Baer[107], P. Bagnaia[75a,75b], M. Bahmani[18], D. Bahner[54], K. Bai[124], J. T. Baines[135], L. Baines[95], O. K. Baker[173], E. Bakos[15], D. Bakshi Gupta[8], V. Balakrishnan[121], R. Balasubramanian[115], E. M. Baldin[37], P. Balek[86a], E. Ballabene[23a,23b], F. Balli[136], L. M. Baltes[63a], W. K. Balunas[32], J. Balz[101], I. Bamwidhi[117b], E. Banas[87], M. Bandieramonte[130], A. Bandyopadhyay[24], S. Bansal[24], L. Barak[152], M. Barakat[48], E. L. Barberio[106], D. Barberis[57a,57b], M. Barbero[103], M. Z. Barel[115], K. N. Barends[33a], T. Barillari[111], M-S. Barisits[36], T. Barklow[144], P. Baron[123], D. A. Baron Moreno[102], A. Baroncelli[62a], G. Barone[29], A. J. Barr[127], J. D. Barr[97], F. Barreiro[100], J. Barreiro Guimarães da Costa[14a], U. Barron[152], M. G. Barros Teixeira[131a], S. Barsov[37], F. Bartels[63a], R. Bartoldus[144], A. E. Barton[92], P. Bartos[28a], A. Basan[101], M. Baselga[49], A. Bassalat[66,b], M. J. Basso[157a], R. Bate[165], R. L. Bates[59], S. Batlamous[100], B. Batool[142], M. Battaglia[137], D. Battulga[18], M. Bauce[75a,75b], M. Bauer[36], P. Bauer[24], L. T. Bazzano Hurrell[30], J. B. Beacham[51], T. Beau[128], J. Y. Beaucamp[91], P. H. Beauchemin[159], P. Bechtle[24], H. P. Beck[19,n], K. Becker[168], A. J. Beddall[82], V. A. Bednyakov[38], C. P. Bee[146], L. J. Beemster[15], T. A. Beermann[36], M. Begalli[83d], M. Begel[29], A. Behera[146], J. K. Behr[48], J. F. Beirer[36], F. Beisiegel[24], M. Belfkir[117b], G. Bella[152], L. Bellagamba[23b], A. Bellerive[34], P. Bellos[20], K. Beloborodov[37], D. Benchekroun[35a], F. Bendebba[35a], Y. Benhammou[152], K. C. Benkendorfer[61], L. Beresford[48], M. Beretta[53], E. Bergeaas Kuutmann[162], N. Berger[4], B. Bergmann[133], J. Beringer[17a], G. Bernardi[5], C. Bernius[144], F. U. Bernlochner[24], F. Bernon[36,103], A. Berrocal Guardia[13], T. Berry[96], P. Berta[134], A. Berthold[50], S. Bethke[111], A. Betti[75a,75b], A. J. Bevan[95], N. K. Bhalla[54], M. Bhamjee[33c], S. Bhatta[146], D. S. Bhattacharya[167], P. Bhattarai[144], K. D. Bhide[54], V. S. Bhopatkar[122], R. M. Bianchi[130], G. Bianco[23a,23b], O. Biebel[110], R. Bielski[124], M. Biglietti[77a], C. S. Billingsley[44], M. Bindi[55], A. Bingul[21b], C. Bini[75a,75b], A. Biondini[93], C. J. Birch-sykes[102], G. A. Bird[32], M. Birman[170], M. Biros[134], S. Biryukov[147], T. Bisanz[49], E. Bisceglie[43a,43b], J. P. Biswal[135], D. Biswas[142], I. Bloch[48], A. Blue[59], U. Blumenschein[95], J. Blumenthal[101], V. S. Bobrovnikov[37], M. Boehler[54], B. Boehm[167], D. Bogavac[36], A. G. Bogdanchikov[37], C. Bohm[47a], V. Boisvert[96], P. Bokan[36], T. Bold[86a], M. Bomben[5], M. Bona[95], M. Boonekamp[136], C. D. Booth[96], A. G. Borbély[59], I. S. Bordulev[37], H. M. Borecka-Bielska[109], G. Borissov[92], D. Bortoletto[127], D. Boscherini[23b], M. Bosman[13], J. D. Bossio Sola[36], K. Bouaouda[35a], N. Bouchhar[164], L. Boudet[4], J. Boudreau[130], E. V. Bouhova-Thacker[92], D. Boumediene[40], R. Bouquet[57a,57b], A. Boveia[120], J. Boyd[36], D. Boye[29], I. R. Boyko[38], L. Bozianu[56], J. Bracinik[20], N. Brahimi[4], G. Brandt[172], O. Brandt[32], F. Braren[48], B. Brau[104], J. E. Brau[124], R. Brener[170],

L. Brenner[115], R. Brenner[162], S. Bressler[170], D. Britton[59], D. Britzger[111], I. Brock[24], G. Brooijmans[41], E. Brost[29], L. M. Brown[166], L. E. Bruce[61], T. L. Bruckler[127], P. A. Bruckman de Renstrom[87], B. Brüers[48], A. Bruni[23b], G. Bruni[23b], M. Bruschi[23b], N. Bruscino[75a,75b], T. Buanes[16], Q. Buat[139], D. Buchin[111], A. G. Buckley[59], O. Bulekov[37], B. A. Bullard[144], S. Burdin[93], C. D. Burgard[49], A. M. Burger[36], B. Burghgrave[8], O. Burlayenko[54], J. T. P. Burr[32], J. C. Burzynski[143], E. L. Busch[41], V. Büscher[101], P. J. Bussey[59], J. M. Butler[25], C. M. Buttar[59], J. M. Butterworth[97], W. Buttinger[135], C. J. Buxo Vazquez[108], A. R. Buzykaev[37], S. Cabrera Urbán[164], L. Cadamuro[66], D. Caforio[58], H. Cai[130], Y. Cai[14a,14e], Y. Cai[14c], V. M. M. Cairo[36], O. Cakir[3a], N. Calace[36], P. Calafiura[17a], G. Calderini[128], P. Calfayan[68], G. Callea[59], L. P. Caloba[83b], D. Calvet[40], S. Calvet[40], M. Calvetti[74a,74b], R. Camacho Toro[128], S. Camarda[36], D. Camarero Munoz[26], P. Camarri[76a,76b], M. T. Camerlingo[72a,72b], D. Cameron[36], C. Camincher[166], M. Campanelli[97], A. Camplani[42], V. Canale[72a,72b], A. C. Canbay[3a], E. Canonero[96], J. Cantero[164], Y. Cao[163], F. Capocasa[26], M. Capua[43a,43b], A. Carbone[71a,71b], R. Cardarelli[76a], J. C. J. Cardenas[8], G. Carducci[43a,43b], T. Carli[36], G. Carlino[72a], J. I. Carlotto[13], B. T. Carlson[130,p], E. M. Carlson[157a,166], J. Carmignani[93], L. Carminati[71a,71b], A. Carnelli[136], M. Carnesale[75a,75b], S. Caron[114], E. Carquin[138f], S. Carrá[71a], G. Carratta[23a,23b], A. M. Carroll[124], T. M. Carter[52], M. P. Casado[13,h], M. Caspar[48], F. L. Castillo[4], L. Castillo Garcia[13], V. Castillo Gimenez[164], N. F. Castro[131a,131e], A. Catinaccio[36], J. R. Catmore[126], T. Cavaliere[4], V. Cavaliere[29], N. Cavalli[23a,23b], Y. C. Cekmecelioglu[48], E. Celebi[21a], S. Cella[36], F. Celli[127], M. S. Centonze[70a,70b], V. Cepaitis[56], K. Cerny[123], A. S. Cerqueira[83a], A. Cerri[147], L. Cerrito[76a,76b], F. Cerutti[17a], B. Cervato[142], A. Cervelli[23b], G. Cesarini[53], S. A. Cetin[82], D. Chakraborty[116], J. Chan[17a], W. Y. Chan[154], J. D. Chapman[32], E. Chapon[136], B. Chargeishvili[150b], D. G. Charlton[20], M. Chatterjee[19], C. Chauhan[134], Y. Che[14c], S. Chekanov[6], S. V. Chekulaev[157a], G. A. Chelkov[38,a], A. Chen[107], B. Chen[152], B. Chen[166], H. Chen[14c], H. Chen[29], J. Chen[62c], J. Chen[143], M. Chen[127], S. Chen[154], S. J. Chen[14c], X. Chen[62c,136], X. Chen[14b,ac], Y. Chen[62a], C. L. Cheng[171], H. C. Cheng[64a], S. Cheong[144], A. Cheplakov[38], E. Cheremushkina[48], E. Cherepanova[115], R. Cherkaoui El Moursli[35e], E. Cheu[7], K. Cheung[65], L. Chevalier[136], V. Chiarella[53], G. Chiarelli[74a], N. Chiedde[103], G. Chiodini[70a], A. S. Chisholm[20], A. Chitan[27b], M. Chitishvili[164], M. V. Chizhov[38], K. Choi[11], Y. Chou[139], E. Y. S. Chow[114], K. L. Chu[170], M. C. Chu[64a], X. Chu[14a,14e], J. Chudoba[132], J. J. Chwastowski[87], D. Cieri[111], K. M. Ciesla[86a], V. Cindro[94], A. Ciocio[17a], F. Cirotto[72a,72b], Z. H. Citron[170], M. Citterio[71a], D. A. Ciubotaru[27b], A. Clark[56], P. J. Clark[52], C. Clarry[156], J. M. Clavijo Columbie[48], S. E. Clawson[48], C. Clement[47a,47b], J. Clercx[48], Y. Coadou[103], M. Cobal[69a,69c], A. Coccaro[57b], R. F. Coelho Barrue[131a], R. Coelho Lopes De Sa[104], S. Coelli[71a], B. Cole[41], J. Collot[60], P. Conde Muiño[131a,131g], M. P. Connell[33c], S. H. Connell[33c], E. I. Conroy[127], F. Conventi[72a,ae], H. G. Cooke[20], A. M. Cooper-Sarkar[127], F. A. Corchia[23a,23b], A. Cordeiro Oudot Choi[128], L. D. Corpe[40], M. Corradi[75a,75b], F. Corriveau[105,v], A. Cortes-Gonzalez[18], M. J. Costa[164], F. Costanza[4], D. Costanzo[140], B. M. Cote[120], J. Couthures[4], G. Cowan[96], K. Cranmer[171], D. Cremonini[23a,23b], S. Crépé-Renaudin[60], F. Crescioli[128], M. Cristinziani[142], M. Cristoforetti[78a,78b], V. Croft[115], J. E. Crosby[122], G. Crosetti[43a,43b], A. Cueto[100], Z. Cui[7], W. R. Cunningham[59], F. Curcio[164], J. R. Curran[52], P. Czodrowski[36], M. M. Czurylo[36], M. J. Da Cunha Sargedas De Sousa[57a,57b], J. V. Da Fonseca Pinto[83b], C. Da Via[102], W. Dabrowski[86a], T. Dado[49], S. Dahbi[149], T. Dai[107], D. Dal Santo[19], C. Dallapiccola[104], M. Dam[42], G. D'amen[29], V. D'Amico[110], J. Damp[101], J. R. Dandoy[34], D. Dannheim[36], M. Danninger[143], V. Dao[36], G. Darbo[57b], S. J. Das[29,af], F. Dattola[48], S. D'Auria[71a,71b], A. D'avanzo[72a,72b], C. David[33a], T. Davidek[134], I. Dawson[95], H. A. Day-hall[133], K. De[8], R. De Asmundis[72a], N. De Biase[48], S. De Castro[23a,23b], N. De Groot[114], P. de Jong[115], H. De la Torre[116], A. De Maria[14c], A. De Salvo[75a], U. De Sanctis[76a,76b], F. De Santis[70a,70b], A. De Santo[147], J. B. De Vivie De Regie[60], D. V. Dedovich[38], J. Degens[93], A. M. Deiana[44], F. Del Corso[23a,23b], J. Del Peso[100], F. Del Rio[63a], L. Delagrange[128], F. Deliot[136], C. M. Delitzsch[49], M. Della Pietra[72a,72b], D. Della Volpe[56], A. Dell'Acqua[36], L. Dell'Asta[71a,71b], M. Delmastro[4], P. A. Delsart[60], S. Demers[173], M. Demichev[38], S. P. Denisov[37], L. D'Eramo[40], D. Derendarz[87], F. Derue[128], P. Dervan[93], K. Desch[24], C. Deutsch[24], F. A. Di Bello[57a,57b], A. Di Ciaccio[76a,76b], L. Di Ciaccio[4], A. Di Domenico[75a,75b], C. Di Donato[72a,72b], A. Di Girolamo[36], G. Di Gregorio[36], A. Di Luca[78a,78b], B. Di Micco[77a,77b], R. Di Nardo[77a,77b], M. Diamantopoulou[34], F. A. Dias[115], T. Dias Do Vale[143], M. A. Diaz[138a,138b], F. G. Diaz Capriles[24], M. Didenko[164], E. B. Diehl[107], S. Díez Cornell[48], C. Diez Pardos[142], C. Dimitriadi[24,162], A. Dimitrievska[20], J. Dingfelder[24], I-M. Dinu[27b], S. J. Dittmeier[63b], F. Dittus[36], M. Divisek[134], F. Djama[103], T. Djobava[150b], C. Doglioni[99,102], A. Dohnalova[28a], J. Dolejsi[134], Z. Dolezal[134], K. Domijan[86a], K. M. Dona[39], M. Donadelli[83c], B. Dong[108], J. Donini[40], A. D'Onofrio[72a,72b],

M. D'Onofrio[93], J. Dopke[135], A. Doria[72a], N. Dos Santos Fernandes[131a], P. Dougan[102], M. T. Dova[91], A. T. Doyle[59], M. A. Draguet[127], E. Dreyer[170], I. Drivas-koulouris[10], M. Drnevich[118], M. Drozdova[56], D. Du[62a], T. A. du Pree[115], F. Dubinin[37], M. Dubovsky[28a], E. Duchovni[170], G. Duckeck[110], O. A. Ducu[27b], D. Duda[52], A. Dudarev[36], E. R. Duden[26], M. D'uffizi[102], L. Duflot[66], M. Dührssen[36], I. Duminica[27g], A. E. Dumitriu[27b], M. Dunford[63a], S. Dungs[49], K. Dunne[47a,47b], A. Duperrin[103], H. Duran Yildiz[3a], M. Düren[58], A. Durglishvili[150b], B. L. Dwyer[116], G. I. Dyckes[17a], M. Dyndal[86a], B. S. Dziedzic[36], Z. O. Earnshaw[147], G. H. Eberwein[127], B. Eckerova[28a], S. Eggebrecht[55], E. Egidio Purcino De Souza[128], L. F. Ehrke[56], G. Eigen[16], K. Einsweiler[17a], T. Ekelof[162], P. A. Ekman[99], S. El Farkh[35b], Y. El Ghazali[35b], H. El Jarrari[36], A. El Moussaouy[109], V. Ellajosyula[162], M. Ellert[162], F. Ellinghaus[172], N. Ellis[36], J. Elmsheuser[29], M. Elsawy[117a], M. Elsing[36], D. Emeliyanov[135], Y. Enari[154], I. Ene[17a], S. Epari[13], P. A. Erland[87], M. Errenst[172], M. Escalier[66], C. Escobar[164], E. Etzion[152], G. Evans[131a], H. Evans[68], L. S. Evans[96], A. Ezhilov[37], S. Ezzarqtouni[35a], F. Fabbri[23a,23b], L. Fabbri[23a,23b], G. Facini[97], V. Fadeyev[137], R. M. Fakhrutdinov[37], D. Fakoudis[101], S. Falciano[75a], L. F. Falda Ulhoa Coelho[36], F. Fallavollita[111], J. Faltova[134], C. Fan[163], Y. Fan[14a], Y. Fang[14a,14e], M. Fanti[71a,71b], M. Faraj[69a,69b], Z. Farazpay[98], A. Farbin[8], A. Farilla[77a], T. Farooque[108], S. M. Farrington[52], F. Fassi[35e], D. Fassouliotis[9], M. Faucci Giannelli[76a,76b], W. J. Fawcett[32], L. Fayard[66], P. Federic[134], P. Federicova[132], O. L. Fedin[37,a], M. Feickert[171], L. Feligioni[103], D. E. Fellers[124], C. Feng[62b], M. Feng[14b], Z. Feng[115], M. J. Fenton[160], L. Ferencz[48], R. A. M. Ferguson[92], S. I. Fernandez Luengo[138f], P. Fernandez Martinez[13], M. J. V. Fernoux[103], J. Ferrando[92], A. Ferrari[162], P. Ferrari[114,115], R. Ferrari[73a], D. Ferrere[56], C. Ferretti[107], F. Fiedler[101], P. Fiedler[133], A. Filipčič[94], E. K. Filmer[1], F. Filthaut[114], M. C. N. Fiolhais[131a,131c,c], L. Fiorini[164], W. C. Fisher[108], T. Fitschen[102], P. M. Fitzhugh[136], I. Fleck[142], P. Fleischmann[107], T. Flick[172], M. Flores[33d,aa], L. R. Flores Castillo[64a], L. Flores Sanz De Acedo[36], F. M. Follega[78a,78b], N. Fomin[16], J. H. Foo[156], A. Formica[136], A. C. Forti[102], E. Fortin[36], A. W. Fortman[17a], M. G. Foti[17a], L. Fountas[9,i], D. Fournier[66], H. Fox[92], P. Francavilla[74a,74b], S. Francescato[61], S. Franchellucci[56], M. Franchini[23a,23b], S. Franchino[63a], D. Francis[36], L. Franco[114], V. Franco Lima[36], L. Franconi[48], M. Franklin[61], G. Frattari[26], Y. Y. Frid[152], J. Friend[59], N. Fritzsche[50], A. Froch[54], D. Froidevaux[36], J. A. Frost[127], Y. Fu[62a], S. Fuenzalida Garrido[138f], M. Fujimoto[103], K. Y. Fung[64a], E. Furtado De Simas Filho[83e], M. Furukawa[154], J. Fuster[164], A. Gabrielli[23a,23b], A. Gabrielli[156], P. Gadow[36], G. Gagliardi[57a,57b], L. G. Gagnon[17a], S. Gaid[161], S. Galantzan[152], E. J. Gallas[127], B. J. Gallop[135], K. K. Gan[120], S. Ganguly[154], Y. Gao[52], F. M. Garay Walls[138a,138b], B. Garcia[29], C. García[164], A. Garcia Alonso[115], A. G. Garcia Caffaro[173], J. E. García Navarro[164], M. Garcia-Sciveres[17a], G. L. Gardner[129], R. W. Gardner[39], N. Garelli[159], D. Garg[80], R. B. Garg[144], J. M. Gargan[52], C. A. Garner[156], C. M. Garvey[33a], V. K. Gassmann[159], G. Gaudio[73a], V. Gautam[13], P. Gauzzi[75a,75b], I. L. Gavrilenko[37], A. Gavrilyuk[37], C. Gay[165], G. Gaycken[48], E. N. Gazis[10], A. A. Geanta[27b], C. M. Gee[137], A. Gekow[120], C. Gemme[57b], M. H. Genest[60], A. D. Gentry[113], S. George[96], W. F. George[20], T. Geralis[46], P. Gessinger-Befurt[36], M. E. Geyik[172], M. Ghani[168], K. Ghorbanian[95], A. Ghosal[142], A. Ghosh[160], A. Ghosh[7], B. Giacobbe[23b], S. Giagu[75a,75b], T. Giani[115], P. Giannetti[74a], A. Giannini[62a], S. M. Gibson[96], M. Gignac[137], D. T. Gil[86b], A. K. Gilbert[86a], B. J. Gilbert[41], D. Gillberg[34], G. Gilles[115], L. Ginabat[128], D. M. Gingrich[2,ad], M. P. Giordani[69a,69c], P. F. Giraud[136], G. Giugliarelli[69a,69c], D. Giugni[71a], F. Giuli[36], I. Gkialas[9,i], L. K. Gladilin[37], C. Glasman[100], G. R. Gledhill[124], G. Glemža[48], M. Glisic[124], I. Gnesi[43b,e], Y. Go[29], M. Goblirsch-Kolb[36], B. Gocke[49], D. Godin[109], B. Gokturk[21a], S. Goldfarb[106], T. Golling[56], M. G. D. Gololo[33g], D. Golubkov[37], J. P. Gombas[108], A. Gomes[131a,131b], G. Gomes Da Silva[142], A. J. Gomez Delegido[164], R. Gonçalo[131a], L. Gonella[20], A. Gongadze[150c], F. Gonnella[20], J. L. Gonski[144], R. Y. González Andana[52], S. González de la Hoz[164], R. Gonzalez Lopez[93], C. Gonzalez Renteria[17a], M. V. Gonzalez Rodrigues[48], R. Gonzalez Suarez[162], S. Gonzalez-Sevilla[56], L. Goossens[36], B. Gorini[36], E. Gorini[70a,70b], A. Gorišek[94], T. C. Gosart[129], A. T. Goshaw[51], M. I. Gostkin[38], S. Goswami[122], C. A. Gottardo[36], S. A. Gotz[110], M. Gouighri[35b], V. Goumarre[48], A. G. Goussiou[139], N. Govender[33c], I. Grabowska-Bold[86a], K. Graham[34], E. Gramstad[126], S. Grancagnolo[70a,70b], C. M. Grant[1,136], P. M. Gravila[27f], F. G. Gravili[70a,70b], H. M. Gray[17a], M. Greco[70a,70b], C. Grefe[24], A. S. Grefsrud[16], I. M. Gregor[48], K. T. Greif[160], P. Grenier[144], S. G. Grewe[111], A. A. Grillo[137], K. Grimm[31], S. Grinstein[13,r], J.-F. Grivaz[66], E. Gross[170], J. Grosse-Knetter[55], J. C. Grundy[127], L. Guan[107], J. G. R. Guerrero Rojas[164], G. Guerrieri[69a,69c], F. Guescini[111], R. Gugel[101], J. A. M. Guhit[107], A. Guida[18], E. Guilloton[168], S. Guindon[36], F. Guo[14a,14e], J. Guo[62c], L. Guo[48], Y. Guo[107], R. Gupta[130], S. Gurbuz[24], S. S. Gurdasani[54], G. Gustavino[36], M. Guth[56], P. Gutierrez[121], L. F. Gutierrez Zagazeta[129], M. Gutsche[50], C. Gutschow[97],

C. Gwenlan[127], C. B. Gwilliam[93], E. S. Haaland[126], A. Haas[118], M. Habedank[48], C. Haber[17a], H. K. Hadavand[8], A. Hadef[50], S. Hadzic[111], A. I. Hagan[92], J. J. Hahn[142], E. H. Haines[97], M. Haleem[167], J. Haley[122], J. J. Hall[140], G. D. Hallewell[103], L. Halser[19], K. Hamano[166], M. Hamer[24], G. N. Hamity[52], E. J. Hampshire[96], J. Han[62b], K. Han[62a], L. Han[14c], L. Han[62a], S. Han[17a], Y. F. Han[156], K. Hanagaki[84], M. Hance[137], D. A. Hangal[41], H. Hanif[143], M. D. Hank[129], J. B. Hansen[42], P. H. Hansen[42], K. Hara[158], D. Harada[56], T. Harenberg[172], S. Harkusha[37], M. L. Harris[104], Y. T. Harris[127], J. Harrison[13], N. M. Harrison[120], P. F. Harrison[168], N. M. Hartman[111], N. M. Hartmann[110], R. Z. Hasan[96,135], Y. Hasegawa[141], S. Hassan[16], R. Hauser[108], C. M. Hawkes[20], R. J. Hawkings[36], Y. Hayashi[154], S. Hayashida[112], D. Hayden[108], C. Hayes[107], R. L. Hayes[115], C. P. Hays[127], J. M. Hays[95], H. S. Hayward[93], F. He[62a], M. He[14a,14e], Y. He[155], Y. He[48], Y. He[97], N. B. Heatley[95], V. Hedberg[99], A. L. Heggelund[126], N. D. Hehir[95,*], C. Heidegger[54], K. K. Heidegger[54], W. D. Heidorn[81], J. Heilman[34], S. Heim[48], T. Heim[17a], J. G. Heinlein[129], J. J. Heinrich[124], L. Heinrich[111,ab], J. Hejbal[132], A. Held[171], S. Hellesund[16], C. M. Helling[165], S. Hellman[47a,47b], R. C. W. Henderson[92], L. Henkelmann[32], A. M. Henriques Correia[36], H. Herde[99], Y. Hernández Jiménez[146], L. M. Herrmann[24], T. Herrmann[50], G. Herten[54], R. Hertenberger[110], L. Hervas[36], M. E. Hesping[101], N. P. Hessey[157a], M. Hidaoui[35b], E. Hill[156], S. J. Hillier[20], J. R. Hinds[108], F. Hinterkeuser[24], M. Hirose[125], S. Hirose[158], D. Hirschbuehl[172], T. G. Hitchings[102], B. Hiti[94], J. Hobbs[146], R. Hobincu[27e], N. Hod[170], M. C. Hodgkinson[140], B. H. Hodkinson[127], A. Hoecker[36], D. D. Hofer[107], J. Hofer[48], T. Holm[24], M. Holzbock[111], L. B. A. H. Hommels[32], B. P. Honan[102], J. J. Hong[68], J. Hong[62c], T. M. Hong[130], B. H. Hooberman[163], W. H. Hopkins[6], M. C. Hoppesch[163], Y. Horii[112], S. Hou[149], A. S. Howard[94], J. Howarth[59], J. Hoya[6], M. Hrabovsky[123], A. Hrynevich[48], T. Hryn'ova[4], P. J. Hsu[65], S.-C. Hsu[139], T. Hsu[66], M. Hu[17a], Q. Hu[62a], S. Huang[64b], X. Huang[14a,14e], Y. Huang[140], Y. Huang[101], Y. Huang[14a], Z. Huang[102], Z. Hubacek[133], M. Huebner[24], F. Huegging[24], T. B. Huffman[127], C. A. Hugli[48], M. Huhtinen[36], S. K. Huiberts[16], R. Hulsken[105], N. Huseynov[12], J. Huston[108], J. Huth[61], R. Hyneman[144], G. Iacobucci[56], G. Iakovidis[29], L. Iconomidou-Fayard[66], J. P. Iddon[36], P. Iengo[72a,72b], R. Iguchi[154], T. Iizawa[127], Y. Ikegami[84], N. Ilic[156], H. Imam[35a], M. Ince Lezki[56], T. Ingebretsen Carlson[47a,47b], G. Introzzi[73a,73b], M. Iodice[77a], V. Ippolito[75a,75b], R. K. Irwin[93], M. Ishino[154], W. Islam[171], C. Issever[18,48], S. Istin[21a,ah], H. Ito[169], R. Iuppa[78a,78b], A. Ivina[170], J. M. Izen[45], V. Izzo[72a], P. Jacka[132], P. Jackson[1], C. S. Jagfeld[110], G. Jain[157a], P. Jain[48], K. Jakobs[54], T. Jakoubek[170], J. Jamieson[59], M. Javurkova[104], L. Jeanty[124], J. Jejelava[150a,y], P. Jenni[54,f], C. E. Jessiman[34], C. Jia[62b], J. Jia[146], X. Jia[61], X. Jia[14a,14e], Z. Jia[14c], C. Jiang[52], S. Jiggins[48], J. Jimenez Pena[13], S. Jin[14c], A. Jinaru[27b], O. Jinnouchi[155], P. Johansson[140], K. A. Johns[7], J. W. Johnson[137], D. M. Jones[147], E. Jones[48], P. Jones[32], R. W. L. Jones[92], T. J. Jones[93], H. L. Joos[55,36], R. Joshi[120], J. Jovicevic[15], X. Ju[17a], J. J. Junggeburth[104], T. Junkermann[63a], A. Juste Rozas[13,r], M. K. Juzek[87], S. Kabana[138e], A. Kaczmarska[87], M. Kado[111], H. Kagan[120], M. Kagan[144], A. Kahn[129], C. Kahra[101], T. Kaji[154], E. Kajomovitz[151], N. Kakati[170], I. Kalaitzidou[54], C. W. Kalderon[29], N. J. Kang[137], D. Kar[33g], K. Karava[127], M. J. Kareem[157b], E. Karentzos[54], O. Karkout[115], S. N. Karpov[38], Z. M. Karpova[38], V. Kartvelishvili[92], A. N. Karyukhin[37], E. Kasimi[153], J. Katzy[48], S. Kaur[34], K. Kawade[141], M. P. Kawale[121], C. Kawamoto[88], T. Kawamoto[62a], E. F. Kay[36], F. I. Kaya[159], S. Kazakos[108], V. F. Kazanin[37], Y. Ke[146], J. M. Keaveney[33a], R. Keeler[166], G. V. Kehris[61], J. S. Keller[34], A. S. Kelly[97], J. J. Kempster[147], P. D. Kennedy[101], O. Kepka[132], B. P. Kerridge[135], S. Kersten[172], B. P. Kerševan[94], L. Keszeghova[28a], S. Ketabchi Haghighat[156], R. A. Khan[130], A. Khanov[122], A. G. Kharlamov[37], T. Kharlamova[37], E. E. Khoda[139], M. Kholodenko[37], T. J. Khoo[18], G. Khoriauli[167], J. Khubua[150b,*], Y. A. R. Khwaira[128], B. Kibirige[33g], D. W. Kim[47a,47b], Y. K. Kim[39], N. Kimura[97], M. K. Kingston[55], A. Kirchhoff[55], C. Kirfel[24], F. Kirfel[24], J. Kirk[135], A. E. Kiryunin[111], C. Kitsaki[10], O. Kivernyk[24], M. Klassen[159], C. Klein[34], L. Klein[167], M. H. Klein[44], S. B. Klein[56], U. Klein[93], P. Klimek[36], A. Klimentov[29], T. Klioutchnikova[36], P. Kluit[115], S. Kluth[111], E. Kneringer[79], T. M. Knight[156], A. Knue[49], R. Kobayashi[88], D. Kobylianskii[170], S. F. Koch[127], M. Kocian[144], P. Kodyš[134], D. M. Koeck[124], P. T. Koenig[24], T. Koffas[34], O. Kolay[50], I. Koletsou[4], T. Komarek[123], K. Köneke[54], A. X. Y. Kong[1], T. Kono[119], N. Konstantinidis[97], P. Kontaxakis[56], B. Konya[99], R. Kopeliansky[41], S. Koperny[86a], K. Korcyl[87], K. Kordas[153,d], A. Korn[97], S. Korn[55], I. Korolkov[13], N. Korotkova[37], B. Kortman[115], O. Kortner[111], S. Kortner[111], W. H. Kostecka[116], V. V. Kostyukhin[142], A. Kotsokechagia[136], A. Koulouris[36], A. Kourkoumeli-Charalampidi[73a,73b], C. Kourkoumelis[9], E. Kourlitis[111,ab], O. Kovanda[124], R. Kowalewski[166], W. Kozanecki[136], A. S. Kozhin[37], V. A. Kramarenko[37], G. Kramberger[94], P. Kramer[101], M. W. Krasny[128], A. Krasznahorkay[36], J. W. Kraus[172], J. A. Kremer[48], T. Kresse[50], J. Kretzschmar[93], K. Kreul[18],

P. Krieger[156], S. Krishnamurthy[104], M. Krivos[134], K. Krizka[20], K. Kroeninger[49], H. Kroha[111], J. Kroll[132], J. Kroll[129], K. S. Krowpman[108], U. Kruchonak[38], H. Krüger[24], N. Krumnack[81], M. C. Kruse[51], O. Kuchinskaia[37], S. Kuday[3a], S. Kuehn[36], R. Kuesters[54], T. Kuhl[48], V. Kukhtin[38], Y. Kulchitsky[37,a], S. Kuleshov[138b,138d], M. Kumar[33g], N. Kumari[48], P. Kumari[157b], A. Kupco[132], T. Kupfer[49], A. Kupich[37], O. Kuprash[54], H. Kurashige[85], L. L. Kurchaninov[157a], O. Kurdysh[66], Y. A. Kurochkin[37], A. Kurova[37], M. Kuze[155], A. K. Kvam[104], J. Kvita[123], T. Kwan[105], N. G. Kyriacou[107], L. A. O. Laatu[103], C. Lacasta[164], F. Lacava[75a,75b], H. Lacker[18], D. Lacour[128], N. N. Lad[97], E. Ladygin[38], A. Lafarge[40], B. Laforge[128], T. Lagouri[173], F. Z. Lahbabi[35a], S. Lai[55], J. E. Lambert[166], S. Lammers[68], W. Lampl[7], C. Lampoudis[153,d], G. Lamprinoudis[101], A. N. Lancaster[116], E. Lançon[29], U. Landgraf[54], M. P. J. Landon[95], V. S. Lang[54], O. K. B. Langrekken[126], A. J. Lankford[160], F. Lanni[36], K. Lantzsch[24], A. Lanza[73a], J. F. Laporte[136], T. Lari[71a], F. Lasagni Manghi[23b], M. Lassnig[36], V. Latonova[132], A. Laudrain[101], A. Laurier[151], S. D. Lawlor[140], Z. Lawrence[102], R. Lazaridou[168], M. Lazzaroni[71a,71b], B. Le[102], E. M. Le Boulicaut[51], L. T. Le Pottier[17a], B. Leban[23a,23b], A. Lebedev[81], M. LeBlanc[102], F. Ledroit-Guillon[60], S. C. Lee[149], S. Lee[47a,47b], T. F. Lee[93], L. L. Leeuw[33c], H. P. Lefebvre[96], M. Lefebvre[166], C. Leggett[17a], G. Lehmann Miotto[36], M. Leigh[56], W. A. Leight[104], W. Leinonen[114], A. Leisos[153,q], M. A. L. Leite[83c], C. E. Leitgeb[18], R. Leitner[134], K. J. C. Leney[44], T. Lenz[24], S. Leone[74a], C. Leonidopoulos[52], A. Leopold[145], C. Leroy[109], R. Les[108], C. G. Lester[32], M. Levchenko[37], J. Levêque[4], L. J. Levinson[170], G. Levrini[23a,23b], M. P. Lewicki[87], C. Lewis[139], D. J. Lewis[4], A. Li[5], B. Li[62b], C. Li[62a], C-Q. Li[111], H. Li[62a], H. Li[62b], H. Li[14c], H. Li[14b], H. Li[62b], J. Li[62c], K. Li[139], L. Li[62c], M. Li[14a,14e], S. Li[14a,14e], S. Li[62c,62d], T. Li[5], X. Li[105], Z. Li[127], Z. Li[154], Z. Li[14a,14e], S. Liang[14a,14e], Z. Liang[14a], M. Liberatore[136], B. Liberti[76a], K. Lie[64c], J. Lieber Marin[83e], H. Lien[68], H. Lin[107], K. Lin[108], R. E. Lindley[7], J. H. Lindon[2], E. Lipeles[129], A. Lipniacka[16], A. Lister[165], J. D. Little[68], B. Liu[14a], B. X. Liu[14d], D. Liu[62c,62d], E. H. L. Liu[20], J. B. Liu[62a], J. K. K. Liu[32], K. Liu[62d], K. Liu[62c,62d], M. Liu[62a], M. Y. Liu[62a], P. Liu[14a], Q. Liu[62c,62d,139], X. Liu[62a], X. Liu[62b], Y. Liu[14d,14e], Y. L. Liu[62b], Y. W. Liu[62a], J. Llorente Merino[143], S. L. Lloyd[95], E. M. Lobodzinska[48], P. Loch[7], T. Lohse[18], K. Lohwasser[140], E. Loiacono[48], M. Lokajicek[132,*], J. D. Lomas[20], J. D. Long[163], I. Longarini[160], R. Longo[163], I. Lopez Paz[67], A. Lopez Solis[48], N. Lorenzo Martinez[4], A. M. Lory[110], M. Losada[117a], G. Löschcke Centeno[147], O. Loseva[37], X. Lou[47a,47b], X. Lou[14a,14e], A. Lounis[66], P. A. Love[92], G. Lu[14a,14e], M. Lu[66], S. Lu[129], Y. J. Lu[65], H. J. Lubatti[139], C. Luci[75a,75b], F. L. Lucio Alves[14c], F. Luehring[68], I. Luise[146], O. Lukianchuk[66], O. Lundberg[145], B. Lund-Jensen[145,*], N. A. Luongo[6], M. S. Lutz[36], A. B. Lux[25], D. Lynn[29], R. Lysak[132], E. Lytken[99], V. Lyubushkin[38], T. Lyubushkina[38], M. M. Lyukova[146], M.Firdaus M. Soberi[52], H. Ma[29], K. Ma[62a], L. L. Ma[62b], W. Ma[62a], Y. Ma[122], G. Maccarrone[53], J. C. MacDonald[101], P. C. Machado De Abreu Farias[83e], R. Madar[40], T. Madula[97], J. Maeda[85], T. Maeno[29], H. Maguire[140], V. Maiboroda[136], A. Maio[131a,131b,131d], K. Maj[86a], O. Majersky[48], S. Majewski[124], N. Makovec[66], V. Maksimovic[15], B. Malaescu[128], Pa. Malecki[87], V. P. Maleev[37], F. Malek[60,m], M. Mali[94], D. Malito[96], U. Mallik[80], S. Maltezos[10], S. Malyukov[38], J. Mamuzic[13], G. Mancini[53], M. N. Mancini[26], G. Manco[73a,73b], J. P. Mandalia[95], I. Mandić[94], L. Manhaes de Andrade Filho[83a], I. M. Maniatis[170], J. Manjarres Ramos[90], D. C. Mankad[170], A. Mann[110], S. Manzoni[36], L. Mao[62c], X. Mapekula[33c], A. Marantis[153,q], G. Marchiori[5], M. Marcisovsky[132], C. Marcon[71a], M. Marinescu[20], S. Marium[48], M. Marjanovic[121], A. Markhoos[54], M. Markovitch[66], E. J. Marshall[92], Z. Marshall[17a], S. Marti-Garcia[164], T. A. Martin[135], V. J. Martin[52], B. Martin dit Latour[16], L. Martinelli[75a,75b], M. Martinez[13,r], P. Martinez Agullo[164], V. I. Martinez Outschoorn[104], P. Martinez Suarez[13], S. Martin-Haugh[135], G. Martinovicova[134], V. S. Martoiu[27b], A. C. Martyniuk[97], A. Marzin[36], D. Mascione[78a,78b], L. Masetti[101], T. Mashimo[154], J. Masik[102], A. L. Maslennikov[37], P. Massarotti[72a,72b], P. Mastrandrea[74a,74b], A. Mastroberardino[43a,43b], T. Masubuchi[154], T. Mathisen[162], J. Matousek[134], N. Matsuzawa[154], J. Maurer[27b], A. J. Maury[66], B. Maček[94], D. A. Maximov[37], A. E. May[102], R. Mazini[149], I. Maznas[116], M. Mazza[108], S. M. Mazza[137], E. Mazzeo[71a,71b], C. Mc Ginn[29], J. P. Mc Gowan[166], S. P. Mc Kee[107], C. C. McCracken[165], E. F. McDonald[106], A. E. McDougall[115], J. A. Mcfayden[147], R. P. McGovern[129], G. Mchedlidze[150b], R. P. Mckenzie[33g], T. C. Mclachlan[48], D. J. Mclaughlin[97], S. J. McMahon[135], C. M. Mcpartland[93], R. A. McPherson[166,v], S. Mehlhase[110], A. Mehta[93], D. Melini[164], B. R. Mellado Garcia[33g], A. H. Melo[55], F. Meloni[48], A. M. Mendes Jacques Da Costa[102], H. Y. Meng[156], L. Meng[92], S. Menke[111], M. Mentink[36], E. Meoni[43a,43b], G. Mercado[116], S. Merianos[153], C. Merlassino[69a,69c], L. Merola[72a,72b], C. Meroni[71a,71b], J. Metcalfe[6], A. S. Mete[6], E. Meuser[101], C. Meyer[68], J-P. Meyer[136], R. P. Middleton[135], L. Mijović[52], G. Mikenberg[170],

M. Mikestikova[132], M. Mikuž[94], H. Mildner[101], A. Milic[36], D. W. Miller[39], E. H. Miller[144], L. S. Miller[34], A. Milov[170], D. A. Milstead[47a,47b], T. Min[14c], A. A. Minaenko[37], I. A. Minashvili[150b], L. Mince[59], A. I. Mincer[118], B. Mindur[86a], M. Mineev[38], Y. Mino[88], L. M. Mir[13], M. Miralles Lopez[59], M. Mironova[17a], A. Mishima[154], M. C. Missio[114], A. Mitra[168], V. A. Mitsou[164], Y. Mitsumori[112], O. Miu[156], P. S. Miyagawa[95], T. Mkrtchyan[63a], M. Mlinarevic[97], T. Mlinarevic[97], M. Mlynarikova[36], S. Mobius[19], P. Mogg[110], M. H. Mohamed Farook[113], A. F. Mohammed[14a,14e], S. Mohapatra[41], G. Mokgatitswane[33g], L. Moleri[170], B. Mondal[142], S. Mondal[133], K. Mönig[48], E. Monnier[103], L. Monsonis Romero[164], J. Montejo Berlingen[13], M. Montella[120], F. Montereali[77a,77b], F. Monticelli[91], S. Monzani[69a,69c], N. Morange[66], A. L. Moreira De Carvalho[48], M. Moreno Llácer[164], C. Moreno Martinez[56], P. Morettini[57b], S. Morgenstern[36], M. Morii[61], M. Morinaga[154], F. Morodei[75a,75b], L. Morvaj[36], P. Moschovakos[36], B. Moser[36], M. Mosidze[150b], T. Moskalets[54], P. Moskvitina[114], J. Moss[31,j], P. Moszkowicz[86a], A. Moussa[35d], E. J. W. Moyse[104], O. Mtintsilana[33g], S. Muanza[103], J. Mueller[130], D. Muenstermann[92], R. Müller[19], G. A. Mullier[162], A. J. Mullin[32], J. J. Mullin[129], D. P. Mungo[156], D. Munoz Perez[164], F. J. Munoz Sanchez[102], M. Murin[102], W. J. Murray[168,135], M. Muškinja[94], C. Mwewa[29], A. G. Myagkov[37,a], A. J. Myers[8], G. Myers[107], M. Myska[133], B. P. Nachman[17a], O. Nackenhorst[49], K. Nagai[127], K. Nagano[84], J. L. Nagle[29,af], E. Nagy[103], A. M. Nairz[36], Y. Nakahama[84], K. Nakamura[84], K. Nakkalil[5], H. Nanjo[125], E. A. Narayanan[113], I. Naryshkin[37], L. Nasella[71a,71b], M. Naseri[34], S. Nasri[117b], C. Nass[24], G. Navarro[22a], J. Navarro-Gonzalez[164], R. Nayak[152], A. Nayaz[18], P. Y. Nechaeva[37], S. Nechaeva[23a,23b], F. Nechansky[48], L. Nedic[127], T. J. Neep[20], A. Negri[73a,73b], M. Negrini[23b], C. Nellist[115], C. Nelson[105], K. Nelson[107], S. Nemecek[132], M. Nessi[36,g], M. S. Neubauer[163], F. Neuhaus[101], J. Neundorf[48], P. R. Newman[20], C. W. Ng[130], Y. W. Y. Ng[48], B. Ngair[117a], H. D. N. Nguyen[109], R. B. Nickerson[127], R. Nicolaidou[136], J. Nielsen[137], M. Niemeyer[55], J. Niermann[55], N. Nikiforou[36], V. Nikolaenko[37,a], I. Nikolic-Audit[128], K. Nikolopoulos[20], P. Nilsson[29], I. Ninca[48], G. Ninio[152], A. Nisati[75a], N. Nishu[2], R. Nisius[111], J-E. Nitschke[50], E. K. Nkadimeng[33g], T. Nobe[154], T. Nommensen[148], M. B. Norfolk[140], R. R. B. Norisam[97], B. J. Norman[34], M. Noury[35a], J. Novak[94], T. Novak[94], L. Novotny[133], R. Novotny[113], L. Nozka[123], K. Ntekas[160], N. M. J. Nunes De Moura Junior[83b], J. Ocariz[128], A. Ochi[85], I. Ochoa[131a], S. Oerdek[48,s], J. T. Offermann[39], A. Ogrodnik[134], A. Oh[102], C. C. Ohm[145], H. Oide[84], R. Oishi[154], M. L. Ojeda[48], Y. Okumura[154], L. F. Oleiro Seabra[131a], S. A. Olivares Pino[138d], G. Oliveira Correa[13], D. Oliveira Damazio[29], D. Oliveira Goncalves[83a], J. L. Oliver[160], Ö. O. Öncel[54], A. P. O'Neill[19], A. Onofre[131a,131e], P. U. E. Onyisi[11], M. J. Oreglia[39], G. E. Orellana[91], D. Orestano[77a,77b], N. Orlando[13], R. S. Orr[156], V. O'Shea[59], L. M. Osojnak[129], R. Ospanov[62a], G. Otero y Garzon[30], H. Otono[89], P. S. Ott[63a], G. J. Ottino[17a], M. Ouchrif[35d], F. Ould-Saada[126], T. Ovsiannikova[139], M. Owen[59], R. E. Owen[135], V. E. Ozcan[21a], F. Ozturk[87], N. Ozturk[8], S. Ozturk[82], H. A. Pacey[127], A. Pacheco Pages[13], C. Padilla Aranda[13], G. Padovano[75a,75b], S. Pagan Griso[17a], G. Palacino[68], A. Palazzo[70a,70b], J. Pampel[24], J. Pan[173], T. Pan[64a], D. K. Panchal[11], C. E. Pandini[115], J. G. Panduro Vazquez[135], H. D. Pandya[1], H. Pang[14b], P. Pani[48], G. Panizzo[69a,69c], L. Panwar[128], L. Paolozzi[56], S. Parajuli[163], A. Paramonov[6], C. Paraskevopoulos[53], D. Paredes Hernandez[64b], A. Pareti[73a,73b], K. R. Park[41], T. H. Park[156], M. A. Parker[32], F. Parodi[57a,57b], E. W. Parrish[116], V. A. Parrish[52], J. A. Parsons[41], U. Parzefall[54], B. Pascual Dias[109], L. Pascual Dominguez[100], E. Pasqualucci[75a], S. Passaggio[57b], F. Pastore[96], P. Patel[87], U. M. Patel[51], J. R. Pater[102], T. Pauly[36], C. I. Pazos[159], J. Pearkes[144], M. Pedersen[126], R. Pedro[131a], S. V. Peleganchuk[37], O. Penc[36], E. A. Pender[52], G. D. Penn[173], K. E. Penski[110], M. Penzin[37], B. S. Peralva[83d], A. P. Pereira Peixoto[139], L. Pereira Sanchez[144], D. V. Perepelitsa[29,af], E. Perez Codina[157a], M. Perganti[10], H. Pernegger[36], S. Perrella[75a,75b], O. Perrin[40], K. Peters[48], R. F. Y. Peters[102], B. A. Petersen[36], T. C. Petersen[42], E. Petit[103], V. Petousis[133], C. Petridou[153,d], T. Petru[134], A. Petrukhin[142], M. Pettee[17a], N. E. Pettersson[36], A. Petukhov[37], K. Petukhova[134], R. Pezoa[138f], L. Pezzotti[36], G. Pezzullo[173], T. M. Pham[171], T. Pham[106], P. W. Phillips[135], G. Piacquadio[146], E. Pianori[17a], F. Piazza[124], R. Piegaia[30], D. Pietreanu[27b], A. D. Pilkington[102], M. Pinamonti[69a,69c], J. L. Pinfold[2], B. C. Pinheiro Pereira[131a], A. E. Pinto Pinoargote[136,136], L. Pintucci[69a,69c], K. M. Piper[147], A. Pirttikoski[56], D. A. Pizzi[34], L. Pizzimento[64b], A. Pizzini[115], M.-A. Pleier[29], V. Pleskot[134], E. Plotnikova[38], G. Poddar[95], R. Poettgen[99], L. Poggioli[128], I. Pokharel[55], S. Polacek[134], G. Polesello[73a], A. Poley[143,157a], A. Polini[23b], C. S. Pollard[168], Z. B. Pollock[120], E. Pompa Pacchi[75a,75b], N. I. Pond[97], D. Ponomarenko[114], L. Pontecorvo[36], S. Popa[27a], G. A. Popeneciu[27d], A. Poreba[36], D. M. Portillo Quintero[157a], S. Pospisil[133], M. A. Postill[140], P. Postolache[27c], K. Potamianos[168], P. A. Potepa[86a], I. N. Potrap[38], C. J. Potter[32], H. Potti[1], J. Poveda[164], M. E. Pozo Astigarraga[36],

A. Prades Ibanez[164], J. Pretel[54], D. Price[102], M. Primavera[70a], M. A. Principe Martin[100], R. Privara[123], T. Procter[59], M. L. Proffitt[139], N. Proklova[129], K. Prokofiev[64c], G. Proto[111], J. Proudfoot[6], M. Przybycien[86a], W. W. Przygoda[86b], A. Psallidas[46], J. E. Puddefoot[140], D. Pudzha[37], D. Pyatiizbyantseva[37], J. Qian[107], D. Qichen[102], Y. Qin[13], T. Qiu[52], A. Quadt[55], M. Queitsch-Maitland[102], G. Quetant[56], R. P. Quinn[165], G. Rabanal Bolanos[61], D. Rafanoharana[54], F. Raffaeli[76a,76b], F. Ragusa[71a,71b], J. L. Rainbolt[39], J. A. Raine[56], S. Rajagopalan[29], E. Ramakoti[37], I. A. Ramirez-Berend[34], K. Ran[48,14e], N. P. Rapheeha[33g], H. Rasheed[27b], V. Raskina[128], D. F. Rassloff[63a], A. Rastogi[17a], S. Rave[101], B. Ravina[55], I. Ravinovich[170], M. Raymond[36], A. L. Read[126], N. P. Readioff[140], D. M. Rebuzzi[73a,73b], G. Redlinger[29], A. S. Reed[111], K. Reeves[26], J. A. Reidelsturz[172], D. Reikher[152], A. Rej[49], C. Rembser[36], M. Renda[27b], M. B. Rendel[111], F. Renner[48], A. G. Rennie[160], A. L. Rescia[48], S. Resconi[71a], M. Ressegotti[57a,57b], S. Rettie[36], J. G. Reyes Rivera[108], E. Reynolds[17a], O. L. Rezanova[37], P. Reznicek[134], H. Riani[35d], N. Ribaric[92], E. Ricci[78a,78b], R. Richter[111], S. Richter[47a,47b], E. Richter-Was[86b], M. Ridel[128], S. Ridouani[35d], P. Rieck[118], P. Riedler[36], E. M. Riefel[47a,47b], J. O. Rieger[115], M. Rijssenbeek[146], M. Rimoldi[36], L. Rinaldi[23a,23b], T. T. Rinn[29], M. P. Rinnagel[110], G. Ripellino[162], I. Riu[13], J. C. Rivera Vergara[166], F. Rizatdinova[122], E. Rizvi[95], B. R. Roberts[17a], S. H. Robertson[105,v], D. Robinson[32], C. M. Robles Gajardo[138f], M. Robles Manzano[101], A. Robson[59], A. Rocchi[76a,76b], C. Roda[74a,74b], S. Rodriguez Bosca[36], Y. Rodriguez Garcia[22a], A. Rodriguez Rodriguez[54], A. M. Rodríguez Vera[116], S. Roe[36], J. T. Roemer[160], A. R. Roepe-Gier[137], J. Roggel[172], O. Røhne[126], R. A. Rojas[104], C. P. A. Roland[128], J. Roloff[29], A. Romaniouk[37], E. Romano[73a,73b], M. Romano[23b], A. C. Romero Hernandez[163], N. Rompotis[93], L. Roos[128], S. Rosati[75a], B. J. Rosser[39], E. Rossi[127], E. Rossi[72a,72b], L. P. Rossi[61], L. Rossini[54], R. Rosten[120], M. Rotaru[27b], B. Rottler[54], C. Rougier[90], D. Rousseau[66], D. Rousso[48], A. Roy[163], S. Roy-Garand[156], A. Rozanov[103], Z. M. A. Rozario[59], Y. Rozen[151], A. Rubio Jimenez[164], A. J. Ruby[93], V. H. Ruelas Rivera[18], T. A. Ruggeri[1], A. Ruggiero[127], A. Ruiz-Martinez[164], A. Rummler[36], Z. Rurikova[54], N. A. Rusakovich[38], H. L. Russell[166], G. Russo[75a,75b], J. P. Rutherfoord[7], S. Rutherford Colmenares[32], M. Rybar[134], E. B. Rye[126], A. Ryzhov[44], J. A. Sabater Iglesias[56], P. Sabatini[164], H.F-W. Sadrozinski[137], F. Safai Tehrani[75a], B. Safarzadeh Samani[135], S. Saha[1], M. Sahinsoy[111], A. Saibel[164], M. Saimpert[136], M. Saito[154], T. Saito[154], A. Sala[71a,71b], D. Salamani[36], A. Salnikov[144], J. Salt[164], A. Salvador Salas[152], D. Salvatore[43a,43b], F. Salvatore[147], A. Salzburger[36], D. Sammel[54], E. Sampson[92], D. Sampsonidis[153,d], D. Sampsonidou[124], J. Sánchez[164], V. Sanchez Sebastian[164], H. Sandaker[126], C. O. Sander[48], J. A. Sandesara[104], M. Sandhoff[172], C. Sandoval[22b], L. Sanfilippo[63a], D. P. C. Sankey[135], T. Sano[88], A. Sansoni[53], L. Santi[75a,75b], C. Santoni[40], H. Santos[131a,131b], A. Santra[170], E. Sanzani[23a,23b], K. A. Saoucha[161], J. G. Saraiva[131a,131d], J. Sardain[7], O. Sasaki[84], K. Sato[158], C. Sauer[63b], E. Sauvan[4], P. Savard[156,ad], R. Sawada[154], C. Sawyer[135], L. Sawyer[98], C. Sbarra[23b], A. Sbrizzi[23a,23b], T. Scanlon[97], J. Schaarschmidt[139], U. Schäfer[101], A. C. Schaffer[66,44], D. Schaile[110], R. D. Schamberger[146], C. Scharf[18], M. M. Schefer[19], V. A. Schegelsky[37], D. Scheirich[134], M. Schernau[160], C. Scheulen[55], C. Schiavi[57a,57b], M. Schioppa[43a,43b], B. Schlag[144,l], K. E. Schleicher[54], S. Schlenker[36], J. Schmeing[172], M. A. Schmidt[172], K. Schmieden[101], C. Schmitt[101], N. Schmitt[101], S. Schmitt[48], L. Schoeffel[136], A. Schoening[63b], P. G. Scholer[34], E. Schopf[127], M. Schott[24], J. Schovancova[36], S. Schramm[56], T. Schroer[56], H-C. Schultz-Coulon[63a], M. Schumacher[54], B. A. Schumm[137], Ph. Schune[136], A. J. Schuy[139], H. R. Schwartz[137], A. Schwartzman[144], T. A. Schwarz[107], Ph. Schwemling[136], R. Schwienhorst[108], A. Sciandra[29], G. Sciolla[26], F. Scuri[74a], C. D. Sebastiani[93], K. Sedlaczek[116], S. C. Seidel[113], A. Seiden[137], B. D. Seidlitz[41], C. Seitz[48], J. M. Seixas[83b], G. Sekhniaidze[72a], L. Selem[60], N. Semprini-Cesari[23a,23b], D. Sengupta[56], V. Senthilkumar[164], L. Serin[66], M. Sessa[76a,76b], H. Severini[121], F. Sforza[57a,57b], A. Sfyrla[56], Q. Sha[14a], E. Shabalina[55], A. H. Shah[32], R. Shaheen[145], J. D. Shahinian[129], D. Shaked Renous[170], L. Y. Shan[14a], M. Shapiro[17a], A. Sharma[36], A. S. Sharma[165], P. Sharma[80], P. B. Shatalov[37], K. Shaw[147], S. M. Shaw[102], Q. Shen[5,62c], D. J. Sheppard[143], P. Sherwood[97], L. Shi[97], X. Shi[14a], C. O. Shimmin[173], J. D. Shinner[96], I. P. J. Shipsey[127], S. Shirabe[89], M. Shiyakova[38,t], M. J. Shochet[39], J. Shojaii[106], D. R. Shope[126], B. Shrestha[121], S. Shrestha[120,ag], M. J. Shroff[166], P. Sicho[132], A. M. Sickles[163], E. Sideras Haddad[33g], A. C. Sidley[115], A. Sidoti[23b], F. Siegert[50], Dj. Sijacki[15], F. Sili[91], J. M. Silva[52], M. V. Silva Oliveira[29], S. B. Silverstein[47a], S. Simion[66], R. Simoniello[36], E. L. Simpson[102], H. Simpson[147], L. R. Simpson[107], N. D. Simpson[99], S. Simsek[82], S. Sindhu[55], P. Sinervo[156], S. Singh[156], S. Sinha[48], S. Sinha[102], M. Sioli[23a,23b], I. Siral[36], E. Sitnikova[48], J. Sjölin[47a,47b], A. Skaf[55], E. Skorda[20], P. Skubic[121], M. Slawinska[87], V. Smakhtin[170], B. H. Smart[135], S.Yu. Smirnov[37], Y. Smirnov[37], L. N. Smirnova[37,a], O. Smirnova[99], A. C. Smith[41], D. R. Smith[160],

E. A. Smith[39], H. A. Smith[127], J. L. Smith[102], R. Smith[144], M. Smizanska[92], K. Smolek[133], A. A. Snesarev[37], S. R. Snider[156], H. L. Snoek[115], S. Snyder[29], R. Sobie[166,v], A. Soffer[152], C. A. Solans Sanchez[36], E.Yu. Soldatov[37], U. Soldevila[164], A. A. Solodkov[37], S. Solomon[26], A. Soloshenko[38], K. Solovieva[54], O. V. Solovyanov[40], P. Sommer[36], A. Sonay[13], W. Y. Song[157b], A. Sopczak[133], A. L. Sopio[97], F. Sopkova[28b], J. D. Sorenson[113], I. R. Sotarriva Alvarez[155], V. Sothilingam[63a], O. J. Soto Sandoval[138b,138c], S. Sottocornola[68], R. Soualah[161], Z. Soumaimi[35e], D. South[48], N. Soybelman[170], S. Spagnolo[70a,70b], M. Spalla[111], D. Sperlich[54], G. Spigo[36], S. Spinali[92], D. P. Spiteri[59], M. Spousta[134], E. J. Staats[34], R. Stamen[63a], A. Stampekis[20], M. Standke[24], E. Stanecka[87], W. Stanek-Maslouska[48], M. V. Stange[50], B. Stanislaus[17a], M. M. Stanitzki[48], B. Stapf[48], E. A. Starchenko[37], G. H. Stark[137], J. Stark[90], P. Staroba[132], P. Starovoitov[63a], S. Stärz[105], R. Staszewski[87], G. Stavropoulos[46], J. Steentoft[162], P. Steinberg[29], B. Stelzer[143,157a], H. J. Stelzer[130], O. Stelzer-Chilton[157a], H. Stenzel[58], T. J. Stevenson[147], G. A. Stewart[36], J. R. Stewart[122], M. C. Stockton[36], G. Stoicea[27b], M. Stolarski[131a], S. Stonjek[111], A. Straessner[50], J. Strandberg[145], S. Strandberg[47a,47b], M. Stratmann[172], M. Strauss[121], T. Strebler[103], P. Strizenec[28b], R. Ströhmer[167], D. M. Strom[124], R. Stroynowski[44], A. Strubig[47a,47b], S. A. Stucci[29], B. Stugu[16], J. Stupak[121], N. A. Styles[48], D. Su[144], S. Su[62a], W. Su[62d], X. Su[62a], D. Suchy[28a], K. Sugizaki[154], V. V. Sulin[37], M. J. Sullivan[93], D. M. S. Sultan[127], L. Sultanaliyeva[37], S. Sultansoy[3b], T. Sumida[88], S. Sun[107], S. Sun[171], O. Sunneborn Gudnadottir[162], N. Sur[103], M. R. Sutton[147], H. Suzuki[158], M. Svatos[132], M. Swiatlowski[157a], T. Swirski[167], I. Sykora[28a], M. Sykora[134], T. Sykora[134], D. Ta[101], K. Tackmann[48,s], A. Taffard[160], R. Tafirout[157a], J. S. Tafoya Vargas[66], Y. Takubo[84], M. Talby[103], A. A. Talyshev[37], K. C. Tam[64b], N. M. Tamir[152], A. Tanaka[154], J. Tanaka[154], R. Tanaka[66], M. Tanasini[146], Z. Tao[165], S. Tapia Araya[138f], S. Tapprogge[101], A. Tarek Abouelfadl Mohamed[108], S. Tarem[151], K. Tariq[14a], G. Tarna[27b], G. F. Tartarelli[71a], M. J. Tartarin[90], P. Tas[134], M. Tasevsky[132], E. Tassi[43a,43b], A. C. Tate[163], G. Tateno[154], Y. Tayalati[35e,u], G. N. Taylor[106], W. Taylor[157b], A. S. Tee[171], R. Teixeira De Lima[144], P. Teixeira-Dias[96], J. J. Teoh[156], K. Terashi[154], J. Terron[100], S. Terzo[13], M. Testa[53], R. J. Teuscher[156,v], A. Thaler[79], O. Theiner[56], N. Themistokleous[52], T. Theveneaux-Pelzer[103], O. Thielmann[172], D. W. Thomas[96], J. P. Thomas[20], E. A. Thompson[17a], P. D. Thompson[20], E. Thomson[129], R. E. Thornberry[44], C. Tian[62a], Y. Tian[55], V. Tikhomirov[37,a], Yu.A. Tikhonov[37], S. Timoshenko[37], D. Timoshyn[134], E. X. L. Ting[1], P. Tipton[173], A. Tishelman-Charny[29], S. H. Tlou[33g], K. Todome[155], S. Todorova-Nova[134], S. Todt[50], L. Toffolin[69a,69c], M. Togawa[84], J. Tojo[89], S. Tokár[28a], K. Tokushuku[84], O. Toldaiev[68], R. Tombs[32], M. Tomoto[84,112], L. Tompkins[144,l], K. W. Topolnicki[86b], E. Torrence[124], H. Torres[90], E. Torró Pastor[164], M. Toscani[30], C. Tosciri[39], M. Tost[11], D. R. Tovey[140], A. Traeet[16], I. S. Trandafir[27b], T. Trefzger[167], A. Tricoli[29], I. M. Trigger[157a], S. Trincaz-Duvoid[128], D. A. Trischuk[26], B. Trocmé[60], L. Truong[33c], M. Trzebinski[87], A. Trzupek[87], F. Tsai[146], M. Tsai[107], A. Tsiamis[153,d], P. V. Tsiareshka[37], S. Tsigaridas[157a], A. Tsirigotis[153,q], V. Tsiskaridze[156], E. G. Tskhadadze[150a], M. Tsopoulou[153], Y. Tsujikawa[88], I. I. Tsukerman[37], V. Tsulaia[17a], S. Tsuno[84], K. Tsuri[119], D. Tsybychev[146], Y. Tu[64b], A. Tudorache[27b], V. Tudorache[27b], A. N. Tuna[61], S. Turchikhin[57a,57b], I. Turk Cakir[3a], R. Turra[71a], T. Turtuvshin[38,w], P. M. Tuts[41], S. Tzamarias[153,d], E. Tzovara[101], F. Ukegawa[158], P. A. Ulloa Poblete[138b,138c], E. N. Umaka[29], G. Unal[36], A. Undrus[29], G. Unel[160], J. Urban[28b], P. Urrejola[138a], G. Usai[8], R. Ushioda[155], M. Usman[109], Z. Uysal[82], V. Vacek[133], B. Vachon[105], T. Vafeiadis[36], A. Vaitkus[97], C. Valderanis[110], E. Valdes Santurio[47a,47b], M. Valente[157a], S. Valentinetti[23a,23b], A. Valero[164], E. Valiente Moreno[164], A. Vallier[90], J. A. Valls Ferrer[164], D. R. Van Arneman[115], T. R. Van Daalen[139], A. Van Der Graaf[49], P. Van Gemmeren[6], M. Van Rijnbach[36], S. Van Stroud[97], I. Van Vulpen[115], P. Vana[134], M. Vanadia[76a,76b], W. Vandelli[36], E. R. Vandewall[122], D. Vannicola[152], L. Vannoli[53], R. Vari[75a], E. W. Varnes[7], C. Varni[17b], T. Varol[149], D. Varouchas[66], L. Varriale[164], K. E. Varvell[148], M. E. Vasile[27b], L. Vaslin[84], G. A. Vasquez[166], A. Vasyukov[38], R. Vavricka[101], T. Vazquez Schroeder[36], J. Veatch[31], V. Vecchio[102], M. J. Veen[104], I. Veliscek[29], L. M. Veloce[156], F. Veloso[131a,131c], S. Veneziano[75a], A. Ventura[70a,70b], S. Ventura Gonzalez[136], A. Verbytskyi[111], M. Verducci[74a,74b], C. Vergis[95], M. Verissimo De Araujo[83b], W. Verkerke[115], J. C. Vermeulen[115], C. Vernieri[144], M. Vessella[104], M. C. Vetterli[143,ad], A. Vgenopoulos[153,d], N. Viaux Maira[138f], T. Vickey[140], O. E. Vickey Boeriu[140], G. H. A. Viehhauser[127], L. Vigani[63b], M. Villa[23a,23b], M. Villaplana Perez[164], E. M. Villhauer[52], E. Vilucchi[53], M. G. Vincter[34], A. Visibile[115], C. Vittori[36], I. Vivarelli[23a,23b], E. Voevodina[111], F. Vogel[110], J. C. Voigt[50], P. Vokac[133], Yu. Volkotrub[86b], J. Von Ahnen[48], E. Von Toerne[24], B. Vormwald[36], V. Vorobel[134], K. Vorobev[37], M. Vos[164], K. Voss[142], M. Vozak[115], L. Vozdecky[121], N. Vranjes[15], M. Vranjes Milosavljevic[15], M. Vreeswijk[115], N. K. Vu[62c,62d], R. Vuillermet[36], O. Vujinovic[101], I. Vukotic[39],

S. Wada[158], C. Wagner[104], J. M. Wagner[17a], W. Wagner[172], S. Wahdan[172], H. Wahlberg[91], M. Wakida[112], J. Walder[135], R. Walker[110], W. Walkowiak[142], A. Wall[129], E. J. Wallin[99], T. Wamorkar[6], A. Z. Wang[137], C. Wang[101], C. Wang[11], H. Wang[17a], J. Wang[64c], R. Wang[61], R. Wang[6], S. M. Wang[149], S. Wang[62b], S. Wang[14a], T. Wang[62a], W. T. Wang[80], W. Wang[14a], X. Wang[14c], X. Wang[163], X. Wang[62c], Y. Wang[62d], Y. Wang[14c], Z. Wang[107], Z. Wang[51,62c,62d], Z. Wang[107], A. Warburton[105], R. J. Ward[20], N. Warrack[59], S. Waterhouse[96], A. T. Watson[20], H. Watson[59], M. F. Watson[20], E. Watton[59,135], G. Watts[139], B. M. Waugh[97], J. M. Webb[54], C. Weber[29], H. A. Weber[18], M. S. Weber[19], S. M. Weber[63a], C. Wei[62a], Y. Wei[54], A. R. Weidberg[127], E. J. Weik[118], J. Weingarten[49], C. Weiser[54], C. J. Wells[48], T. Wenaus[29], B. Wendland[49], T. Wengler[36], N. S. Wenke[111], N. Wermes[24], M. Wessels[63a], A. M. Wharton[92], A. S. White[61], A. White[8], M. J. White[1], D. Whiteson[160], L. Wickremasinghe[125], W. Wiedenmann[171], M. Wielers[135], C. Wiglesworth[42], D. J. Wilbern[121], H. G. Wilkens[36], J. J. H. Wilkinson[32], D. M. Williams[41], H. H. Williams[129], S. Williams[32], S. Willocq[104], B. J. Wilson[102], P. J. Windischhofer[39], F. I. Winkel[30], F. Winklmeier[124], B. T. Winter[54], J. K. Winter[102], M. Wittgen[144], M. Wobisch[98], T. Wojtkowski[60], Z. Wolffs[115], J. Wollrath[160], M. W. Wolter[87], H. Wolters[131a,131c], M. C. Wong[137], E. L. Woodward[41], S. D. Worm[48], B. K. Wosiek[87], K. W. Woźniak[87], S. Wozniewski[55], K. Wraight[59], C. Wu[20], M. Wu[14d], M. Wu[114], S. L. Wu[171], X. Wu[56], Y. Wu[62a], Z. Wu[4], J. Wuerzinger[111,ab], T. R. Wyatt[102], B. M. Wynne[52], S. Xella[42], L. Xia[14c], M. Xia[14b], J. Xiang[64c], M. Xie[62a], S. Xin[14a,14e], A. Xiong[124], J. Xiong[17a], D. Xu[14a], H. Xu[62a], L. Xu[62a], R. Xu[129], T. Xu[107], Y. Xu[14b], Z. Xu[52], Z. Xu[14c], B. Yabsley[148], S. Yacoob[33a], Y. Yamaguchi[155], E. Yamashita[154], H. Yamauchi[158], T. Yamazaki[17a], Y. Yamazaki[85], J. Yan[62c], S. Yan[59], Z. Yan[104], H. J. Yang[62c,62d], H. T. Yang[62a], S. Yang[62a], T. Yang[64c], X. Yang[36], X. Yang[14a], Y. Yang[44], Y. Yang[62a], Z. Yang[62a], W-M. Yao[17a], H. Ye[14c], H. Ye[55], J. Ye[14a], S. Ye[29], X. Ye[62a], Y. Yeh[97], I. Yeletskikh[38], B. K. Yeo[17b], M. R. Yexley[97], T. P. Yildirim[127], P. Yin[41], K. Yorita[169], S. Younas[27b], C. J. S. Young[36], C. Young[144], C. Yu[14a,14e], Y. Yu[62a], M. Yuan[107], R. Yuan[62c,62d], L. Yue[97], M. Zaazoua[62a], B. Zabinski[87], E. Zaid[52], Z. K. Zak[87], T. Zakareishvili[164], N. Zakharchuk[34], S. Zambito[56], J. A. Zamora Saa[138b,138d], J. Zang[154], D. Zanzi[54], O. Zaplatilek[133], C. Zeitnitz[172], H. Zeng[14a], J. C. Zeng[163], D. T. Zenger Jr[26], O. Zenin[37], T. Ženiš[28a], S. Zenz[95], S. Zerradi[35a], D. Zerwas[66], M. Zhai[14a,14e], D. F. Zhang[140], J. Zhang[62b], J. Zhang[6], K. Zhang[14a,14e], L. Zhang[62a], L. Zhang[14c], P. Zhang[14a,14e], R. Zhang[171], S. Zhang[107], S. Zhang[90], T. Zhang[154], X. Zhang[62c], X. Zhang[62b], Y. Zhang[62c], Y. Zhang[97], Y. Zhang[14c], Z. Zhang[17a], Z. Zhang[62b], Z. Zhang[66], H. Zhao[139], T. Zhao[62b], Y. Zhao[137], Z. Zhao[62a], Z. Zhao[62a], A. Zhemchugov[38], J. Zheng[14c], K. Zheng[163], X. Zheng[62a], Z. Zheng[144], D. Zhong[163], B. Zhou[107], H. Zhou[7], N. Zhou[62c], Y. Zhou[14b], Y. Zhou[14c], Y. Zhou[7], C. G. Zhu[62b], J. Zhu[107], X. Zhu[62d], Y. Zhu[62c], Y. Zhu[62a], X. Zhuang[14a], K. Zhukov[37], N. I. Zimine[38], J. Zinsser[63b], M. Ziolkowski[142], L. Živković[15], A. Zoccoli[23a,23b], K. Zoch[61], T. G. Zorbas[140], O. Zormpa[46], W. Zou[41], L. Zwalinski[36]

[1] Department of Physics, University of Adelaide, Adelaide, Australia
[2] Department of Physics, University of Alberta, Edmonton, AB, Canada
[3] [(a)]Department of Physics, Ankara University, Ankara, Türkiye; [(b)]Division of Physics, TOBB University of Economics and Technology, Ankara, Türkiye
[4] LAPP, Université Savoie Mont Blanc, CNRS/IN2P3, Annecy, France
[5] APC, Université Paris Cité, CNRS/IN2P3, Paris, France
[6] High Energy Physics Division, Argonne National Laboratory, Argonne, IL, USA
[7] Department of Physics, University of Arizona, Tucson, AZ, USA
[8] Department of Physics, University of Texas at Arlington, Arlington, TX, USA
[9] Physics Department, National and Kapodistrian University of Athens, Athens, Greece
[10] Physics Department, National Technical University of Athens, Zografou, Greece
[11] Department of Physics, University of Texas at Austin, Austin, TX, USA
[12] Institute of Physics, Azerbaijan Academy of Sciences, Baku, Azerbaijan
[13] Institut de Física d'Altes Energies (IFAE), Barcelona Institute of Science and Technology, Barcelona, Spain
[14] [(a)]Institute of High Energy Physics, Chinese Academy of Sciences, Beijing, China; [(b)]Physics Department, Tsinghua University, Beijing, China; [(c)]Department of Physics, Nanjing University, Nanjing, China; [(d)]School of Science, Shenzhen Campus of Sun Yat-sen University, Shenzhen, China; [(e)]University of Chinese Academy of Science (UCAS), Beijing, China
[15] Institute of Physics, University of Belgrade, Belgrade, Serbia

[16] Department for Physics and Technology, University of Bergen, Bergen, Norway
[17] [(a)]Physics Division, Lawrence Berkeley National Laboratory, Berkeley, CA, USA; [(b)]University of California, Berkeley, CA, USA
[18] Institut für Physik, Humboldt Universität zu Berlin, Berlin, Germany
[19] Albert Einstein Center for Fundamental Physics and Laboratory for High Energy Physics, University of Bern, Bern, Switzerland
[20] School of Physics and Astronomy, University of Birmingham, Birmingham, UK
[21] [(a)]Department of Physics, Bogazici University, Istanbul, Türkiye; [(b)]Department of Physics Engineering, Gaziantep University, Gaziantep, Türkiye; [(c)]Department of Physics, Istanbul University, Istanbul, Türkiye
[22] [(a)]Facultad de Ciencias y Centro de Investigaciónes, Universidad Antonio Nariño, Bogotá, Colombia; [(b)]Departamento de Física, Universidad Nacional de Colombia, Bogotá, Colombia
[23] [(a)]Dipartimento di Fisica e Astronomia A. Righi, Università di Bologna, Bologna, Italy; [(b)]INFN Sezione di Bologna, Bologna, Italy
[24] Physikalisches Institut, Universität Bonn, Bonn, Germany
[25] Department of Physics, Boston University, Boston, MA, USA
[26] Department of Physics, Brandeis University, Waltham, MA, USA
[27] [(a)]Transilvania University of Brasov, Brasov, Romania; [(b)]Horia Hulubei National Institute of Physics and Nuclear Engineering, Bucharest, Romania; [(c)]Department of Physics, Alexandru Ioan Cuza University of Iasi, Iasi, Romania; [(d)]Physics Department, National Institute for Research and Development of Isotopic and Molecular Technologies, Cluj-Napoca, Romania; [(e)]National University of Science and Technology Politechnica, Bucharest, Romania; [(f)]West University in Timisoara, Timisoara, Romania; [(g)]Faculty of Physics, University of Bucharest, Bucharest, Romania
[28] [(a)]Faculty of Mathematics, Physics and Informatics, Comenius University, Bratislava, Slovak Republic; [(b)]Department of Subnuclear Physics, Institute of Experimental Physics of the Slovak Academy of Sciences, Kosice, Slovak Republic
[29] Physics Department, Brookhaven National Laboratory, Upton, NY, USA
[30] Universidad de Buenos Aires, Facultad de Ciencias Exactas y Naturales, Departamento de Física, y CONICET, Instituto de Física de Buenos Aires (IFIBA), Buenos Aires, Argentina
[31] California State University, Los Angeles, CA, USA
[32] Cavendish Laboratory, University of Cambridge, Cambridge, UK
[33] [(a)]Department of Physics, University of Cape Town, Cape Town, South Africa; [(b)]iThemba Labs, Cape Town, Western Cape, South Africa; [(c)]Department of Mechanical Engineering Science, University of Johannesburg, Johannesburg, South Africa; [(d)]National Institute of Physics, University of the Philippines Diliman (Philippines), Quezon City, Philippines; [(e)]Department of Physics, University of South Africa, Pretoria, South Africa; [(f)]University of Zululand, KwaDlangezwa, South Africa; [(g)]School of Physics, University of the Witwatersrand, Johannesburg, South Africa
[34] Department of Physics, Carleton University, Ottawa, ON, Canada
[35] [(a)]Faculté des Sciences Ain Chock, Réseau Universitaire de Physique des Hautes Energies-Université Hassan II, Casablanca, Morocco; [(b)]Faculté des Sciences, Université Ibn-Tofail, Kénitra, Morocco; [(c)]Faculté des Sciences Semlalia, Université Cadi Ayyad, LPHEA, Marrakech, Morocco; [(d)]LPMR, Faculté des Sciences, Université Mohamed Premier, Oujda, Morocco; [(e)]Faculté des sciences, Université Mohammed V, Rabat, Morocco; [(f)]Institute of Applied Physics, Mohammed VI Polytechnic University, Ben Guerir, Morocco
[36] CERN, Geneva, Switzerland
[37] Affiliated with an institute covered by a cooperation agreement with CERN, Geneva, Switzerland
[38] Affiliated with an international laboratory covered by a cooperation agreement with CERN, Geneva, Switzerland
[39] Enrico Fermi Institute, University of Chicago, Chicago, IL, USA
[40] LPC, Université Clermont Auvergne, CNRS/IN2P3, Clermont-Ferrand, France
[41] Nevis Laboratory, Columbia University, Irvington, NY, USA
[42] Niels Bohr Institute, University of Copenhagen, Copenhagen, Denmark
[43] [(a)]Dipartimento di Fisica, Università della Calabria, Rende, Italy; [(b)]Laboratori Nazionali di Frascati, INFN Gruppo Collegato di Cosenza, Cosenza, Italy
[44] Physics Department, Southern Methodist University, Dallas, TX, USA
[45] Physics Department, University of Texas at Dallas, Richardson, TX, USA
[46] National Centre for Scientific Research "Demokritos", Agia Paraskevi, Greece
[47] [(a)]Department of Physics, Stockholm University, Stockholm, Sweden; [(b)]Oskar Klein Centre, Stockholm, Sweden

[48] Deutsches Elektronen-Synchrotron DESY, Hamburg and Zeuthen, Germany
[49] Fakultät Physik , Technische Universität Dortmund, Dortmund, Germany
[50] Institut für Kern- und Teilchenphysik, Technische Universität Dresden, Dresden, Germany
[51] Department of Physics, Duke University, Durham, NC, USA
[52] SUPA-School of Physics and Astronomy, University of Edinburgh, Edinburgh, UK
[53] INFN e Laboratori Nazionali di Frascati, Frascati, Italy
[54] Physikalisches Institut, Albert-Ludwigs-Universität Freiburg, Freiburg, Germany
[55] II. Physikalisches Institut, Georg-August-Universität Göttingen, Göttingen, Germany
[56] Département de Physique Nucléaire et Corpusculaire, Université de Genève, Genève, Switzerland
[57] [(a)]Dipartimento di Fisica, Università di Genova, Genova, Italy; [(b)]INFN Sezione di Genova, Genova, Italy
[58] II. Physikalisches Institut, Justus-Liebig-Universität Giessen, Giessen, Germany
[59] SUPA-School of Physics and Astronomy, University of Glasgow, Glasgow, UK
[60] LPSC, Université Grenoble Alpes, CNRS/IN2P3, Grenoble INP, Grenoble, France
[61] Laboratory for Particle Physics and Cosmology, Harvard University, Cambridge, MA, USA
[62] [(a)]Department of Modern Physics and State Key Laboratory of Particle Detection and Electronics, University of Science and Technology of China, Hefei, China; [(b)]Institute of Frontier and Interdisciplinary Science and Key Laboratory of Particle Physics and Particle Irradiation (MOE), Shandong University, Qingdao, China; [(c)]School of Physics and Astronomy, Shanghai Jiao Tong University, Key Laboratory for Particle Astrophysics and Cosmology (MOE), SKLPPC, Shanghai, China; [(d)]Tsung-Dao Lee Institute, Shanghai, China; [(e)]School of Physics and Microelectronics, Zhengzhou University, Zhengzhou, China
[63] [(a)]Kirchhoff-Institut für Physik, Ruprecht-Karls-Universität Heidelberg, Heidelberg, Germany; [(b)]Physikalisches Institut, Ruprecht-Karls-Universität Heidelberg, Heidelberg, Germany
[64] [(a)]Department of Physics, Chinese University of Hong Kong, Shatin, N.T., Hong Kong, China; [(b)]Department of Physics, University of Hong Kong, Hong Kong, China; [(c)]Department of Physics and Institute for Advanced Study, Hong Kong University of Science and Technology, Clear Water Bay, Kowloon, Hong Kong, China
[65] Department of Physics, National Tsing Hua University, Hsinchu, Taiwan
[66] IJCLab, Université Paris-Saclay, CNRS/IN2P3, 91405 Orsay, France
[67] Centro Nacional de Microelectrónica (IMB-CNM-CSIC), Barcelona, Spain
[68] Department of Physics, Indiana University, Bloomington, IN, USA
[69] [(a)]INFN Gruppo Collegato di Udine, Sezione di Trieste, Udine, Italy; [(b)]ICTP, Trieste, Italy; [(c)]Dipartimento Politecnico di Ingegneria e Architettura, Università di Udine, Udine, Italy
[70] [(a)]INFN Sezione di Lecce, Lecce, Italy; [(b)]Dipartimento di Matematica e Fisica, Università del Salento, Lecce, Italy
[71] [(a)]INFN Sezione di Milano, Milan, Italy; [(b)]Dipartimento di Fisica, Università di Milano, Milan, Italy
[72] [(a)]INFN Sezione di Napoli, Naples, Italy; [(b)]Dipartimento di Fisica, Università di Napoli, Naples, Italy
[73] [(a)]INFN Sezione di Pavia, Pavia, Italy; [(b)]Dipartimento di Fisica, Università di Pavia, Pavia, Italy
[74] [(a)]INFN Sezione di Pisa, Pisa, Italy; [(b)]Dipartimento di Fisica E. Fermi, Università di Pisa, Pisa, Italy
[75] [(a)]INFN Sezione di Roma, Rome, Italy; [(b)]Dipartimento di Fisica, Sapienza Università di Roma, Rome, Italy
[76] [(a)]INFN Sezione di Roma Tor Vergata, Rome, Italy; [(b)]Dipartimento di Fisica, Università di Roma Tor Vergata, Rome, Italy
[77] [(a)]INFN Sezione di Roma Tre, Rome, Italy; [(b)]Dipartimento di Matematica e Fisica, Università Roma Tre, Rome, Italy
[78] [(a)]INFN-TIFPA, Povo, Italy; [(b)]Università degli Studi di Trento, Trento, Italy
[79] Universität Innsbruck, Department of Astro and Particle Physics, Innsbruck, Austria
[80] University of Iowa, Iowa City, IA, USA
[81] Department of Physics and Astronomy, Iowa State University, Ames, IA, USA
[82] Istinye University, Sariyer, Istanbul, Türkiye
[83] [(a)]Departamento de Engenharia Elétrica, Universidade Federal de Juiz de Fora (UFJF), Juiz de Fora, Brazil; [(b)]Universidade Federal do Rio De Janeiro COPPE/EE/IF, Rio de Janeiro, Brazil; [(c)]Instituto de Física, Universidade de São Paulo, São Paulo, Brazil; [(d)]Rio de Janeiro State University, Rio de Janeiro, Brazil; [(e)]Federal University of Bahia, Bahia, Brazil
[84] KEK, High Energy Accelerator Research Organization, Tsukuba, Japan
[85] Graduate School of Science, Kobe University, Kobe, Japan
[86] [(a)]AGH University of Krakow, Faculty of Physics and Applied Computer Science, Krakow, Poland; [(b)]Marian Smoluchowski Institute of Physics, Jagiellonian University, Krakow, Poland

[87] Institute of Nuclear Physics Polish Academy of Sciences, Krakow, Poland
[88] Faculty of Science, Kyoto University, Kyoto, Japan
[89] Research Center for Advanced Particle Physics and Department of Physics, Kyushu University, Fukuoka , Japan
[90] L2IT, Université de Toulouse, CNRS/IN2P3, UPS, Toulouse, France
[91] Instituto de Física La Plata, Universidad Nacional de La Plata and CONICET, La Plata, Argentina
[92] Physics Department, Lancaster University, Lancaster, UK
[93] Oliver Lodge Laboratory, University of Liverpool, Liverpool, UK
[94] Department of Experimental Particle Physics, Jožef Stefan Institute and Department of Physics, University of Ljubljana, Ljubljana, Slovenia
[95] School of Physics and Astronomy, Queen Mary University of London, London, UK
[96] Department of Physics, Royal Holloway University of London, Egham, UK
[97] Department of Physics and Astronomy, University College London, London, UK
[98] Louisiana Tech University, Ruston, LA, USA
[99] Fysiska institutionen, Lunds universitet, Lund, Sweden
[100] Departamento de Física Teorica C-15 and CIAFF, Universidad Autónoma de Madrid, Madrid, Spain
[101] Institut für Physik, Universität Mainz, Mainz, Germany
[102] School of Physics and Astronomy, University of Manchester, Manchester, UK
[103] CPPM, Aix-Marseille Université, CNRS/IN2P3, Marseille, France
[104] Department of Physics, University of Massachusetts, Amherst, MA, USA
[105] Department of Physics, McGill University, Montreal, QC, Canada
[106] School of Physics, University of Melbourne, Victoria, Australia
[107] Department of Physics, University of Michigan, Ann Arbor, MI, USA
[108] Department of Physics and Astronomy, Michigan State University, East Lansing, MI, USA
[109] Group of Particle Physics, University of Montreal, Montreal, QC, Canada
[110] Fakultät für Physik, Ludwig-Maximilians-Universität München, München, Germany
[111] Max-Planck-Institut für Physik (Werner-Heisenberg-Institut), München, Germany
[112] Graduate School of Science and Kobayashi-Maskawa Institute, Nagoya University, Nagoya, Japan
[113] Department of Physics and Astronomy, University of New Mexico, Albuquerque, NM, USA
[114] Institute for Mathematics, Astrophysics and Particle Physics, Radboud University/Nikhef, Nijmegen, Netherlands
[115] Nikhef National Institute for Subatomic Physics and University of Amsterdam, Amsterdam, Netherlands
[116] Department of Physics, Northern Illinois University, DeKalb, IL, USA
[117] [(a)]New York University Abu Dhabi, Abu Dhabi, United Arab Emirates; [(b)]United Arab Emirates University, Al Ain, United Arab Emirates
[118] Department of Physics, New York University, New York, NY, USA
[119] Ochanomizu University, Otsuka, Bunkyo-ku, Tokyo, Japan
[120] Ohio State University, Columbus, OH, USA
[121] Homer L. Dodge Department of Physics and Astronomy, University of Oklahoma, Norman, OK, USA
[122] Department of Physics, Oklahoma State University, Stillwater, OK, USA
[123] Palacký University, Joint Laboratory of Optics, Olomouc, Czech Republic
[124] Institute for Fundamental Science, University of Oregon, Eugene, OR, USA
[125] Graduate School of Science, Osaka University, Osaka, Japan
[126] Department of Physics, University of Oslo, Oslo, Norway
[127] Department of Physics, Oxford University, Oxford, UK
[128] LPNHE, Sorbonne Université, Université Paris Cité, CNRS/IN2P3, Paris, France
[129] Department of Physics, University of Pennsylvania, Philadelphia, PA, USA
[130] Department of Physics and Astronomy, University of Pittsburgh, Pittsburgh, PA, USA
[131] [(a)]Laboratório de Instrumentação e Física Experimental de Partículas-LIP, Lisbon, Portugal; [(b)]Departamento de Física, Faculdade de Ciências, Universidade de Lisboa, Lisbon, Portugal; [(c)]Departamento de Física, Universidade de Coimbra, Coimbra, Portugal; [(d)]Centro de Física Nuclear da Universidade de Lisboa, Lisbon, Portugal; [(e)]Departamento de Física, Universidade do Minho, Braga, Portugal; [(f)]Departamento de Física Teórica y del Cosmos, Universidad de Granada, Granada, Spain; [(g)]Departamento de Física, Instituto Superior Técnico, Universidade de Lisboa, Lisbon, Portugal
[132] Institute of Physics of the Czech Academy of Sciences, Prague, Czech Republic
[133] Czech Technical University in Prague, Prague, Czech Republic

[134] Charles University, Faculty of Mathematics and Physics, Prague, Czech Republic
[135] Particle Physics Department, Rutherford Appleton Laboratory, Didcot, UK
[136] IRFU, CEA, Université Paris-Saclay, Gif-sur-Yvette, France
[137] Santa Cruz Institute for Particle Physics, University of California Santa Cruz, Santa Cruz, CA, USA
[138] [(a)]Departamento de Física, Pontificia Universidad Católica de Chile, Santiago, Chile; [(b)]Millennium Institute for Subatomic physics at high energy frontier (SAPHIR), Santiago, Chile; [(c)]Instituto de Investigación Multidisciplinario en Ciencia y Tecnología y Departamento de Física, Universidad de La Serena, La Serena, Chile; [(d)]Universidad Andres Bello, Department of Physics, Santiago, Chile; [(e)]Instituto de Alta Investigación, Universidad de Tarapacá, Arica, Chile; [(f)]Departamento de Física, Universidad Técnica Federico Santa María, Valparaíso, Chile
[139] Department of Physics, University of Washington, Seattle, WA, USA
[140] Department of Physics and Astronomy, University of Sheffield, Sheffield, UK
[141] Department of Physics, Shinshu University, Nagano, Japan
[142] Department Physik, Universität Siegen, Siegen, Germany
[143] Department of Physics, Simon Fraser University, Burnaby, BC, Canada
[144] SLAC National Accelerator Laboratory, Stanford, CA, USA
[145] Department of Physics, Royal Institute of Technology, Stockholm, Sweden
[146] Departments of Physics and Astronomy, Stony Brook University, Stony Brook, NY, USA
[147] Department of Physics and Astronomy, University of Sussex, Brighton, UK
[148] School of Physics, University of Sydney, Sydney, Australia
[149] Institute of Physics, Academia Sinica, Taipei, Taiwan
[150] [(a)]E. Andronikashvili Institute of Physics, Iv. Javakhishvili Tbilisi State University, Tbilisi, Georgia; [(b)]High Energy Physics Institute, Tbilisi State University, Tbilisi, Georgia; [(c)]University of Georgia, Tbilisi, Georgia
[151] Department of Physics, Technion, Israel Institute of Technology, Haifa, Israel
[152] Raymond and Beverly Sackler School of Physics and Astronomy, Tel Aviv University, Tel Aviv, Israel
[153] Department of Physics, Aristotle University of Thessaloniki, Thessaloniki, Greece
[154] International Center for Elementary Particle Physics and Department of Physics, University of Tokyo, Tokyo, Japan
[155] Department of Physics, Tokyo Institute of Technology, Tokyo, Japan
[156] Department of Physics, University of Toronto, Toronto, ON, Canada
[157] [(a)]TRIUMF, Vancouver, BC, Canada; [(b)]Department of Physics and Astronomy, York University, Toronto, ON, Canada
[158] Division of Physics and Tomonaga Center for the History of the Universe, Faculty of Pure and Applied Sciences, University of Tsukuba, Tsukuba, Japan
[159] Department of Physics and Astronomy, Tufts University, Medford, MA, USA
[160] Department of Physics and Astronomy, University of California Irvine, Irvine, CA, USA
[161] University of Sharjah, Sharjah, United Arab Emirates
[162] Department of Physics and Astronomy, University of Uppsala, Uppsala, Sweden
[163] Department of Physics, University of Illinois, Urbana, IL, USA
[164] Instituto de Física Corpuscular (IFIC), Centro Mixto Universidad de Valencia-CSIC, Valencia, Spain
[165] Department of Physics, University of British Columbia, Vancouver, BC, Canada
[166] Department of Physics and Astronomy, University of Victoria, Victoria, BC, Canada
[167] Fakultät für Physik und Astronomie, Julius-Maximilians-Universität Würzburg, Würzburg, Germany
[168] Department of Physics, University of Warwick, Coventry, UK
[169] Waseda University, Tokyo, Japan
[170] Department of Particle Physics and Astrophysics, Weizmann Institute of Science, Rehovot, Israel
[171] Department of Physics, University of Wisconsin, Madison, WI, USA
[172] Fakultät für Mathematik und Naturwissenschaften, Fachgruppe Physik, Bergische Universität Wuppertal, Wuppertal, Germany
[173] Department of Physics, Yale University, New Haven, CT, USA

[a] Also Affiliated with an institute covered by a cooperation agreement with CERN, Geneva, Switzerland
[b] Also at An-Najah National University, Nablus, Palestine
[c] Also at Borough of Manhattan Community College, City University of New York, New York, NY, USA
[d] Also at Center for Interdisciplinary Research and Innovation (CIRI-AUTH), Thessaloniki, Greece
[e] Also at Centro Studi e Ricerche Enrico Fermi, Rome, Italy

[f] Also at CERN, Geneva, Switzerland
[g] Also at Département de Physique Nucléaire et Corpusculaire, Université de Genève, Genève, Switzerland
[h] Also at Departament de Fisica de la Universitat Autonoma de Barcelona, Barcelona, Spain
[i] Also at Department of Financial and Management Engineering, University of the Aegean, Chios, Greece
[j] Also at Department of Physics, California State University, Sacramento, USA
[k] Also at Department of Physics, King's College London, London, UK
[l] Also at Department of Physics, Stanford University, Stanford, CA, USA
[m] Also at Department of Physics, Stellenbosch University, South Africa
[n] Also at Department of Physics, University of Fribourg, Fribourg, Switzerland
[o] Also at Department of Physics, University of Thessaly, Greece
[p] Also at Department of Physics, Westmont College, Santa Barbara, USA
[q] Also at Hellenic Open University, Patras, Greece
[r] Also at Institucio Catalana de Recerca i Estudis Avancats, ICREA, Barcelona, Spain
[s] Also at Institut für Experimentalphysik, Universität Hamburg, Hamburg, Germany
[t] Also at Institute for Nuclear Research and Nuclear Energy (INRNE) of the Bulgarian Academy of Sciences, Sofia, Bulgaria
[u] Also at Institute of Applied Physics, Mohammed VI Polytechnic University, Ben Guerir, Morocco
[v] Also at Institute of Particle Physics (IPP), Toronto, Canada
[w] Also at Institute of Physics and Technology, Mongolian Academy of Sciences, Ulaanbaatar, Mongolia
[x] Also at Institute of Physics, Azerbaijan Academy of Sciences, Baku, Azerbaijan
[y] Also at Institute of Theoretical Physics, Ilia State University, Tbilisi, Georgia
[z] Also at Lawrence Livermore National Laboratory, Livermore, USA
[aa] Also at National Institute of Physics, University of the Philippines Diliman (Philippines), Philippines
[ab] Also at Technical University of Munich, Munich, Germany
[ac] Also at The Collaborative Innovation Center of Quantum Matter (CICQM), Beijing, China
[ad] Also at TRIUMF, Vancouver, BC, Canada
[ae] Also at Università di Napoli Parthenope, Napoli, Italy
[af] Also at University of Colorado Boulder, Department of Physics, Colorado, USA
[ag] Also at Washington College, Chestertown, MD, USA
[ah] Also at Yeditepe University, Physics Department, Istanbul, Türkiye
[*] Deceased